



University of Tennessee, Knoxville

TRACE: Tennessee Research and Creative Exchange

Doctoral Dissertations

Graduate School

8-2002

KN and J/[psi]-nucleon scattering in the quark model

Noel F. Black
University of Tennessee

Follow this and additional works at: https://trace.tennessee.edu/utk_graddiss

Recommended Citation

Black, Noel F., "KN and J/[psi]-nucleon scattering in the quark model. " PhD diss., University of Tennessee, 2002.
https://trace.tennessee.edu/utk_graddiss/6204

This Dissertation is brought to you for free and open access by the Graduate School at TRACE: Tennessee Research and Creative Exchange. It has been accepted for inclusion in Doctoral Dissertations by an authorized administrator of TRACE: Tennessee Research and Creative Exchange. For more information, please contact trace@utk.edu.

To the Graduate Council:

I am submitting herewith a dissertation written by Noel F. Black entitled "KN and J/[psi]-nucleon scattering in the quark model." I have examined the final electronic copy of this dissertation for form and content and recommend that it be accepted in partial fulfillment of the requirements for the degree of Doctor of Philosophy, with a major in Physics.

T. Barnes, Major Professor

We have read this dissertation and recommend its acceptance:

Accepted for the Council:

Carolyn R. Hodges

Vice Provost and Dean of the Graduate School

(Original signatures are on file with official student records.)

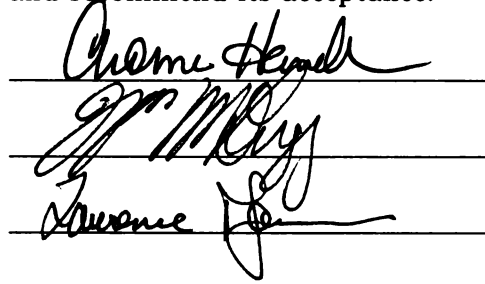
To the Graduate Council:

I am submitting herewith a thesis written by Noel Franklin Black entitled "Kaon-nucleon and J/ψ -nucleon Scattering in the Quark Model." I have examined the final paper copy of this thesis for form and content and recommend that it be accepted in partial fulfillment of the requirements for the degree of Doctor of Philosophy, with a major in Physics.

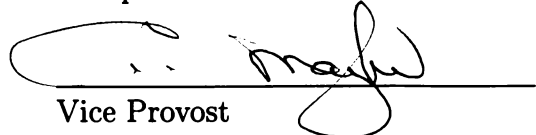


T. Barnes, Major Professor

We have read this thesis
and recommend its acceptance:



Accepted for the Council:



Vice Provost
and Dean of Graduate Studies

KN and $J/\psi N$ scattering in the Quark Model

A Dissertation
Presented for the
Doctor of Philosophy
Degree
The University of Tennessee, Knoxville

Noel F. Black
August 2002

Acknowledgements

I am grateful to my family and friends for all their support and encouragement. I wish to thank Vicki Vandaveer, Melanie Black, Dorothy Hollister, Tom and Jeanie Drake, John and Kelly Hunter, Mary Gilbreth, and Kenneth Roche for always being there for me. I wish to thank my advisor Ted Barnes for his guidance and help along the way, Philip Page for introducing me to Los Alamos and hybrid baryons, and David Blaschke for his wonderful hospitality in Rostock and Dubna.

Abstract

We calculate KN elastic scattering phase shifts at Born order in a quark interchange model with one-gluon exchange and linear scalar confinement. We find that quark-gluon forces are insufficient to explain the experimentally large spin-orbit interaction, especially evident in the P-waves. DN scattering amplitudes are simply related to the KN amplitudes, the only new parameter being the charm quark mass, and phase shifts for DN scattering are calculated. No DN bound states are found. Phase shifts for K^*N elastic scattering are calculated, and the formalism developed may be easily generalized to the scattering of hadrons of arbitrary spins. Inelasticities in KN scattering are large experimentally, and as a first step toward including the inelastic contribution to the elastic scattering phase shifts we compute the $KN \rightarrow K^*N$ scattering amplitudes. Finally, we develop the model for J/ψ -nucleon scattering and calculate cross sections for the reactions $J/\psi \rightarrow \bar{D}^0 \Sigma_c^+$, $\bar{D}^0 \Lambda_c^+$, and $D^{-*} \Sigma_c^{++}$.

Contents

1	Introduction	1
1.1	Prologue	1
1.2	Quantum Chromodynamics	5
1.3	Quark Model	9
2	KN Elastic Scattering	12
2.1	Introduction	12
2.2	The Calculation	13
2.2.1	Hamiltonian	13
2.2.2	Post-prior Ambiguity	15
2.2.3	Hadron States	16
2.2.4	Diagrams	18
2.3	Scattering Amplitudes	19
2.3.1	Signature	19
2.3.2	Color	20
2.3.3	Spin-flavor	20
2.3.4	Space	26
2.3.5	Spin-spin	29
2.3.6	Coulomb	30
2.3.7	Linear Confinement	31
2.3.8	OGE Spin-orbit	32
2.3.9	Scalar Confinement Spin-orbit	33
2.4	K^*N Phase Shifts	34
2.4.1	Spin-spin Hyperfine, Coulomb, and Linear Interactions	35
2.4.2	Spin-orbit Interactions	35
2.5	KN Results	36
2.6	KN Conclusions and Extensions	39
3	DN Scattering	41
4	K^*N Elastic Scattering and $KN \rightarrow K^*N$ Inelastic Amplitudes	42
5	$J/\psi N$ Scattering Cross Sections	43
5.1	Parameters	44
5.2	T-matrix	44
5.3	Space Wave Functions	45

5.4	Space Overlap	47
5.5	Spin-flavor Wave Functions	52
5.6	Spin-flavor Factors	53
5.7	Cross Sections	53
6	Conclusion	55
	References	56
	Appendix	62
A	Vectors and Spherical Tensors	63
B	Integrals	64
C	KN, K^*N Space Amplitudes	65
C.1	Reduced Forms	65
C.2	Explicit Amplitudes	69
C.2.1	Spin-spin	69
C.2.2	Coulomb	70
C.2.3	Linear	71
C.2.4	OGE Spin-orbit	72
C.2.5	Confinement Spin-orbit	74
D	$J/\psi N$ Space Amplitudes	76
D.1	Spin-spin	76
D.2	Coulomb	78
D.3	Linear	82
E	Figures	87
	Vita	143

List of Figures

1	Quark line diagrams.	87
2	Theoretical S_{11} KN phase shift. The experimental phase shifts of Hashimoto (triangles with error bars) and the RGM theoretical phase shifts of Lemaire, <i>et al.</i> (circles and squares, two wave functions) are shown.	88
3	Theoretical P_{11} KN phase shift. The symbols are as in Fig. 1.	89
4	Theoretical P_{13} KN phase shift. The symbols are as in Fig. 1.	90
5	Theoretical D_{13} KN phase shift. The symbols are as in Fig. 1.	91
6	Theoretical D_{15} KN phase shift. The symbols are as in Fig. 1.	92
7	Theoretical $I=1$ KN total phase shifts. The data points are from Hashimoto	93
8	Theoretical $I=1$ KN OGE spin-orbit phase shifts. The data points are from Hashimoto	94
9	Theoretical $I=1$ KN confinement spin-orbit phase shifts. The data points are from Hashimoto	95
10	Theoretical S_{01} KN phase shift. The symbols are as in Fig. 1.	96
11	Theoretical P_{01} KN phase shift. The symbols are as in Fig. 1.	97
12	Theoretical P_{03} KN phase shift. The symbols are as in Fig. 1.	98
13	Theoretical D_{03} KN phase shift. The symbols are as in Fig. 1.	99
14	Theoretical D_{05} KN phase shift. The symbols are as in Fig. 1.	100
15	Theoretical $I=0$ KN total phase shifts. The data points are from Hashimoto	101
16	Theoretical $I=0$ KN OGE spin-orbit phase shifts. The data points are from Hashimoto	102
17	Theoretical $I=0$ KN confinement spin-orbit phase shifts. The data points are from Hashimoto	103
18	Theoretical $I=1$ DN phase shifts.	104
19	Theoretical S_{11} DN phase shift.	105
20	Theoretical P_{11} DN phase shift.	106
21	Theoretical P_{13} DN phase shift.	107
22	Theoretical D_{13} DN phase shift.	108
23	Theoretical D_{15} DN phase shift.	109
24	Theoretical $I=0$ DN phase shifts.	110
25	Theoretical S_{01} DN phase shift.	111
26	Theoretical P_{01} DN phase shift.	112
27	Theoretical P_{03} DN phase shift.	113

28	Theoretical D_{03} DN phase shift.	114
29	Theoretical D_{05} DN phase shift.	115
30	Theoretical $S=1/2$ S_{11} K^*N phase shift.	116
31	Theoretical $I=1$ $S=1/2$ P- and D-wave K^*N phase shifts. . . .	117
32	Theoretical $S=3/2$ S_{11} K^*N phase shift.	118
33	Theoretical $I=1$ $S=3/2$ P- and D-wave K^*N phase shifts. . . .	119
34	Theoretical $S=1/2$ S_{01} K^*N phase shift.	120
35	Theoretical $I=0$ $S=1/2$ P- and D-wave K^*N phase shifts. . . .	121
36	Theoretical $S=3/2$ S_{01} K^*N phase shift.	122
37	Theoretical $I=0$ $S=3/2$ P- and D-wave K^*N phase shifts. . . .	123
38	Theoretical $I=1$ $S=1/2$ K^*N total phase shifts.	124
39	Theoretical $I=0$ $S=1/2$ K^*N total phase shifts.	125
40	Theoretical $I=1$ $S=3/2$ K^*N total phase shifts.	126
41	Theoretical $I=0$ $S=3/2$ K^*N total phase shifts.	127
42	Theoretical $I=1,0$ $S=1/2,3/2$ K^*N OGE spin-orbit phase shifts.	128
43	Theoretical $I=1,0$ $S=1/2,3/2$ K^*N confinement spin-orbit phase shifts.	129
44	Theoretical S_{11} $KN \rightarrow K^*N$ inelasticity.	130
45	Theoretical $I=1$ P- and D-wave $KN \rightarrow K^*N$ inelasticities. . .	131
46	Theoretical S_{01} $KN \rightarrow K^*N$ inelasticity.	132
47	Theoretical $I=0$ P- and D-wave $KN \rightarrow K^*N$ inelasticities. . .	133
48	Theoretical $I=1$ $KN \rightarrow K^*N$ total inelasticities.	134
49	Theoretical $I=0$ $KN \rightarrow K^*N$ total inelasticities.	135
50	Theoretical $I=1$ $KN \rightarrow K^*N$ OGE spin-orbit inelasticities. . .	136
51	Theoretical $I=0$ $KN \rightarrow K^*N$ OGE spin-orbit inelasticities. . .	137
52	Theoretical $I=1$ $KN \rightarrow K^*N$ confinement spin-orbit inelas- ticities.	138
53	Theoretical $I=0$ $KN \rightarrow K^*N$ confinement spin-orbit inelas- ticities.	139
54	Theoretical $J/\psi p \rightarrow \bar{D}^0 \Sigma_c^+$ cross section.	140
55	Theoretical $J/\psi p \rightarrow \bar{D}^0 \Lambda_c^+$ cross section.	141
56	Theoretical $J/\psi p \rightarrow \bar{D}^{*-} \Sigma_c^{++}$ cross section.	142

1 Introduction

1.1 Prologue

Despite widespread acceptance of quantum chromodynamics (QCD) as the theory of the strong interaction, our knowledge of QCD's predictions for hadron properties and interactions is extremely limited. We can hardly be satisfied with our understanding of hadron physics when we do not even know the physical states of the theory. QCD allows a perturbative solution, as is the method for precision tests of QED (quantum electrodynamics), only for high energy processes and so-called hard processes, where the coupling is weak. It is prohibitively difficult to solve QCD in the strongly coupled, non-perturbative regime which governs hadron spectra and soft processes. There are perhaps two important approaches for dealing with this situation. The first is to reformulate the theory on a space-time lattice. Lattice gauge theory (LGT) allows numerical calculation of QCD quantities from first principles and is the most promising approach for the long term. Progress, however, is slow because of the technical complexity and the large computing capacity required. The second is to develop QCD-inspired models. (Other methods such as QCD sum rules, large N_c QCD, and effective field theories can also provide insight but are not expected to be as widely applicable.) There exist many specific quark models but they generally share the same basic ingredients, which are motivated by QCD. The constituent-quark model (CQM) has been applied to a wide range of hadron phenomena with many successes. "The constituent-quark model offers the most complete description of hadron properties and is probably the most successful phenomenological model of hadron structure" [39]. The spectra and static properties of mesons and baryons are generally well described in this model, as are their strong, weak, and electromagnetic decays. It is therefore interesting to investigate its extension to hadron scattering. Scattering is, after all, the experimental arrangement by which we study hadrons.

It would be invaluable to have a consistent quark model description of hadron scattering. Although in principle it is possible to calculate any measurable quantity in LGT, we are a long way from lattice calculations of scattering [80]. LGT has been used up to now mainly for the calculation of static properties and ground state spectra. Calculations of excited state spectra have only recently been performed. Furthermore, LGT provides only numerical results with no direct physical insight. A quark model description of the

strong scattering process would make definite predictions for scattering amplitudes and would allow physical interpretation of the mechanisms involved in specific channels. The list of applications is long and includes searches for nuclei and hypernuclei, modeling stellar interiors, interpreting CP violation through final state interactions, and interpreting J/ψ -production suppression as signature for QGP in relativistic heavy-ion collisions. It would be satisfying if the same forces which are responsible for hadron masses also give rise to hadron scattering dynamics. We would then have a unified description of hadrons.

We take the nonrelativistic quark potential model (NQPM) as our starting point. There are many possible criticisms of the nonrelativistic quark model. Indeed, the world is known to be relativistic, so why should we even consider a model that is not relativistic at the outset? The main reasons are its previous successes and its relative technical simplicity. The NQPM has been successful in describing, at least qualitatively, a very wide range of phenomena. One of its great strengths is its consistent treatment of phenomena. Although admittedly coarse, it nevertheless has provided a “recognizable portrait” [36] of many aspects of hadron phenomenology. It is natural to suppose therefore that the NQPM contains much of the correct physics. For calculations of spectra, the nonrelativistic approximation is expected to be more applicable for heavy quarks. Light quarks are known to be relativistic in hadrons, yet the nonrelativistic model works surprisingly well for light quarks as well. It is an open and interesting question as to why a nonrelativistic model should work so well. Attempts to relativize the model are fraught with technical difficulties and typically fail to find better agreement with experiment than the naive NQPM. For these reasons, the results of the nonrelativistic scattering calculations should be pursued first. In order to elucidate the connection between NQPM and QCD it is important to test the extension of the NQPM to other aspects of hadron physics, in particular scattering. It is important to know where the NQPM works and where it fails.

There are different mechanisms at work in a hadron scattering interaction. Valence annihilation and s -channel resonance formation is known to be the dominant process when allowed. Pion exchange, when allowed, generally dominates the long distance behavior, as it clearly does in NN scattering. It is unlikely, however, that meson exchange is the scattering mechanism at short distances. It is difficult, for instance, to conceive of a physical meson being exchanged between nucleons whose wavefunctions are overlapping. Is-

gur has argued that the appropriate degrees of freedom at this scale should be the quarks and gluons. The repulsive core has been derived in the quark model from the spin-spin hyperfine interaction arising from one-gluon exchange (OGE) followed by quark interchange. The other OGE interactions (namely spin-orbit and tensor) are assumed small, and there is one calculation by Faessler [72] which reaches this conclusion. The transition between the short and long distance components of NN scattering is unclear. In the Yukawa-type models, the intermediate range attraction is traditionally ascribed to the exchange of a light scalar-isoscalar meson, referred to as the σ , but no evidence for such a resonance has been found in the $\pi - \pi$ S-wave system, and Faessler argues that the exchange of a correlated $\pi - \pi$ in relative S-wave between nucleons leads to a repulsive rather than attractive interaction [73]. It is important to understand the role of the quark-gluon degrees of freedom in the NN scattering problem. Isgur has called the spin-orbit problem in NN scattering the ‘Holy Grail’ of quark model scattering calculations.

KN scattering is ideally suited for studying the origins of the nonresonant ‘nuclear’ force. Conventional s -channel baryon resonance production is excluded because the nucleon contains no s -quark to annihilate against the \bar{s} of the kaon, and OPE is forbidden because of the vanishing three-pseudoscalar vertex. We may therefore study the nonresonant part of hadron scattering in relative isolation, uncomplicated by OPE. In this work we calculate KN phase shifts at Born order in a quark exchange model with OGE and linear scalar confinement. The Born approximation is expected to be a good one since the interaction is known experimentally to be only moderately strong. The dominant hyperfine term has given very good results in S-wave for $I = 2\pi\pi$ [67], $I = 3/2K\pi$ [68], and $I = 0, 1 KN$ [69] and NN [70] scattering. Here we include the spin-orbit and subdominant spin-independent contributions and give results for higher-L waves. KN scattering is an excellent place to test our model because data exists and there is a large spin-orbit effect evident in the P-waves. Understanding the spin-orbit effect here will motivate predictions for other hadronic interactions. The quark model calculation of KN scattering is a natural step toward the more combinatorically complicated NN calculation.

The effect of the spin-orbit interaction in hadron phenomenology is interesting for several reasons. The spin-orbit force is intimately connected with the Lorentz nature of the confining interaction. It is well known that scalar confinement is preferred in the meson spectra because the Thomas preces-

sion spin-orbit interaction arising from OGE in a scalar confining potential is inverted, and so partly cancels the ‘ordinary’ spin-orbit force due to OGE. The net spin-orbit splittings are then small, as observed experimentally. The baryon spectra have a well known “spin-orbit problem” because of three-body spin-orbit forces. The OGE and confinement spin-orbit effects approximately cancel as in the mesons but there seems to be no way to arrange a cancellation for these three-body forces, which give large splittings, in disagreement with the observed small splittings in the baryon spectra. Isgur and Karl’s original treatment left spin-orbit forces out altogether as a first approximation, suggesting a more thorough treatment of spin-orbit forces was necessary to resolve the problem. Capstick and Isgur [37] have suggested that relativistic effects may enhance the size of the spin-spin relative to the spin-orbit interaction. Page *et al.* [42] have shown that the near perfect cancellation of OGE and Thomas precession spin-orbit interactions in heavy-light quark systems may arise from a symmetry of QCD and so may not be a numerical accident. Isgur [44] has shown that the three-body spin-orbit force for Λ_Q states is a pseudo-two-body effect and does exhibit meson-like cancellation. The spin-orbit problem in hadron spectroscopy is an area of active interest. We feel it is valuable and complementary to investigate the spin-orbit interaction in hadron scattering in the NQPM.

We can readily apply our KN scattering calculation to DN scattering. All that is required is to replace the strange quark with a charm quark. Knowledge of vacuum DN scattering amplitudes is important, for example, for understanding open-charm hadronic interactions in relativistic heavy-ion collisions, for example.

Since the S-wave phase shifts found previously have good agreement with experiment in the cases where data exists, we can make useful predictions for other S-wave scattering interactions that are not directly accessible to experiment. We will apply the model to compute cross sections for $J/\psi N$ scattering and related channels. This calculation requires a generalization of the model. The charm baryons produced in the final state of such processes contain one heavy (charm) quark and two light quarks, so it will be necessary to use asymmetric wave functions for these baryons. The previous calculations involved only the symmetric nucleon wave function. It is essential to know the size of these cross sections in order to understand charmonium-nucleon interactions in hot, dense media, as occur in heavy-ion collisions. In order for a suppression in the rate of J/ψ production to be interpreted as a signal for the QGP, we must be able to rule out the possibility of signifi-

cant charmonium dissociation from inelastic scattering in the collision region. This requires knowledge of $J/\psi N$ cross sections as we calculate here.

1.2 Quantum Chromodynamics

Quantum chromodynamics [7, 8, 9] is the gauge field theory of the strong interaction between colored quarks and gluons and is one component of the $SU(3)_c \otimes SU(2)_L \otimes U(1)_Y$ Standard Model of particle interactions. It is constructed in analogy with the spectacularly successful theory of photons and electrons, quantum electrodynamics (QED). In QED, photon exchange mediates the electromagnetic interaction between charged electrons (or positrons). The photons are the massless quanta of the electromagnetic field. Their existence is required, and the form of the interaction between them and the electrons prescribed, by the principle of local gauge invariance. The QED Lagrangian is invariant under a local $U(1)$ gauge transformation of the fields, and the modern viewpoint is that physically relevant field theories are locally gauge invariant.

The choice of the theory of the strong interaction is well understood with reference to the early quark model, which has its origins in the observations by Gell-Mann [16] and Ne'eman [17] in 1961 that the then known hadrons seemed to be arranged according to their quantum numbers in certain representations of the group $SU(3)$. In 1964 Zweig [19] and Gell-Mann [18] proposed that the hadrons could be understood as composites of fractionally charged spin-1/2 'quarks' (Gell-Mann) or 'aces' (Zweig) of three flavors: up (u), down (d), and strange (s). Mesons were postulated to be composed of a quark-antiquark pair and baryons were assumed to be made of three quarks. This early model successfully related static properties like magnetic moments in terms of spin-flavor matrix elements and explained the observed pattern of states. The nonobservation of quarks, however, made it difficult for many to believe in quarks as real objects; they seemed merely a convenient bookkeeping device. It was not understood why only representations corresponding to $q\bar{q}$ and qqq should be realized and not others, particularly the fundamental representation q . There was also a statistics problem. The quarks, being fermions, should obey Fermi-Dirac statistics in baryons, yet the baryon spectrum seemed to indicate symmetric wavefunctions. The Δ^{++} is a simple example; its aligned spins, uuu flavor content, and zero orbital angular momentum clearly make it symmetric in spin, flavor, and space quantum numbers and therefore symmetric overall. To solve the statistics problem it

was postulated [20, 21] that the quarks carry an additional internal quantum number now realized as color with respect to which the baryon states could be antisymmetrized, thus making them totally antisymmetric as required by the spin-statistics theorem. The simplest model is to presume that quarks come in three colors, i.e. to assign them to the fundamental triplet representation of a new internal $SU(3)_c$ symmetry. The three quarks in a baryon are in the antisymmetric color singlet state. The antiquarks should be assigned to the conjugate representation of $SU(3)$, so the $q\bar{q}$ pair in a meson can be in a color singlet state as well. In fact these are the only simple combinations that can be color singlets. The other possible combinations are multiples of these states, eg. $qq\bar{q}\bar{q}$. With the postulate that only color singlets can be observed in nature, the color hypothesis could simultaneously solve the statistics problem and ‘explain’ why mesons and baryons are the only quark combinations seen. Isolated quarks thus cannot exist; the quarks are confined within hadrons.

Further evidence regarding the internal constituents of hadrons came from deep inelastic scattering experiments at SLAC in the 1960s [84]. There a 20 GeV electron beam was incident on a hydrogen target. Substantial rates for hard scattering events were observed in the deep inelastic region of phase space, in which the electron breaks up the proton producing many outgoing hadrons in the final state. The proton behaves in these reactions as if it were composed of essentially free pointlike constituents, called ‘partons’ in the parton model of Bjorken and Feynman [85, 86]. The parton model was also motivated by the observation that in high energy hadron-hadron collisions, many pions are produced with momenta nearly parallel to the collision axis. The limited transverse momenta of the final state particles in such processes indicates that the constituents in the proton appear to be loosely bound. A more quantitative test of this notion came in the observation that the measured structure functions of the proton in deep inelastic lepton-hadron scattering depend on the momentum transfer $Q^2 = -q^2$ (> 0 , since q is space-like) only in the dimensionless combination $\frac{Q^2}{P \cdot q}$ (where P is the total proton momentum), as was anticipated by Bjorken [10]. This ‘Bjorken scaling’ indicated that interactions between the proton constituents were negligible over the short time scales associated with the electromagnetic scattering. If the partons are to be identified with the quarks, then a successful theory of the strong interaction between quarks should somehow account for their apparent freedom at short distances as well as their confinement.

The coupling constant in a quantum field theory must be renormalized, and the effective coupling depends on the distance scale. In QED, the coupling increases with decreasing distance (increasing momentum transfer) because the QED vacuum is a normal dielectric. A bare charge polarizes the surrounding virtual e^+e^- pairs, which exist as a result of vacuum fluctuations, and hence is screened at large distances. At shorter distances, a test charge is less screened by the virtual cloud and feels more of the bare charge, so that the effective coupling is greater. In some field theories, the effective coupling has the opposite behavior, increasing at large distances and becoming weak at short distances. This feature, called ‘asymptotic freedom,’ is apparently required for the theory of the strong interaction. ‘t Hooft, Politzer, Gross, Wilczek showed that the only asymptotically free theories in four dimensions are the non-Abelian gauge theories [?]. It remained only to determine the symmetry group, and $SU(3)_c$ emerged as the natural choice after theories built on flavor symmetry were ruled out. Demanding the QCD Lagrangian \mathcal{L}_{QCD} to be invariant under local $SU(3)_c$ transformations requires the existence of the massless gluons, the quanta of the color field, and determines the form of the interactions.

The QCD Lagrangian is

$$\mathcal{L}_{QCD} = \sum_q \bar{q}^i (i\gamma^\mu (D_\mu)_{ij} - \delta_{ij} m_q) q^j - \frac{1}{4} F_{\mu\nu}^{(a)} F^{(a)\mu\nu} \quad (1)$$

with field strength tensor

$$F_{\mu\nu}^{(a)} = \partial_\mu A_\nu^a - \partial_\nu A_\mu^a + g f_{abc} A_\mu^b A_\nu^c \quad (2)$$

and covariant derivative

$$(D_\mu)_{ij} = \delta_{ij} \partial_\mu - ig \sum_a \frac{\lambda_{ij}^a}{2} A_\mu^a, \quad (3)$$

where the $\{q^i\}$ are four-component Dirac spinor fields for the quarks of flavor q and color i and the $\{A_\mu^{(a)}\}$ are the eight gluon fields. The $\{\lambda_{ij}^a\}$ are the generators of $SU(3)$, the $\{f_{abc}\}$ are the structure constants of the $SU(3)$ algebra, and g is the strong coupling constant [65].

The last term in the field strength tensor $F_{\mu\nu}^a$ is present because the local $SU(3)$ symmetry is non-Abelian. It gives terms in \mathcal{L}_{QCD} trilinear and quartic in the gluon fields, corresponding to three- and four-gluon vertices.

Such terms do not occur in the Abelian theory QED; there are no vertices in \mathcal{L}_{QED} involving only photons. Thus gluons are quite different from photons in that the former interact with each other whereas the latter do not; gluons carry color but photons do not carry electric charge. This feature makes the theory nonlinear and has profound consequences. The virtual $q\bar{q}$ pairs do screen a bare color charge, analagous to the charge screening in QED, but the gluon self-interactions give rise to an antiscreening effect which dominates.

The effective QCD coupling constant $\alpha_s = g_s^2/4\pi$ is governed by the β -function, and its dependence on the energy scale Q^2 can be parametrized approximately as

$$\alpha_s(Q^2) = \frac{4\pi}{(11 - \frac{2}{3}n_f) \ln(Q^2/\Lambda^2)} \quad (4)$$

where $\Lambda \approx 200\text{MeV}$ sets the QCD scale. This expression clearly shows that the ‘running coupling constant’ is weak at large momentum transfer and becomes strong at small Q^2 . Perturbation theory will only work when the coupling is small, which corresponds to energies of approximately 1 GeV or greater. The increasing of the coupling at large distances is inherently a nonperturbative effect and is thought to lead to confinement, although it has yet to be shown that confinement follows rigorously from QCD.

Although the QCD coupling vanishes asymptotically, it is still nonzero and finite at any finite distance, and hence a deviation from strict Bjorken scaling is expected. QCD predicts a slow, logarithmic evolution of the parton distribution functions, and the observation of violation of Bjorken scaling in just this manner is strong verification of the theory. Further verification comes from tests of perturbative QCD, some important processes being τ decay, heavy quarkonium decay, e^+e^- annihilation to hadrons, and high energy hadron-hadron collisions. Often there are perturbative and nonperturbative parts to a given process. In high energy hadron-hadron scattering, for example, the parton process is perturbatively calculable but the relation between the partons and the produced hadrons is described by structure and fragmentation functions which must be taken from experiment. Hadronization is an important part of inelastic processes and is a highly nonperturbative, noncalculable effect.

A second qualitative difference between QED and QCD involves the nature of the force between two sources. The flux lines of the electromagnetic force between electric charges are spread out, whereas the gluon self-couplings cause the flux lines of the color force between color charges to condense into

stringlike configurations [12, 13]. As the quark and antiquark of a meson are pulled apart, the energy density of the color flux between the two remains essentially constant. It becomes energetically favorable for the string to break, producing a $q\bar{q}$ pair somewhere in the middle. It is in this manner that color is confined; in trying to remove a quark from a meson we obtain two $q\bar{q}$ mesons rather than isolated quarks.

The color singlet mesons and baryons are thus the low energy states of the theory. Color singlet multiquark states (eg. $qq\bar{q}\bar{q}$ or $q\bar{q}qqq$) tend to fall apart into ordinary hadrons, for instance in nuclei, because it is energetically favorable to do so. A color singlet state may also be composed entirely of gluons, and since the gluons interact with each other these ‘glueballs’ are expected. So far there is no unambiguous proof that any of the known states are glueballs although there are several candidates, the most likely being the scalar $f_0(1500)$ [66]. ‘Hybrids,’ which contain both valence quarks and gluons in color singlet combinations like $q\bar{q}g$ and $qqqg$ are also possible. The flux tube model describes such hybrid mesons or hybrid baryons as having an excitation in the string of gluon flux binding the quarks [87, 88, 89]. $\hat{\rho}(1600)$ and $\hat{\rho}(1400)$ are possible hybrid mesons [39].

1.3 Quark Model

The discovery of the J/ψ simultaneously at SLAC and BNL [2, 1] was quickly interpreted as the discovery of a $c\bar{c}$ bound state, c being a fourth quark flavor, charm. This convinced almost all physicists that quarks were real, and other members of the $c\bar{c}$ family were subsequently found. Quark potential models incorporating asymptotic freedom and confinement, qualitative features of QCD, were able to reproduce the charmonium spectrum rather well [29, 30, 31, 32]. DeRujula, Georgi, and Glashow [28] showed these ideas could be applied to light quark spectroscopy. They argued that the effective short range force between quarks arises from OGE and is Coulomb-like at short distances, while the long range confining forces should be independent of quark spins and masses and depend only on the spatial separations of the constituent quarks. The confining force is typically taken to be a Lorentz scalar.

The basic idea of the simplest version of the quark potential model is to assume the spin- $\frac{1}{2}$ quarks in hadrons are bound by this Coulomb-plus-linear

quark-quark potential

$$V_{q\bar{q}} = -\frac{4}{3} \frac{\alpha_s}{r} + br \quad (5)$$

(mesons) with phenomenological coupling constant α_s and string tension b . Fits to light quark spectroscopy (u,d, and s quarks) require $\alpha_s \approx 0.6$ and $b \approx 0.18 \text{ GeV}^2$. The charmonium spectrum requires a slightly reduced $\alpha_s \approx 0.4$ and the bottomonium spectrum uses $\alpha_s \approx 0.15$. The wave function length scales of $q\bar{q}$ systems decrease with increasing quark mass, so heavier quarks require smaller values of α_s due to antiscreening effects. The energy levels and wavefunctions may be determined by solving the Schrodinger equation or a relativized Schrodinger equation, or by solving the Bethe-Salpeter equation. This elucidates the spectroscopy, and the wave functions can then be used to calculate matrix elements for transitions.

The OGE amplitude leads to spin dependent interactions as well, namely spin-spin, spin-orbit and tensor. The $O(P^2/m^2)$ reduction of the OGE amplitude gives the analog of the Fermi-Breit interaction, well known from atomic physics, times a color factor which is $-4/3$ for color singlet $q\bar{q}$ in mesons (this factor appears explicitly in Eq. (5)) and $-2/3$ for qq in baryons. The spin-dependent part of the $q\bar{q}$ Hamiltonian has the form

$$H_{ij}^{spin} = H_{ij}^{hyp} + H_{ij}^{cm S.O.} + H_{ij}^{tp S.O.} \quad (6)$$

where

$$H_{ij}^{hyp} = \frac{4}{3} \frac{\alpha_s(r)}{m_i m_j} \left\{ \frac{8\pi}{3} \mathbf{S}_i \cdot \mathbf{S}_j \delta^3(\mathbf{r}_{ij}) + \frac{1}{r_{ij}^3} \left(\frac{3 \mathbf{S}_i \cdot \mathbf{r}_{ij} \mathbf{S}_j \cdot \mathbf{r}_{ij}}{r_{ij}^2} - \mathbf{S}_i \cdot \mathbf{S}_j \right) \right\} \quad (7)$$

is the color hyperfine interaction,

$$H_{ij}^{cm S.O.} = \frac{4}{3} \frac{\alpha_s(r)}{r_{ij}^3} \left(\frac{1}{m_i} + \frac{1}{m_j} \right) \left(\frac{\mathbf{S}_i}{m_i} + \frac{\mathbf{S}_j}{m_j} \right) \cdot \mathbf{L} \quad (8)$$

is the color magnetic OGE spin-orbit interaction, and

$$H_{ij}^{tp S.O.} = - \frac{1}{2r_{ij}} \frac{\partial V(r)}{\partial r_{ij}} \left(\frac{\mathbf{S}_i}{m_i^2} + \frac{\mathbf{S}_j}{m_j^2} \right) \cdot \mathbf{L} \quad (9)$$

($V(r)$ is the $q\bar{q}$ potential) arises from Thomas precession of the confining potential [39].

This form of the $q\bar{q}$ interaction has direct support from the lattice. The $Q\bar{Q}$ potential between infinitely heavy quarks can be calculated on the lattice by evaluating the expectation value of the Wilson loop for fixed quark positions, and the result is indeed Coulomb-like at short distances and linear at large separations (see for instance [43]). Values for the coupling α_s and the string tension b can be extracted and agree with the values obtained from spectroscopic fits. The spin-dependent potentials can be determined by expanding the Wilson loop to order v^2/c^2 and agree reasonably well with the spin-dependent potential arising from OGE [3, 4, 5, 6].

2 KN Elastic Scattering

2.1 Introduction

Kaon-nucleon (KN , as distinct from $\bar{K}N$) scattering is interesting experimentally because of the possible existence of Z^* resonances. These resonances must have some flavor-exotic $q^4\bar{s}$ structure if they exist, since a three-quark system cannot have hypercharge = 2. Searches have been made since the early 1960s, and although candidates have been announced the results are inconclusive. Different analyses have drawn different conclusions as to which channels contain Z^* resonances, and in general multiple solutions which fit the data are possible. Typically the evidence of a given solution is incomplete, so for instance some counterclockwise resonance-like motion in the Argand diagram may not be accompanied by any sharp variation with energy of the speed plot dT/dE or any peak in the cross section in the same energy range. It may be difficult to distinguish between moderate to strong attraction and the existence of exotic Z^* resonances in a given channel. There may be some dynamical mechanism by which the resonance-like nature of these reactions arises. It is well known, for instance, that the rapid opening of an inelastic channel can simulate a resonance, and the inelasticities are known to be large in KN (as is evident in the Argand plots of KN scattering amplitudes). It is clearly of interest to calculate the KN elastic and inelastic scattering amplitudes at Born order in the constituent quark interchange model to see if attractive forces support bound states. The Born approximation is expected to be a good one since the KN interaction is known experimentally to be only moderately strong. The dominant hyperfine interaction has been calculated in this model for $I=2 \pi\pi$, $I=3/2 K\pi$, KN , and NN scattering and has given good results in S-wave, so there is reason to believe that we can make accurate predictions for KN scattering using the full OGE plus linear scalar confinement interaction.

KN elastic scattering is interesting in its own right for several reasons, the most significant being its large spin-orbit effect which is evident experimentally in the P-waves. KN scattering is almost entirely elastic below the $K\Delta$ threshold. Since KN elastic scattering data exists, this reaction is the ideal place to test whether our method can give correct results for the spin-orbit interaction, and for the higher-L channels in general. We are interested to know if we can understand the origins of the nonresonant “nuclear” force from the more fundamental quark and gluon interactions. If we

have included the most important physics in our model, we should find good results for higher-L KN partial waves. The model can then be extended to the spin-orbit force in NN scattering. We proceed first with a calculation of the KN elastic scattering amplitudes and phase shifts.

There are some basic experimental features which are generally agreed upon. The $I=1$ channel is relatively well determined from K^+P scattering. In $L_I 2J$ notation, the S_{11} and P_{11} channels are repulsive and the P_{13} channel is attractive. $I=0$ is more in doubt because of inherent difficulties of the experimental analysis. The $I=0$ KN scattering amplitudes must be extracted from K^2H scattering, using a model of deuteron breakup and form factors. It is clear, however, that the P_{01} channel is strongly attractive and may support a Z^* resonance. Inelasticities are also known to be important above the inelastic thresholds. $K\Delta$ ($I=1$ only) opens at $P_{lab} = 0.870$ GeV and K^*N opens at $P_{lab} = 1.075$ GeV. $K^*\Delta$ opens somewhat higher.

2.2 The Calculation

2.2.1 Hamiltonian

The fundamental interactions in hadron-hadron scattering are between the constituents, especially between quarks. Pairs of quarks interact in our model by exchanging a single gluon, and through a linear scalar confining interaction. We have thus included two important qualitative features of QCD: It is perturbative at short distances and is confining at large distances. In the perturbative regime OGE should dominate the interaction, so it is natural to include it; the OGE interaction should still be large at the intermediate distances we are considering. Confinement is known to be a nonperturbative phenomenon, which we model as a linear scalar interaction. There is evidence from LGT that the confining interaction is linear; the potential energy between a $q\bar{q}$ pair grows linearly with their separation on the lattice. The quark-quark OGE T_{fi} is derived as the nonrelativistic reduction to order P^2/m^2 of the Feynman amplitude for two quarks to exchange a gluon, with phenomenological strength α_s . The result is the usual Breit-Fermi Hamiltonian, which is well known from atomic physics and which includes the spin-spin hyperfine interaction as well as Coulomb, spin-orbit, tensor, and spin-independent contributions. The confining interaction is the reduction of the amplitude for a scalar interaction with strength b (the string tension) between a pair of quarks, and yields linear and inverted spin-orbit contri-

butions, as well as smaller spin-independent terms. The momentum-space quark-quark T_{fi} we consider (with color factors removed) is

$$T_{fi}^{qq}(\vec{q}, \vec{p}_1, \vec{p}_2) = \begin{cases} -\frac{8\pi\alpha_s}{3m_1m_2} [\vec{S}_1 \cdot \vec{S}_2] \\ +\frac{4\pi\alpha_s}{\vec{q}^2} \\ +\frac{6\pi b}{\vec{q}^4} \\ +\frac{4\pi\alpha_s}{\vec{q}^2} \left[\frac{\vec{S}_1}{m_1} \cdot \left(\vec{q} \times \left(\frac{\vec{p}_1}{2m_1} - \frac{\vec{p}_2}{m_2} \right) \right) + \frac{\vec{S}_2}{m_2} \cdot \left(\vec{q} \times \left(\frac{\vec{p}_1}{m_1} - \frac{\vec{p}_2}{2m_2} \right) \right) \right] \\ -\frac{3\pi b}{\vec{q}^4} \left[\frac{\vec{S}_1}{m_1} \cdot \left(\vec{q} \times \frac{\vec{p}_1}{m_1} \right) - \frac{\vec{S}_2}{m_2} \cdot \left(\vec{q} \times \frac{\vec{p}_2}{m_2} \right) \right] \\ +\frac{4\pi\alpha_s}{m_1m_2\vec{q}^2} \left[\vec{S}_1 \cdot \vec{q} \vec{S}_2 \cdot \vec{q} - \frac{1}{3} \vec{q}^2 \vec{S}_1 \cdot \vec{S}_2 \right] \end{cases} \quad (10)$$

for quarks with initial momenta $k_{1,2}$, final momenta $k'_{1,2}$, and spins $s_{1,2}$,

where

$$\begin{aligned} p_1 &= \frac{k_1 + k'_1}{2} \\ p_2 &= \frac{k_2 + k'_2}{2} \\ q &= k'_1 - k_1 = k_2 - k'_2. \end{aligned} \quad (11)$$

The terms in Eq. (10) correspond respectively to the spin-spin, Coulomb, linear, OGE spin-orbit, confinement spin-orbit, and tensor interactions.

For the general two-body scattering process $AB \rightarrow CD$ we partition the Hamiltonian into a part H_0 which includes interactions between quarks in the same initial hadron and the kinetic energies of these quarks and a part H_{int} which includes interactions between quarks initially in different hadrons. We have

$$H = H_0 + H_{int} = (H_0^A + H_0^B) + H_{int} \quad (12)$$

where

$$H_0^A = -\sum_{i \in A} \frac{\hbar^2}{2m_i^2} \nabla_i^2 + \sum_{\substack{i, j \in A \\ i < j}} H_{fi}^{q_i q_j} \quad (13)$$

(and similarly for H_0^B), and

$$H_{int} = \sum_{\substack{i \in A \\ j \in B}} H_{fi}^{q_i q_j}. \quad (14)$$

The scattering in this model arises from the interactions between quarks in different hadrons, i.e. from H_{int} . At Born order the interaction must be followed by quark interchange so that the hadrons C and D emerge as color singlet states. The Born scattering amplitude is given by the matrix element of H_{int} between external hadron states which are eigenstates of the respective free Hamiltonians.

$$T_{fi}^{AB \rightarrow CD} = \langle AB | H_{int} | CD \rangle \delta(\mathbf{P}_f - \mathbf{P}_i) \quad (15)$$

where

$$H_0^A |A\rangle = E_A |A\rangle \quad (16)$$

and similarly for B, C, and D.

2.2.2 Post-prior Ambiguity

It is possible to partition the Hamiltonian so that the final states C and D, instead of the initial states A and B, are diagonal on H_0 . The remaining terms then comprise a CD interaction Hamiltonian which we call H_{int}^{post} since this interaction follows quark interchange. This describes the scattering as due to interactions between quarks in final state hadrons instead of initial state hadrons. In the original partition the interaction preceeds quark interchange. Thus there are two possible partitions with different interaction Hamiltonians,

$$H = (H_0^A + H_0^B) + H_{int}^{prior} \quad (17)$$

$$H = (H_0^C + H_0^D) + H_{int}^{post}. \quad (18)$$

This is the post-prior ambiguity. It can be shown that H_{int}^{post} and H_{int}^{prior} give the same matrix element between external hadron states, provided these states are indeed eigenstates of the respective free Hamiltonians. Since we use approximate wave functions to derive analytical amplitudes, the post and prior forms of our results will differ in general. If the wave functions we

use are good approximations the difference is expected to be small. We will demonstrate the calculation of

$$T_{fi}^{prior}(AB \rightarrow CD) = \langle AB | H_{int}^{prior} | CD \rangle \delta(\mathbf{P}_f - \mathbf{P}_i). \quad (19)$$

The calculation of T_{fi}^{post} proceeds analogously.

2.2.3 Hadron States

The hadron states are direct products of color, spin, flavor, and spatial states. A meson $|A(\mathbf{P}, \lambda)\rangle$ with momentum \mathbf{P} and polarization λ is written as

$$\begin{aligned} |A(\mathbf{P}, \lambda)\rangle = & \sum_{c, \bar{c}=1}^3 \frac{1}{\sqrt{3}} \delta_{c, \bar{c}} \sum_{\substack{s, \bar{s} \\ q, \bar{q}}} \iint d^3k \, d^3\bar{k} \, \delta(\mathbf{P} - \mathbf{k} - \bar{\mathbf{k}}) \, \chi_{s\bar{s}}^\lambda \, \Omega_{q\bar{q}} \, \Phi_A(\mathbf{p}_{rel}) \, b_{\mathbf{k}, s}^{q, c \dagger} \, d_{\bar{\mathbf{k}}, \bar{s}}^{\bar{q}, \bar{c} \dagger} |0\rangle \end{aligned} \quad (20)$$

where

$$\mathbf{p}_{rel} = \frac{m_{\bar{q}}\mathbf{k} - m_q\bar{\mathbf{k}}}{(m_q + m_{\bar{q}})/2} \quad (21)$$

$b_{\mathbf{k}, s}^{q, c \dagger}$ is a creation operator for a flavor q quark with color label c , spin label s , and three-momentum \mathbf{k} , and $d_{\bar{\mathbf{k}}, \bar{s}}^{\bar{q}, \bar{c} \dagger}$ is the antiquark creation operator. $\sum_{c, \bar{c}=1}^3 \frac{1}{\sqrt{3}} \delta_{c, \bar{c}}$ is the antisymmetric color combination for a $q\bar{q}$ pair. $\chi_{s\bar{s}}^\lambda$ is the spin wave function for a spin- S^A meson and $\Omega_{q\bar{q}}$ is the appropriate flavor wave function. $\Phi_A(\mathbf{p}_{rel})$ is the $q\bar{q}$ momentum-space wave function, and the delta function $\delta(\mathbf{P} - \mathbf{k} - \bar{\mathbf{k}})$ ensures that the meson momentum is the sum of the quark and antiquark momenta. Similarly, a baryon state is

$$\begin{aligned} |B(\mathbf{P}, \lambda)\rangle = & \sum_{c_1, c_2, c_3=1}^3 \frac{1}{\sqrt{6}} \epsilon_{c_1, c_2, c_3} \sum_{\substack{s_1, s_2, s_3 \\ q_1, q_2, q_3}} \iiint d^3k_1 \, d^3k_2 \, d^3k_3 \, \delta(\mathbf{P} - \mathbf{k}_1 - \mathbf{k}_2 - \mathbf{k}_3) \\ & \cdot \chi_{s_1, s_2, s_3}^\lambda \, \Omega_{q_1, q_2, q_3} \, \Phi_A(\mathbf{k}_1, \mathbf{k}_2, \mathbf{k}_3) \, b_{\mathbf{k}_1, s_1}^{q_1, c_1 \dagger} \, b_{\mathbf{k}_2, s_2}^{q_2, c_2 \dagger} \, b_{\mathbf{k}_3, s_3}^{q_3, c_3 \dagger} |0\rangle. \end{aligned} \quad (22)$$

Note that, contrary to the usual quark model convention, the baryon spin-flavor wave function generally factors. Our states are not explicitly symmetrized. Instead, symmetrization is part of the diagrammatic evaluation of a matrix element and is realized by summing over all possible quark line diagrams. Our $\Delta^+(+3/2)$ state, for instance, is

$$|\Delta^+(+3/2)\rangle = \frac{1}{\sqrt{2}}|u_+u_+d_+\rangle \quad (23)$$

whereas the usual convention is to write

$$|\Delta^+(+3/2)\rangle = \frac{1}{\sqrt{3}}(|u_+u_+d_+\rangle + |u_+d_+u_+\rangle + |d_+u_+u_+\rangle). \quad (24)$$

In our convention the three terms are equivalent. Of course the $\Delta^+(+3/2)$ factors in either convention, but the proton for instance factors only in ours.

The kaons K^0 and K^+ form an isospin doublet as do the nucleons n and p , so the isospin can be 0 or 1 in KN scattering. The spin-flavor wave functions for the kaons and nucleons are

$$|K^+\rangle = \frac{1}{\sqrt{2}} \left(\left| \begin{smallmatrix} u_+ \\ \bar{s}_- \end{smallmatrix} \right\rangle - \left| \begin{smallmatrix} u_- \\ \bar{s}_+ \end{smallmatrix} \right\rangle \right) \quad (25)$$

$$|K^0\rangle = \frac{1}{\sqrt{2}} \left(\left| \begin{smallmatrix} d_+ \\ \bar{s}_- \end{smallmatrix} \right\rangle - \left| \begin{smallmatrix} d_- \\ \bar{s}_+ \end{smallmatrix} \right\rangle \right) \quad (26)$$

$$|p(+1/2)\rangle = \frac{1}{\sqrt{3}} \left(\left| \begin{smallmatrix} u_+ \\ u_+ \\ d_- \end{smallmatrix} \right\rangle - \left| \begin{smallmatrix} u_+ \\ u_- \\ d_+ \end{smallmatrix} \right\rangle \right) \quad (27)$$

$$|p(-1/2)\rangle = -\frac{1}{\sqrt{3}} \left(\left| \begin{smallmatrix} u_- \\ u_- \\ d_+ \end{smallmatrix} \right\rangle - \left| \begin{smallmatrix} u_+ \\ u_- \\ d_- \end{smallmatrix} \right\rangle \right) \quad (28)$$

$$|n(+1/2)\rangle = -\frac{1}{\sqrt{3}} \left(\left| \begin{smallmatrix} d_+ \\ d_+ \\ u_- \end{smallmatrix} \right\rangle - \left| \begin{smallmatrix} d_+ \\ d_- \\ u_+ \end{smallmatrix} \right\rangle \right) \quad (29)$$

$$|n(-1/2)\rangle = \frac{1}{\sqrt{3}} \left(\left| \begin{smallmatrix} d_- \\ d_- \\ u_+ \end{smallmatrix} \right\rangle - \left| \begin{smallmatrix} d_+ \\ d_- \\ u_- \end{smallmatrix} \right\rangle \right). \quad (30)$$

We use the usual harmonic oscillator momentum-space wave functions so we can get closed form results for the scattering amplitudes. One can solve the Schroedinger equation with a Coulomb plus linear potential and use the wave functions thus obtained, but the overlap must then be evaluated numerically and in practice differs little from the analytical result. The kaon momentum-space wave function is

$$\phi_K(\mathbf{p}_{rel}) = \frac{1}{\pi^{3/4} \beta^{3/2}} \exp \left\{ -\frac{\mathbf{p}_{rel}^2}{8\beta^2} \right\} \quad (31)$$

where

$$\mathbf{p}_{rel} = \frac{m_{\bar{q}}\mathbf{p}_q - m_q\mathbf{p}_{\bar{q}}}{(m_q + m_{\bar{q}})/2} \quad (32)$$

and the nucleon wave function is

$$\phi_N(\mathbf{p}_1, \mathbf{p}_2, \mathbf{p}_3) = \frac{3^{3/4}}{\pi^{3/2} \alpha^3} \exp \left\{ -\frac{\mathbf{p}_1^2 + \mathbf{p}_2^2 + \mathbf{p}_3^2 - \mathbf{p}_1 \cdot \mathbf{p}_2 - \mathbf{p}_1 \cdot \mathbf{p}_3 - \mathbf{p}_2 \cdot \mathbf{p}_3}{3\alpha^2} \right\}. \quad (33)$$

The standard parameters are relatively well determined in hadron phenomenology and we use the ones below for our numerical evaluation.

α_s	$= 0.6$	strong coupling constant	
b	$= 0.18 \text{ GeV}^2$	string tension	
β	$= 0.4 \text{ GeV}$	width parameter for $\phi_K(\mathbf{p}_{rel})$	
α	$= 0.35 \text{ GeV}$	width parameter for $\phi_N(\mathbf{p}_1, \mathbf{p}_2, \mathbf{p}_3)$	(34)
$m_{u,d}$	$= 0.330 \text{ GeV}$	nonstrange constituent quark mass	
m_s	$= 0.550 \text{ GeV}$	strange constituent quark mass	

2.2.4 Diagrams

The quarks of the incoming hadrons must connect to those of the outgoing hadrons in all possible ways, and we must include all pairwise interactions between quarks initially in different hadrons. For the general meson-nucleon scattering process there are $5!$ possible line permutations and $2 \cdot 3$ ways to attach the interactions giving 720 possible diagrams, but the color factor vanishes if all quark lines go straight through. Since the interaction includes a $\lambda \cdot \lambda$ color factor, the hadrons are in a color octet state after the interaction and must exchange quarks to emerge as color singlets. Flavor conservation further reduces the number of nonzero diagrams.

For Kp scattering, for example, the s antiquark of the incident kaon must connect to the s antiquark of the outgoing kaon and the d quark in the incident proton must connect to the d quark in the outgoing proton. The u quark in the incident kaon may connect to either of the u quarks in the outgoing proton and the u quark in the outgoing kaon may connect to either of the u quarks in the incident proton, so there are 24 nonvanishing diagrams. We can use the symmetry of the momentum wave functions and the antisymmetry of the color wave functions to factor this set. ϕ_K and ϕ_N are symmetric functions of the quark momenta, so interchanging quark lines within a hadron does not change the overlap in the spatial sector. The color factor in the overlap changes sign under such an interchange but this is compensated by a sign change in the signature which comes from the anticommutation of the quark creation operators, so the signature-color sector of the overlap is also even under this operation. All diagrams that differ only through permuting quark lines within a hadron are therefore equal in all sectors of the overlap except the spin sector. There are thus four diagrams to evaluate, given in Fig. (1) (all figures are in App. E). Each diagram includes a sum over subdiagrams in the spin sector. The subdiagrams are generated by permuting quark lines inside each of the hadrons in all possible ways consistent with flavor conservation.

2.3 Scattering Amplitudes

Since the hadron states factor as in Eqs. (20) and (22), the overlap factors as well:

$$T_{fi} = \textit{signature} \cdot \textit{color} \cdot \textit{spin} \cdot \textit{flavor} \cdot \textit{space}. \quad (35)$$

Each of these factors is discussed below.

2.3.1 Signature

The signature is the overall phase in the overlap that results from the anticommutation of the quark creation operators. It is equal to $(-1)^{N_x}$, where N_x is the number of quark line crossings in a diagram. The signature is $(-1)^3 = -1$ for all four diagrams.

2.3.2 Color

The color factors are easy to evaluate with the usual meson and baryon antisymmetric combinations contained in Eqs. (20) and (22) respectively. The results are

$$\begin{aligned}
color(D_1) &= +4/9 \\
color(D_2) &= -2/9 \\
color(D_3) &= -4/9 \\
color(D_4) &= +2/9
\end{aligned} \tag{36}$$

2.3.3 Spin-flavor

Since the total spin of the KN system is $1/2$, the matrix elements of the quark spin operators can be expressed in terms of the nucleon spin identity \hat{I}^N and the nucleon spin S^N . The spin-flavor matrix elements are evaluated with the states in Eqs. (25)-(30) and the results are given below for both isospins.

$KN \quad I = 1$	D_1	D_2	D_3	D_4
$\mathbf{s}^{(1)} \cdot \mathbf{s}^{(2)}$	$+3/4$	$-1/4$	$-3/4$	$+1/4$
\hat{I}	$+1$	$+2$	$+1$	$+2$
$s^{(1)}$	$+ 2/3 S^N$	$+ 4/3 S^N$	$- 2/3 S^N$	$- 4/3 S^N$
$s^{(2)}$	$+ 2/3 S^N$	$+ 1/3 S^N$	$+ 2/3 S^N$	$+ 1/3 S^N$
$s_i^{(1)} s_j^{(2)}$	$+ \frac{1}{4} \delta_{ij} - \frac{i}{3} \epsilon_{ijk} S^N$	$- \frac{1}{12} \delta_{ij}$	$- \frac{1}{4} \delta_{ij} + \frac{i}{3} \epsilon_{ijk} S^N$	$+ \frac{1}{12} \delta_{ij}$

(37)

$KN \quad I = 0$

	D_1	D_2	D_3	D_4	
$\mathbf{s}^{(1)} \cdot \mathbf{s}^{(2)}$	0	$-3/4$	0	$+3/4$	
\hat{I}	0	0	0	0	
$s^{(1)}$	$-S^N$	$-2S^N$	$+S^N$	$+2S^N$	(38)
$s^{(2)}$	$-S^N$	$+S^N$	$-S^N$	$+S^N$	
$s_i^{(1)} s_j^{(2)}$	$+\frac{i}{2} \epsilon_{ijk} S^N$	$-\frac{1}{4} \delta_{ij}$	$-\frac{i}{2} \epsilon_{ijk} S^N$	$+\frac{1}{4} \delta_{ij}$	

Note that the Coulomb and linear interactions vanish identically in $I = 0$. It is clear that there is no tensor interaction since $S_i^N S_j^N$ is not independent of \hat{I}^N and ϵ_{ijk} for a spin-1/2 nucleon.

The K^*N system has total spin 3/2 or 1/2. The hyperfine spin, coulomb, and linear interactions are diagonal, whereas the spin-orbit and tensor interactions allow transitions between the spin states. The spin-flavor matrix elements of the quark spin operators may be expressed as follows:

$$(\mathbf{s}^{(1)} \cdot \mathbf{s}^{(2)})_{S'm';Sm} = \delta_{S'S} \delta_{m'm} (a \delta_{S\frac{3}{2}} + d \delta_{S\frac{1}{2}}) \quad (39)$$

$$(\hat{I})_{S'm';Sm} = \delta_{S'S} \delta_{m'm} (a \delta_{S\frac{3}{2}} + d \delta_{S\frac{1}{2}}) \quad (40)$$

$$\begin{aligned} (s_\mu^{(1)})_{S'm';Sm} &= a C_{\frac{3}{2}m \ 1\mu}^{\frac{3}{2}m'} \delta_{S'\frac{3}{2}} \delta_{S\frac{3}{2}} + b C_{\frac{1}{2}m \ 1\mu}^{\frac{3}{2}m'} \delta_{S'\frac{3}{2}} \delta_{S\frac{1}{2}} \\ &+ c C_{\frac{3}{2}m \ 1\mu}^{\frac{1}{2}m'} \delta_{S'\frac{1}{2}} \delta_{S\frac{3}{2}} + d C_{\frac{1}{2}m \ 1\mu}^{\frac{1}{2}m'} \delta_{S'\frac{1}{2}} \delta_{S\frac{1}{2}} \end{aligned} \quad (41)$$

$$\begin{aligned} (s_\nu^{(2)})_{S'm';Sm} &= a C_{\frac{3}{2}m \ 1\nu}^{\frac{3}{2}m'} \delta_{S'\frac{3}{2}} \delta_{S\frac{3}{2}} + b C_{\frac{1}{2}m \ 1\nu}^{\frac{3}{2}m'} \delta_{S'\frac{3}{2}} \delta_{S\frac{1}{2}} \\ &+ c C_{\frac{3}{2}m \ 1\nu}^{\frac{1}{2}m'} \delta_{S'\frac{1}{2}} \delta_{S\frac{3}{2}} + d C_{\frac{1}{2}m \ 1\nu}^{\frac{1}{2}m'} \delta_{S'\frac{1}{2}} \delta_{S\frac{1}{2}} \end{aligned} \quad (42)$$

$$(s_\mu^{(1)} s_\nu^{(2)})_{S'm';Sm} =$$

$$\begin{aligned}
& \left(a_2 C_{\frac{3}{2}m, 2m'-m}^{\frac{3}{2}m'} T_{\mu\nu}^{2m'-m} + a_1 C_{\frac{3}{2}m, 1m'-m}^{\frac{3}{2}m'} T_{\mu\nu}^{1m'-m} + a_0 \delta_{m'm} T_{\mu\nu}^{00} \right) \delta_{S'\frac{3}{2}} \delta_{S\frac{3}{2}} \\
& + \left(b_2 C_{\frac{1}{2}m, 2m'-m}^{\frac{3}{2}m'} T_{\mu\nu}^{2m'-m} + b_1 C_{\frac{1}{2}m, 1m'-m}^{\frac{3}{2}m'} T_{\mu\nu}^{1m'-m} \right) \delta_{S'\frac{3}{2}} \delta_{S\frac{1}{2}} \\
& + \left(c_2 C_{\frac{3}{2}m, 2m'-m}^{\frac{1}{2}m'} T_{\mu\nu}^{2m'-m} + c_1 C_{\frac{3}{2}m, 1m'-m}^{\frac{1}{2}m'} T_{\mu\nu}^{1m'-m} \right) \delta_{S'\frac{1}{2}} \delta_{S\frac{3}{2}} \\
& + \left(d_1 C_{\frac{1}{2}m, 1m'-m}^{\frac{1}{2}m'} T_{\mu\nu}^{1m'-m} + d_0 \delta_{m'm} T_{\mu\nu}^{00} \right) \delta_{S'\frac{1}{2}} \delta_{S\frac{1}{2}}
\end{aligned} \tag{43}$$

The $\hat{\mathbf{e}}_\mu$ are the usual spherical basis vectors

$$\begin{aligned}
\hat{\mathbf{e}}_+ &= \frac{-\hat{\mathbf{x}} - i\hat{\mathbf{y}}}{\sqrt{2}} \equiv \hat{\mathbf{p}} \\
\hat{\mathbf{e}}_0 &= \hat{\mathbf{z}} \\
\hat{\mathbf{e}}_- &= \frac{+\hat{\mathbf{x}} - i\hat{\mathbf{y}}}{\sqrt{2}} \equiv \hat{\mathbf{m}}.
\end{aligned} \tag{44}$$

The $T_{\mu\nu}^{LM}$ are the components of the spherical tensors of rank L formed by coupling the $\hat{\mathbf{e}}_\mu$:

$$\hat{T}^{LM} = \sum_{\mu\nu} (-)^{\mu+\nu} \hat{\mathbf{e}}_{-\mu} \hat{\mathbf{e}}_{-\nu} C_{1\mu, 1\nu}^{LM} \tag{45}$$

so that

$$T_{\mu\nu}^{LM} = C_{1\mu, 1\nu}^{LM}. \tag{46}$$

The spin-flavor matrix elements are evaluated using the spin-flavor states for the K^* 's

$$|K^+(+1)\rangle = \left| \begin{array}{c} u_+ \\ \bar{s}_+ \end{array} \right\rangle \tag{47}$$

$$|K^+(0)\rangle = \frac{1}{\sqrt{2}} \left(\left| \begin{array}{c} u_+ \\ \bar{s}_- \end{array} \right\rangle + \left| \begin{array}{c} u_- \\ \bar{s}_+ \end{array} \right\rangle \right) \tag{48}$$

$$|K^+(-1)\rangle = \left| \begin{array}{c} u_- \\ \bar{s}_- \end{array} \right\rangle \tag{49}$$

$$|K^0(+1)\rangle = \left| \begin{array}{c} d_+ \\ \bar{s}_+ \end{array} \right\rangle \tag{50}$$

$$|K^0(0)\rangle = \frac{1}{\sqrt{2}} \left(\left| \begin{array}{c} d_+ \\ \bar{s}_- \end{array} \right\rangle + \left| \begin{array}{c} d_- \\ \bar{s}_+ \end{array} \right\rangle \right) \tag{51}$$

$$|K^0(-1)\rangle = \left| \frac{d_-}{\bar{s}_-} \right\rangle. \quad (52)$$

The coefficients of the quark spin operator expansions are given below for all four line diagrams and both isospins.

$K^*N \quad I = 1 \text{ (prior)}$

	D_1	D_2	D_3	D_4
$(\mathbf{s}^{(1)} \cdot \mathbf{s}^{(2)})$	$\begin{cases} a = 7/12 \\ d = 13/12 \end{cases}$	$\begin{cases} -1/6 \\ -5/12 \end{cases}$	$\begin{cases} 5/12 \\ -1/12 \end{cases}$	$\begin{cases} 0 \\ -1/4 \end{cases}$
(\hat{I})	$\begin{cases} a = 5/3 \\ d = -1/3 \end{cases}$	$\begin{cases} 10/3 \\ -2/3 \end{cases}$	$\begin{cases} 5/3 \\ -1/3 \end{cases}$	$\begin{cases} 10/3 \\ -2/3 \end{cases}$
$(\mathbf{s}_\mu^{(1)})$	$\begin{cases} a = 5\sqrt{15}/18 \\ b = -7\sqrt{3}/18 \\ c = -5\sqrt{6}/18 \\ d = 2\sqrt{3}/9 \end{cases}$	$\begin{cases} 5\sqrt{15}/9 \\ -7\sqrt{3}/9 \\ -5\sqrt{6}/9 \\ 4\sqrt{3}/9 \end{cases}$	$\begin{cases} 5\sqrt{15}/18 \\ 5\sqrt{3}/18 \\ -5\sqrt{6}/18 \\ -4\sqrt{3}/9 \end{cases}$	$\begin{cases} 5\sqrt{15}/9 \\ 5\sqrt{3}/9 \\ -5\sqrt{6}/9 \\ -8\sqrt{3}/9 \end{cases}$
$(\mathbf{s}_\nu^{(2)})$	$\begin{cases} a = 5\sqrt{15}/18 \\ b = 5\sqrt{3}/18 \\ c = 7\sqrt{6}/18 \\ d = 2\sqrt{3}/9 \end{cases}$	$\begin{cases} 0 \\ -\sqrt{3}/6 \\ \sqrt{6}/6 \\ -\sqrt{3}/6 \end{cases}$	$\begin{cases} 5\sqrt{15}/18 \\ 5\sqrt{3}/18 \\ 7\sqrt{6}/18 \\ 2\sqrt{3}/9 \end{cases}$	$\begin{cases} 0 \\ -\sqrt{3}/6 \\ \sqrt{6}/6 \\ -\sqrt{3}/6 \end{cases}$
$(\mathbf{s}_\mu^{(1)} \mathbf{s}_\nu^{(2)})$	$\begin{cases} a_2 = \sqrt{30}/9 \\ a_1 = -\sqrt{30}/36 \\ a_0 = -7\sqrt{3}/36 \\ b_2 = -\sqrt{30}/18 \\ b_1 = -7\sqrt{6}/36 \\ c_2 = \sqrt{15}/9 \\ c_1 = 7\sqrt{3}/18 \\ d_1 = -2\sqrt{6}/9 \\ d_0 = -13\sqrt{3}/36 \end{cases}$	$\begin{cases} \sqrt{30}/36 \\ \sqrt{30}/36 \\ \sqrt{3}/18 \\ -\sqrt{30}/72 \\ 5\sqrt{6}/72 \\ \sqrt{15}/36 \\ \sqrt{3}/36 \\ \sqrt{6}/18 \\ 5\sqrt{3}/36 \end{cases}$	$\begin{cases} 5\sqrt{30}/36 \\ 0 \\ -5\sqrt{3}/36 \\ 5\sqrt{30}/36 \\ 0 \\ \sqrt{15}/18 \\ \sqrt{3}/3 \\ \sqrt{6}/6 \\ \sqrt{3}/36 \end{cases}$	$\begin{cases} 0 \\ 0 \\ 0 \\ -\sqrt{30}/24 \\ \sqrt{6}/24 \\ \sqrt{15}/12 \\ \sqrt{3}/12 \\ 0 \\ \sqrt{3}/12 \end{cases}$

(53)

$K^*N \quad I = 0 \text{ (prior)}$

$$\begin{array}{l}
\begin{array}{c} (s^{(1)} \cdot s^{(2)}) \\ (\hat{I}) \\ (s_\mu^{(1)}) \\ (s_\nu^{(2)}) \\ (s_\mu^{(1)} s_\nu^{(2)}) \end{array} \begin{cases} \begin{array}{l} a = \\ d = \end{array} \\ \begin{array}{l} a = \\ d = \end{array} \\ \begin{array}{l} a = \\ b = \\ c = \\ d = \end{array} \\ \begin{array}{l} a = \\ b = \\ c = \\ d = \end{array} \\ \begin{array}{l} a_2 = \\ a_1 = \\ a_0 = \\ b_2 = \\ b_1 = \\ c_2 = \\ c_1 = \\ d_1 = \\ d_0 = \end{array} \end{cases} \begin{array}{ccccc} D_1 & D_2 & D_3 & D_4 & \\ \begin{array}{c} 1/4 \\ -1/2 \end{array} & \begin{array}{c} -1/2 \\ -5/4 \end{array} & \begin{array}{c} -1/4 \\ 1/2 \end{array} & \begin{array}{c} 0 \\ -3/4 \end{array} & \\ \begin{array}{c} -1 \\ 2 \end{array} & \begin{array}{c} -2 \\ 4 \end{array} & \begin{array}{c} -1 \\ 2 \end{array} & \begin{array}{c} -2 \\ 4 \end{array} & \\ \begin{array}{c} -\sqrt{15}/6 \\ 5\sqrt{3}/6 \\ \sqrt{6}/6 \\ \sqrt{3}/6 \end{array} & \begin{array}{c} -\sqrt{15}/3 \\ 5\sqrt{3}/3 \\ \sqrt{6}/3 \\ \sqrt{3}/3 \end{array} & \begin{array}{c} -\sqrt{15}/6 \\ -\sqrt{3}/6 \\ \sqrt{6}/6 \\ 7\sqrt{3}/6 \end{array} & \begin{array}{c} -\sqrt{15}/3 \\ -\sqrt{3}/3 \\ \sqrt{6}/3 \\ 7\sqrt{3}/3 \end{array} & \\ \begin{array}{c} -\sqrt{15}/6 \\ -\sqrt{3}/6 \\ -5\sqrt{6}/6 \\ \sqrt{3}/6 \end{array} & \begin{array}{c} 0 \\ -\sqrt{3}/2 \\ \sqrt{6}/2 \\ -\sqrt{3}/2 \end{array} & \begin{array}{c} -\sqrt{15}/6 \\ -\sqrt{3}/6 \\ -5\sqrt{6}/6 \\ \sqrt{3}/6 \end{array} & \begin{array}{c} 0 \\ -\sqrt{3}/2 \\ \sqrt{6}/2 \\ -\sqrt{3}/2 \end{array} & \\ \begin{array}{c} -\sqrt{30}/6 \\ -\sqrt{30}/12 \\ -\sqrt{3}/12 \\ \sqrt{30}/12 \\ \sqrt{6}/6 \\ -\sqrt{15}/6 \\ -\sqrt{3}/3 \\ \sqrt{6}/12 \\ \sqrt{3}/6 \end{array} & \begin{array}{c} \sqrt{30}/12 \\ \sqrt{30}/12 \\ \sqrt{3}/6 \\ -\sqrt{30}/24 \\ 5\sqrt{6}/24 \\ \sqrt{15}/12 \\ \sqrt{3}/12 \\ \sqrt{6}/6 \\ 5\sqrt{3}/12 \end{array} & \begin{array}{c} -\sqrt{30}/12 \\ 0 \\ \sqrt{3}/12 \\ -\sqrt{30}/12 \\ 0 \\ -\sqrt{15}/3 \\ -\sqrt{3}/2 \\ -\sqrt{6}/4 \\ -\sqrt{3}/6 \end{array} & \begin{array}{c} 0 \\ 0 \\ 0 \\ -\sqrt{30}/8 \\ \sqrt{6}/8 \\ \sqrt{15}/4 \\ \sqrt{3}/4 \\ 0 \\ \sqrt{3}/4 \end{array} & \end{array} \quad (54)
\end{array}$$

The coefficients for the *post* case are related to those of the *prior* case when the outgoing particles are the same as the incoming particles. The matrix element of a quark spin operator implicitly contains the quark interchange operator \mathcal{P} . We may write the matrix element for a quark spin operator O^{quark} in the *prior* and *post* cases with \mathcal{P} made explicit as follows:

$$(O^{quark})_{S'm';Sm}^{prior} = \langle (K^*N)_{S'm'} | O^{quark} \mathcal{P} | (K^*N)_{Sm} \rangle \quad (55)$$

$$(O^{quark})_{S'm';Sm}^{post} = \langle (K^*N)_{S'm'} | \mathcal{P} O^{quark} | (K^*N)_{Sm} \rangle \quad (56)$$

\mathcal{P} is Hermitian, so

$$(O^{quark})_{S'm';Sm}^{post} = \langle (K^*N)_{Sm} | O^{quark\dagger} \mathcal{P} | (K^*N)_{S'm'} \rangle = (O^{quark\dagger})_{Sm;S'm'}^{prior} \quad (57)$$

The hyperfine and confinement quark operators are Hermitian: $(\mathbf{s}^{(1)} \cdot \mathbf{s}^{(2)})^\dagger = \mathbf{s}^{(1)} \cdot \mathbf{s}^{(2)}$ and $\hat{I}^\dagger = \hat{I}$, and $\delta_{S'S} \delta_{m'm} = \delta_{SS'} \delta_{mm'}$ in Eqs. (39) and (40) so the *post* form is the same as the *prior* form for these operators. A component of the quark spin operator appearing in the spin-orbit interactions is not by itself Hermitian: $(S_\mu^{(1)})^\dagger = (-)^\mu S_{-\mu}^{(1)}$. Using this relation and the symmetry properties of the CG coefficients

$$\begin{aligned} C_{S'm' \ 1-\mu}^{Sm} &= (-)^{1-\mu} \sqrt{\frac{2S+1}{2S'+1}} C_{S-m \ 1-\mu}^{S'-m'} \\ &= (-)^{1-\mu} \sqrt{\frac{2S+1}{2S'+1}} (-)^{S+1-S'} C_{Sm \ 1\mu}^{S'm'} \end{aligned} \quad (58)$$

in Eqs. (41) and (42) we find the relations between the *post* and *prior* coefficients a, b, c , and d . The coefficients in the expansion of $(s_\mu^{(1)} s_\nu^{(2)})_{S'm';Sm}$ may similarly be determined for the *post* case. The relations are given below for all five quark spin operators and have been checked by explicit calculation of the *post* operator matrix elements.

$$\begin{aligned}
(\mathbf{s}^{(1)} \cdot \mathbf{s}^{(2)}) & \left\{ \begin{array}{l} a^{post} = a^{prior} \\ d^{post} = d^{prior} \end{array} \right. \\
(\hat{I}) & \left\{ \begin{array}{l} a^{post} = a^{prior} \\ d^{post} = d^{prior} \end{array} \right. \\
(\mathbf{s}_\mu^{(1)}) & \left\{ \begin{array}{l} a^{post} = a^{prior} \\ b^{post} = -c^{prior}/\sqrt{2} \\ c^{post} = -\sqrt{2} b^{prior} \\ d^{post} = d^{prior} \end{array} \right. \\
(\mathbf{s}_\nu^{(2)}) & \left\{ \begin{array}{l} a^{post} = a^{prior} \\ b^{post} = -c^{prior}/\sqrt{2} \\ c^{post} = -\sqrt{2} b^{prior} \\ d^{post} = d^{prior} \end{array} \right. \\
(\mathbf{s}_\mu^{(1)} \mathbf{s}_\nu^{(2)}) & \left\{ \begin{array}{l} a_2^{post} = a_2^{prior} \\ a_1^{post} = -a_1^{prior} \\ a_0^{post} = a_0^{prior} \\ b_2^{post} = -c_2^{prior}/\sqrt{2} \\ b_1^{post} = c_1^{prior}/\sqrt{2} \\ c_2^{post} = -\sqrt{2} b_2^{prior} \\ c_1^{post} = \sqrt{2} b_1^{prior} \\ d_1^{post} = -d_1^{prior} \\ d_0^{post} = d_0^{prior} \end{array} \right.
\end{aligned} \tag{59}$$

2.3.4 Space

The space factor T_{space} is obtained by integrating the hadron wave functions $\phi_{A,B,C,D}$ and the quark T_{fi} (10) over all quark momenta. Delta functions are included to enforce momentum conservation along the spectator lines and within the hadrons. With A, B, C , and D the external hadron momenta, we have

$$T_{space}^{D_1} = \int \dots d^3 a \, d^3 \bar{a} \, d^3 b_1 \, d^3 b_2 \, d^3 b_3 \, d^3 c \, d^3 \bar{c} \, d^3 d_1 \, d^3 d_2 \, d^3 d_3$$

$$\begin{aligned}
& \phi_A(a - \bar{a}) \phi_B(b_1, b_2, b_3) \phi_C(c - \bar{c}) \phi_D(d_1, d_2, d_3) T_{fi}^{qq} \left(d_1 - a, \frac{a + d_1}{2}, \frac{b_1 + c}{2} \right) \\
& \delta(\bar{a} - \bar{c}) \delta(b_2 - d_2) \delta(b_3 - d_3) \\
& \delta(A - a - \bar{a}) \delta(B - b_1 - b_2 - b_3) \delta(C - c - \bar{c}) \delta(D - d_1 - d_2 - d_3) \quad (60)
\end{aligned}$$

$$\begin{aligned}
T_{space}^{D_2} = & \int \dots d^3 a \, d^3 \bar{a} \, d^3 b_1 \, d^3 b_2 \, d^3 b_3 \, d^3 c \, d^3 \bar{c} \, d^3 d_1 \, d^3 d_2 \, d^3 d_3 \\
& \phi_A(a - \bar{a}) \phi_B(b_1, b_2, b_3) \phi_C(c - \bar{c}) \phi_D(d_1, d_2, d_3) T_{fi}^{qq} \left(d_1 - a, \frac{a + d_1}{2}, \frac{b_2 + d_2}{2} \right) \\
& \delta(\bar{a} - \bar{c}) \delta(b_1 - c) \delta(b_3 - d_3) \\
& \delta(A - a - \bar{a}) \delta(B - b_1 - b_2 - b_3) \delta(C - c - \bar{c}) \delta(D - d_1 - d_2 - d_3) \quad (61)
\end{aligned}$$

$$\begin{aligned}
T_{space}^{D_3} = & \int \dots d^3 a \, d^3 \bar{a} \, d^3 b_1 \, d^3 b_2 \, d^3 b_3 \, d^3 c \, d^3 \bar{c} \, d^3 d_1 \, d^3 d_2 \, d^3 d_3 \\
& \phi_A(a - \bar{a}) \phi_B(b_1, b_2, b_3) \phi_C(c - \bar{c}) \phi_D(d_1, d_2, d_3) T_{fi}^{qq} \left(\bar{c} - \bar{a}, \frac{\bar{a} + \bar{c}}{2}, \frac{b_1 + c}{2} \right) \\
& \delta(a - d_1) \delta(b_2 - d_2) \delta(b_3 - d_3) \\
& \delta(A - a - \bar{a}) \delta(B - b_1 - b_2 - b_3) \delta(C - c - \bar{c}) \delta(D - d_1 - d_2 - d_3) \quad (62)
\end{aligned}$$

$$\begin{aligned}
T_{space}^{D_4} = & \int \dots d^3 a \, d^3 \bar{a} \, d^3 b_1 \, d^3 b_2 \, d^3 b_3 \, d^3 c \, d^3 \bar{c} \, d^3 d_1 \, d^3 d_2 \, d^3 d_3 \\
& \phi_A(a - \bar{a}) \phi_B(b_1, b_2, b_3) \phi_C(c - \bar{c}) \phi_D(d_1, d_2, d_3) T_{fi}^{qq} \left(\bar{c} - \bar{a}, \frac{\bar{a} + \bar{c}}{2}, \frac{b_2 + d_2}{2} \right) \\
& \delta(a - d_1) \delta(b_1 - c) \delta(b_3 - d_3) \\
& \delta(A - a - \bar{a}) \delta(B - b_1 - b_2 - b_3) \delta(C - c - \bar{c}) \delta(D - d_1 - d_2 - d_3) \quad (63)
\end{aligned}$$

Integrating over the delta functions we can eliminate all but two integration variables, and a suitable choice allows us to write $T_{space}^{D_1}$ in the convenient

form of shifted gaussians times T_{fi}^{qq} after inserting the oscillator forms (31) and (33) for the hadron wave functions. Diagram 3 can likewise be reduced to an integral over two momenta, but in diagrams 2 and 4 the variables appearing in the quark T_{fi}^{qq} are all independent and we have three momenta to integrate over. Defining $\rho = m_{u,d}/m_s$ and setting $\alpha = \beta$ as a first approximation, the reduced forms are

$$\begin{aligned}
T_{space}^{D_1} &= \frac{3^{3/2}}{2^{3/2}\pi^3\beta^6} \exp \left\{ -\frac{(2\rho^2 + 4\rho + 5)}{12\beta^2(\rho + 1)^2} (\mathbf{A} - \mathbf{C})^2 \right\} \\
&\quad \int d^3q \int d^3P \exp \left\{ -\frac{5}{2\beta^2} (\mathbf{P} - \mathbf{P}_0)^2 \right\} \exp \left\{ -\frac{3}{5\beta^2} (\mathbf{q} - \mathbf{q}_0)^2 \right\} \\
&\quad T_{fi}^{qq}(\mathbf{q}, \mathbf{P}, \mathbf{P} + \mathbf{C} - \mathbf{A}) \\
\mathbf{P}_0 &= -\frac{1}{10(\rho + 1)} [(4\rho + 6)\mathbf{C} - (6\rho + 4)\mathbf{A} + (\rho + 1)\mathbf{q}] \\
\mathbf{q}_0 &= -\frac{1}{6(\rho + 1)} [(4\rho + 1)(\mathbf{C} + \mathbf{A})]
\end{aligned} \tag{64}$$

$$\begin{aligned}
T_{space}^{D_2} &= \frac{3^{3/2}}{\pi^{9/2}\beta^9} \\
&\quad \exp \left\{ -\frac{[(19\rho^2 + 8\rho + 46)A^2 + (67\rho^2 + 68\rho + 58)C^2 + (42\rho^2 - 12\rho - 96)\mathbf{A} \cdot \mathbf{C}]}{156\beta^2(\rho + 1)^2} \right\} \\
&\quad \int d^3q \int d^3P \int d^3P' \exp \left\{ -\frac{2}{\beta^2} (\mathbf{P}' - \mathbf{P}'_0)^2 \right\} \exp \left\{ -\frac{5}{2\beta^2} (\mathbf{P} - \mathbf{P}_0)^2 \right\} \\
&\quad \exp \left\{ -\frac{13}{20\beta^2} (\mathbf{q} - \mathbf{q}_0)^2 \right\} T_{fi}^{qq}(\mathbf{q}, \mathbf{P}, \mathbf{P}') \\
\mathbf{P}'_0 &= -\frac{1}{2} (\mathbf{C} + \mathbf{P}) \\
\mathbf{P}_0 &= -\frac{1}{5(\rho + 1)} [(2\rho + 3)\mathbf{C} - (3\rho + 2)\mathbf{A} - (\rho + 1)\mathbf{q}] \\
\mathbf{q}_0 &= \frac{1}{13(\rho + 1)} [(\rho + 4)\mathbf{C} - 3(3\rho + 2)\mathbf{A}]
\end{aligned} \tag{65}$$

$$T_{space}^{D_3} = \frac{3^{3/2}}{2^{3/2}\pi^3\beta^6}$$

$$\begin{aligned}
& \exp \left\{ - \frac{[(8\rho^2 + 4\rho + 5)A^2 + (8\rho^2 + 16\rho + 8)C^2 - 12(\rho + 1)\mathbf{A} \cdot \mathbf{C}]}{24 \beta^2 (\rho + 1)^2} \right\} \\
& \int d^3 q \int d^3 P \exp \left\{ - \frac{5}{2\beta^2} (\mathbf{P} - \mathbf{P}_0)^2 \right\} \exp \left\{ - \frac{2}{5\beta^2} (\mathbf{q} - \mathbf{q}_0)^2 \right\} \\
& T_{fi}^{qq}(\mathbf{q}, \mathbf{P}, \mathbf{C} - \mathbf{P}) \\
& \mathbf{P}_0 = \frac{1}{10(\rho + 1)} [(4\rho + 6)(\mathbf{C} + \mathbf{A}) + 3(\rho + 1)\mathbf{q}] \\
& \mathbf{q}_0 = -\frac{1}{4(\rho + 1)} [(2\rho - 2)\mathbf{C} + (2\rho + 3)\mathbf{A}]
\end{aligned} \tag{66}$$

$$\begin{aligned}
T_{space}^{D_4} &= \frac{3^{3/2}}{\pi^{9/2} \beta^9} \\
& \exp \left\{ - \frac{[(21\rho^2 + 8\rho + 6)(A^2 + C^2) + (22\rho^2 + 16\rho - 8)\mathbf{A} \cdot \mathbf{C}]}{60 \beta^2 (\rho + 1)^2} \right\} \\
& \int d^3 q \int d^3 P \int d^3 P' \exp \left\{ - \frac{2}{\beta^2} (\mathbf{P}' - \mathbf{P}'_0)^2 \right\} \exp \left\{ - \frac{5}{2\beta^2} (\mathbf{P} - \mathbf{P}_0)^2 \right\} \\
& \exp \left\{ - \frac{3}{4\beta^2} (\mathbf{q} - \mathbf{q}_0)^2 \right\} T_{fi}^{qq}(\mathbf{q}, \mathbf{P}, \mathbf{P}') \\
& \mathbf{P}'_0 = \frac{1}{2} (\mathbf{P} - \mathbf{C} - \mathbf{A}) \\
& \mathbf{P}_0 = \frac{2\rho + 3}{5(\rho + 1)} (\mathbf{C} + \mathbf{A}) \\
& \mathbf{q}_0 = \frac{\rho + 2}{13(\rho + 1)} (\mathbf{C} - \mathbf{A})
\end{aligned} \tag{67}$$

Useful integrals over shifted Gaussians have been worked out and are collected in App. B. The final integrations can be done with our specific T_{fi}^{qq} 's (Eq. (10)) inserted, giving analytical expressions for the scattering amplitudes. In the following, $f_{a,c}(x) = {}_1F_1(a, c; x)$ is the confluent hypergeometric function.

2.3.5 Spin-spin

$$T_{space}^{(D1)}(\vec{S} \cdot \vec{S}) = - \frac{2^3 \pi \alpha_s}{3m^2} \exp \left\{ - \frac{(2\rho^2 + 4\rho + 5)(\vec{C} - \vec{A})^2}{12(\rho + 1)^2} \right\} \tag{68}$$

$$T_{space}^{(D2)}(\vec{S} \cdot \vec{S}) = - \frac{2^6 3^{1/2} \pi \alpha_s}{13^{3/2} m^2} \exp \left\{ - \frac{[(43\rho^2 + 38\rho + 52)A^2 + 3(7\rho^2 - 2\rho - 16)\vec{A} \cdot \vec{C}]}{78(\rho + 1)^2} \right\} \quad (69)$$

$$T_{space}^{(D3)}(\vec{S} \cdot \vec{S}) = - \frac{2^{3/2} 3^{1/2} \pi \alpha_s \rho}{m^2} \exp \left\{ - \frac{[(16\rho^2 + 20\rho + 13)A^2 - 12(\rho + 1)\vec{A} \cdot \vec{C}]}{24(\rho + 1)^2} \right\} \quad (70)$$

$$T_{space}^{(D4)}(\vec{S} \cdot \vec{S}) = - \frac{2^6 \pi \alpha_s \rho}{3 \cdot 5^{3/2} m^2} \exp \left\{ - \frac{[(21\rho^2 + 8\rho + 6)A^2 + (11\rho^2 + 8\rho - 4)\vec{A} \cdot \vec{C}]}{30(\rho + 1)^2} \right\} \quad (71)$$

2.3.6 Coulomb

$$T_{space}^{(D1)}(\text{coul}) = + \frac{2^3 3 \pi \alpha_s}{5} f_{1/2,3/2} \left(\frac{(4\rho + 1)^2}{60(\rho + 1)^2} (\vec{C} + \vec{A})^2 \right) \exp \left\{ - \frac{[(13\rho^2 + 14\rho + 13)A^2 + 3(\rho^2 - 2\rho - 4)\vec{A} \cdot \vec{C}]}{15(\rho + 1)^2} \right\} \quad (72)$$

$$T_{space}^{(D2)}(\text{coul}) = + \frac{2^4 3^{3/2} \pi \alpha_s}{5 \cdot 13^{1/2}} f_{1/2,3/2} \left(\frac{[2(41\rho^2 + 58\rho + 26)A^2 - 3(3\rho^2 + 14\rho + 8)\vec{A} \cdot \vec{C}]}{130(\rho + 1)^2} \right) \exp \left\{ - \frac{[(13\rho^2 + 14\rho + 13)A^2 + 3(\rho^2 - 2\rho - 4)\vec{A} \cdot \vec{C}]}{15(\rho + 1)^2} \right\} \quad (73)$$

$$\begin{aligned}
T_{space}^{(D3)}(\text{coul}) &= + \frac{2^{5/2}3^{3/2}\pi\alpha_s}{5} \\
&f_{1/2,3/2} \left(\frac{[(8\rho^2 + 4\rho + 13)A^2 + 4(2\rho^2 + \rho - 3)\vec{A} \cdot \vec{C}]}{40(\rho + 1)^2} \right) \\
&\exp \left\{ - \frac{[(13\rho^2 + 14\rho + 13)A^2 + 3(\rho^2 - 2\rho - 4)\vec{A} \cdot \vec{C}]}{15(\rho + 1)^2} \right\} \quad (74)
\end{aligned}$$

$$\begin{aligned}
T_{space}^{(D4)}(\text{coul}) &= + \frac{2^4 3 \pi \alpha_s}{5^{3/2}} \\
&f_{1/2,3/2} \left(\frac{(\rho + 2)^2}{12(\rho + 1)^2} (\vec{C} - \vec{A})^2 \right) \\
&\exp \left\{ - \frac{[(13\rho^2 + 14\rho + 13)A^2 + 3(\rho^2 - 2\rho - 4)\vec{A} \cdot \vec{C}]}{15(\rho + 1)^2} \right\} \quad (75)
\end{aligned}$$

2.3.7 Linear Confinement

$$\begin{aligned}
T_{space}^{(D1)}(\text{lin}) &= - \frac{2^3 3^3 \pi b}{5^2} \\
&f_{-1/2,3/2} \left(\frac{(4\rho + 1)^2}{60(\rho + 1)^2} (\vec{C} + \vec{A})^2 \right) \\
&\exp \left\{ - \frac{[(13\rho^2 + 14\rho + 13)A^2 + 3(\rho^2 - 2\rho - 4)\vec{A} \cdot \vec{C}]}{15(\rho + 1)^2} \right\} \quad (76)
\end{aligned}$$

$$\begin{aligned}
T_{space}^{(D2)}(\text{lin}) &= - \frac{2^2 3^{5/2} 13^{1/2} \pi b}{5^2} \\
&f_{-1/2,3/2} \left(\frac{[2(41\rho^2 + 58\rho + 26)A^2 - 3(3\rho^2 + 14\rho + 8)\vec{A} \cdot \vec{C}]}{130(\rho + 1)^2} \right) \\
&\exp \left\{ - \frac{[(13\rho^2 + 14\rho + 13)A^2 + 3(\rho^2 - 2\rho - 4)\vec{A} \cdot \vec{C}]}{15(\rho + 1)^2} \right\} \quad (77)
\end{aligned}$$

$$T_{space}^{(D3)}(\text{lin}) = - \frac{2^{7/2} 3^{5/2} \pi b}{5^2}$$

$$\begin{aligned}
& f_{-1/2,3/2} \left(\frac{[(8\rho^2 + 4\rho + 13)A^2 + 4(2\rho^2 + \rho - 3)\vec{A} \cdot \vec{C}]}{40(\rho + 1)^2} \right) \\
& \exp \left\{ - \frac{[(13\rho^2 + 14\rho + 13)A^2 + 3(\rho^2 - 2\rho - 4)\vec{A} \cdot \vec{C}]}{15(\rho + 1)^2} \right\} \quad (78)
\end{aligned}$$

$$\begin{aligned}
T_{space}^{(D4)}(\text{lin}) &= - \frac{2^2 3^3 \pi b}{5^{3/2}} \\
& f_{-1/2,3/2} \left(\frac{(\rho + 2)^2}{12(\rho + 1)^2} (\vec{C} - \vec{A})^2 \right) \\
& \exp \left\{ - \frac{[(13\rho^2 + 14\rho + 13)A^2 + 3(\rho^2 - 2\rho - 4)\vec{A} \cdot \vec{C}]}{15(\rho + 1)^2} \right\} \quad (79)
\end{aligned}$$

2.3.8 OGE Spin-orbit

$$\begin{aligned}
T_{space}^{(D1)}(\text{OGE } \vec{L} \cdot \vec{S}) &= - \frac{2}{5} \frac{i\pi\alpha_s}{m^2} \frac{(4\rho + 1)}{(\rho + 1)} (\vec{s}_1 + \vec{s}_2) \cdot \vec{C} \times \vec{A} \\
& f_{3/2,5/2} \left(\frac{(4\rho + 1)^2}{60(\rho + 1)^2} (\vec{C} + \vec{A})^2 \right) \\
& \exp \left\{ - \frac{[(13\rho^2 + 14\rho + 13)A^2 + 3(\rho^2 - 2\rho - 4)\vec{A} \cdot \vec{C}]}{15(\rho + 1)^2} \right\} \quad (80)
\end{aligned}$$

$$\begin{aligned}
T_{space}^{(D2)}(\text{OGE } \vec{L} \cdot \vec{S}) &= + \frac{2^3 3^{1/2}}{5 \cdot 13^{3/2}} \frac{i\pi\alpha_s}{m^2} \frac{(3\rho + 2)}{(\rho + 1)} (\vec{s}_1 - \vec{s}_2) \cdot \vec{C} \times \vec{A} \\
& f_{3/2,5/2} \left(\frac{[2(41\rho^2 + 58\rho + 26)A^2 - 3(3\rho^2 + 14\rho + 8)\vec{A} \cdot \vec{C}]}{130(\rho + 1)^2} \right) \\
& \exp \left\{ - \frac{[(13\rho^2 + 14\rho + 13)A^2 + 3(\rho^2 - 2\rho - 4)\vec{A} \cdot \vec{C}]}{15(\rho + 1)^2} \right\} \quad (81)
\end{aligned}$$

$$T_{space}^{(D3)}(\text{OGE } \vec{L} \cdot \vec{S}) = - \frac{3^{1/2}}{2^{1/2} 5} \frac{i\pi\alpha_s}{m^2} \frac{\rho(2\rho + 3)}{(\rho + 1)^2} (\rho\vec{s}_1 - \vec{s}_2) \cdot \vec{C} \times \vec{A}$$

$$f_{3/2,5/2} \left(\frac{[(8\rho^2 + 4\rho + 13)A^2 + 4(2\rho^2 + \rho - 3)\vec{A} \cdot \vec{C}]}{40(\rho + 1)^2} \right) \\ \exp \left\{ - \frac{[(13\rho^2 + 14\rho + 13)A^2 + 3(\rho^2 - 2\rho - 4)\vec{A} \cdot \vec{C}]}{15(\rho + 1)^2} \right\} \quad (82)$$

$$T_{space}^{(D4)}(\text{OGE } \vec{L} \cdot \vec{S}) = + \frac{2^3}{3 \cdot 5^{5/2}} \frac{i\pi\alpha_s}{m^2} \frac{(\rho + 2)}{(\rho + 1)^2} \\ [4\rho(\rho^2 + 3\rho + 1)\vec{s}_1 + (8\rho^2 + 15\rho + 2)\vec{s}_2] \cdot \vec{C} \times \vec{A} \\ f_{3/2,5/2} \left(\frac{(\rho + 2)^2}{12(\rho + 1)^2} (\vec{C} - \vec{A})^2 \right) \\ \exp \left\{ - \frac{[(13\rho^2 + 14\rho + 13)A^2 + 3(\rho^2 - 2\rho - 4)\vec{A} \cdot \vec{C}]}{15(\rho + 1)^2} \right\} \quad (83)$$

2.3.9 Scalar Confinement Spin-orbit

$$T_{space}^{(D1)}(\text{lin } \vec{L} \cdot \vec{S}) = + \frac{2 \cdot 3}{5^2} \frac{i\pi b}{m^2} \frac{(4\rho + 1)}{(\rho + 1)} (\vec{s}_1 + \vec{s}_2) \cdot \vec{C} \times \vec{A} \\ f_{1/2,5/2} \left(\frac{(4\rho + 1)^2}{60(\rho + 1)^2} (\vec{C} + \vec{A})^2 \right) \\ \exp \left\{ - \frac{[(13\rho^2 + 14\rho + 13)A^2 + 3(\rho^2 - 2\rho - 4)\vec{A} \cdot \vec{C}]}{15(\rho + 1)^2} \right\} \quad (84)$$

$$T_{space}^{(D2)}(\text{lin } \vec{L} \cdot \vec{S}) = + \frac{2 \cdot 3^{3/2}}{5^2 13^{1/2}} \frac{i\pi b}{m^2} \frac{(3\rho + 2)}{(\rho + 1)} (\vec{s}_1 - \vec{s}_2) \cdot \vec{C} \times \vec{A} \\ f_{1/2,5/2} \left(\frac{[2(41\rho^2 + 58\rho + 26)A^2 - 3(3\rho^2 + 14\rho + 8)\vec{A} \cdot \vec{C}]}{130(\rho + 1)^2} \right) \\ \exp \left\{ - \frac{[(13\rho^2 + 14\rho + 13)A^2 + 3(\rho^2 - 2\rho - 4)\vec{A} \cdot \vec{C}]}{15(\rho + 1)^2} \right\} \quad (85)$$

$$T_{space}^{(D3)}(\text{lin } \vec{L} \cdot \vec{S}) = - \frac{2^{1/2} 3^{3/2}}{5^2} \frac{i\pi b}{m^2} \frac{\rho(2\rho + 3)}{(\rho + 1)^2} (\rho\vec{s}_1 - \vec{s}_2) \cdot \vec{C} \times \vec{A}$$

$$f_{1/2,5/2} \left(\frac{[(8\rho^2 + 4\rho + 13)A^2 + 4(2\rho^2 + \rho - 3)\vec{A} \cdot \vec{C}]}{40(\rho + 1)^2} \right) \\ \exp \left\{ - \frac{[(13\rho^2 + 14\rho + 13)A^2 + 3(\rho^2 - 2\rho - 4)\vec{A} \cdot \vec{C}]}{15(\rho + 1)^2} \right\} \quad (86)$$

$$T_{space}^{(D^4)}(\text{lin } \vec{L} \cdot \vec{S}) = - \frac{2 \cdot 3}{5^{5/2}} \frac{i\pi b}{m^2} \frac{(\rho + 2)}{(\rho + 1)^2} \\ [2\rho^2(2\rho + 3)\vec{s}_1 + (3\rho + 2)\vec{s}_2] \cdot \vec{C} \times \vec{A} \\ f_{1/2,5/2} \left(\frac{(\rho + 2)^2}{12(\rho + 1)^2} (\vec{C} - \vec{A})^2 \right) \\ \exp \left\{ - \frac{[(13\rho^2 + 14\rho + 13)A^2 + 3(\rho^2 - 2\rho - 4)\vec{A} \cdot \vec{C}]}{15(\rho + 1)^2} \right\} \quad (87)$$

2.4 K^*N Phase Shifts

The phase shifts can be computed from the T-matrix

$$T_{S',\lambda';S,\lambda}(\Omega', \Omega) = \langle (AB)_{S'\lambda'} | T_{fi}^{qq} | (CD)_{S\lambda} \rangle. \quad (88)$$

Ω and Ω' are the directions of the incident and scattered mesons in the CM frame: $\mathbf{A} = \mathbf{A}(\Omega')$ and $\mathbf{C} = \mathbf{C}(\Omega)$. The elastic scattering phase shift is

$$\delta_{JLS} = - \frac{1}{8\pi^2} \frac{|\mathbf{A}| E_A E_B}{\sqrt{s}} T_{JLS} \quad (89)$$

T_{JLS} is just the diagonal part of the T-matrix $T_{L'L;S'S}^J$. The off-diagonal matrix elements give the inelasticities

$$\epsilon_{L'L;S'S}^J = - \frac{1}{4\pi^2} \frac{|\mathbf{A}| E_A E_B}{\sqrt{s}} T_{L'L;S'S}^J. \quad (90)$$

We get $T_{L'L;S'S}^J$ by coupling the initial and final states to total angular momentum J :

$$T_{L'L;S'S}^{JM_J} = \sum_{M'\lambda'} C_{L'M' S'\lambda'}^{JM_J} \sum_{M\lambda} C_{LM S\lambda}^{JM_J} T_{L'M'S'\lambda';LMS\lambda} \quad (91)$$

where

$$T_{L'M'S'\lambda';LMS\lambda} = \iint d\Omega' d\Omega Y_{L'M'}^*(\Omega') Y_{LM}(\Omega) T_{S'\lambda';S,\lambda}(\Omega', \Omega). \quad (92)$$

We omit the index M_J and write $T_{L'L;S'S}^J$ since $T_{L'L;S'S}^{JM_J}$ is independent of M_J . We must compute $T_{L'L;S'S}^J$ from $T_{L'M'S'\lambda';LMS\lambda}$ for each type of interaction.

2.4.1 Spin-spin Hyperfine, Coulomb, and Linear Interactions

The hyperfine, Coulomb, and linear T-matrices are diagonal in the total spin and have the general form

$$T_{S'\lambda';S,\lambda}(\Omega', \Omega) = f(\mu) \delta_{S'S} \delta_{\lambda'\lambda} \quad (93)$$

where μ is the cosine of the CM scattering angle: $\mathbf{A} \cdot \mathbf{C} = |\mathbf{A}| |\mathbf{C}| \mu$. In this case we get $T_{L'L;S'S}^J$ by integrating over the scattering angles,

$$T_{L'L;S'S}^J = \delta_{L'L} \delta_{S'S} 2\pi \int_{-1}^1 d\mu P_l(\mu) f(\mu). \quad (94)$$

Note that this result does not depend on J .

2.4.2 Spin-orbit Interactions

The spin-orbit T-matrices have the general form

$$T_{S'\lambda';S,\lambda}(\Omega', \Omega) = f(\mu) (\mathbf{s}^{quark})_{S'\lambda';S\lambda} \cdot i(\mathbf{A} \times \mathbf{C}) \quad (95)$$

which becomes

$$T_{S'\lambda';S,\lambda}(\Omega', \Omega) = f(\mu) \sum_{\mu} (-)^{\mu} C_{S\lambda 1\mu}^{S'\lambda'} i(\mathbf{A} \times \mathbf{C}) \quad (96)$$

since $(s_{\mu}^{quark})_{S'\lambda';S\lambda}$ is expanded in terms of Clebsch-Gordon coefficients coupling the initial and final total spins S' and S , as in Eqns. (41) and (42). We find

$$\begin{aligned} T_{L'L;S'S}^J &= \delta_{L'L} |\mathbf{A}| |\mathbf{C}| (-)^{2S+S'+L-J} \sqrt{2S'+1} \sqrt{\frac{L(L+1)}{2L+1}} \\ &\quad \left\{ \begin{matrix} J & L & S \\ 1 & S' & L \end{matrix} \right\} (f_{L+1} - f_{L-1}) \end{aligned} \quad (97)$$

where

$$f_L = 2\pi \int_{-1}^1 d\mu P_L(\mu) f(\mu). \quad (98)$$

The elastic sectors of the T-matrix for K^*N scattering have $S' = S = 1/2, 3/2$. The $6j$ symbols for these cases have simple expressions with the $L \cdot S$ structure clearly evident.

$$\left\{ \begin{matrix} J & L & \frac{1}{2} \\ 1 & \frac{1}{2} & L \end{matrix} \right\} = \frac{(-)^{L+J+\frac{1}{2}}}{\sqrt{2} \sqrt{3} \sqrt{(L+1)(2L+1)L}} \left[J(J+1) - L(L+1) - \frac{3}{4} \right] \quad (99)$$

$$\left\{ \begin{matrix} J & L & \frac{3}{2} \\ 1 & \frac{3}{2} & L \end{matrix} \right\} = \frac{(-)^{L+J+\frac{3}{2}}}{2 \sqrt{3} \sqrt{5} \sqrt{(L+1)(2L+1)L}} \left[J(J+1) - L(L+1) - \frac{15}{4} \right] \quad (100)$$

so that

$$T_{L'L; \frac{1}{2} \frac{1}{2}}^J = \delta_{L'L} \frac{|\mathbf{A}| |\mathbf{C}|}{\sqrt{3} (2L+1)} \left[J(J+1) - L(L+1) - \frac{3}{4} \right] (f_{L+1} - f_{L-1}) \quad (101)$$

and

$$T_{L'L; \frac{3}{2} \frac{3}{2}}^J = \delta_{L'L} \frac{|\mathbf{A}| |\mathbf{C}|}{\sqrt{3} \sqrt{5} (2L+1)} \left[J(J+1) - L(L+1) - \frac{15}{4} \right] (f_{L+1} - f_{L-1}). \quad (102)$$

For $\rho\pi$ scattering we needed $S' = S = 1$, for which the relevant $6j$ symbol is

$$\left\{ \begin{matrix} J & L & 1 \\ 1 & 1 & L \end{matrix} \right\} = \frac{(-)^{L+J+1}}{2 \sqrt{2} \sqrt{3} \sqrt{(L+1)(2L+1)L}} [J(J+1) - L(L+1) - 2] \quad (103)$$

giving

$$T_{L'L; 11}^J = \delta_{L'L} \frac{|\mathbf{A}| |\mathbf{C}|}{2 \sqrt{2} (2L+1)} [J(J+1) - L(L+1) - 2] (f_{L+1} - f_{L-1}). \quad (104)$$

2.5 KN Results

The phase shifts are calculated for both isospins and the S, P, and D-waves are shown in Figs.(2)-(7) and (10)-(15). Hashimoto [52] has performed the

most recent comprehensive single-energy phase shift analysis, and his data are shown for comparison. The data analysis incorporates polarization data for the $I = 0$ system [55, 56] and so has resolved some ambiguities present in earlier analyses. Also shown is the recent resonating group method (RGM) calculation of Lemaire *et al.* [58]. In the $I=1$ channel, the Born order results are in approximate agreement with the RGM calculation. Both models agree qualitatively with the data except in the P_{13} wave, for which they both give the wrong sign.

The theoretical S_{11} wave is too repulsive at low energies and too weak at higher energies. It has a minimum near 0.6 GeV, and crosses the data at $P_{lab} \approx 1$ GeV. The RGM calculation also overestimates the size of this wave. It agrees well with the Born order result at low energies but shows no sign of turning around. The spin-spin term by itself agrees well with the data at low energies, but the Coulomb and linear interactions are both negative at low energies and including them has worsened the agreement. Barnes and Swanson [69] noted that the approximation of single Gaussian wavefunctions likely breaks down at higher energies, leading to a more rapid retreat of the phase shift than is observed. The single Gaussian wavefunctions we use are expected to underestimate the short distance components of the hadron wave functions because the Coulomb and hyperfine interactions are attractive at short distances for $q\bar{q}$ and qq in spin singlet states. More realistic Coulomb plus linear plus hyperfine wave functions should have enhanced short distance components and lead to high energy scattering amplitudes of increased magnitude. Inelasticities are thought to be small in $I=1$ S-wave [54] so the opening of inelastic channels is not likely to be the main reason for disagreement here.

The P_{11} phase shift is similar to the data at low energies but falls away too quickly at higher energies. The quark model gives the wrong sign in the P_{13} channel. The OGE spin-orbit term is not nearly large enough and is more than cancelled by the negative spin-spin and confinement spin-orbit contributions. This channel is thought to contain a Z^* resonance [53]. There is good agreement in the D_{13} channel at low energies but again the quark model phase shift is too weak at higher energies. The D_{15} channel appears to have reasonable agreement. Lemaire *et al.* [58] claim good results for the P_{11} , D_{13} , and D_{15} waves. My calculation has excellent agreement with the RGM phase shifts in these channels, but the RGM calculation ends at 1 GeV. In the P_{11} and D_{13} channels, this is just where the Born order phase shifts start to diverge from the data.

In $I=0$ the calculated phase shifts give the right sign but are in general too small, especially in the large P_{01} wave. It is interesting, however, that the OGE spin-orbit P_{01} phase shift is exceptionally large relative to the other channels Fig.16. There is perhaps an indication here that we have included some of the correct physics. It is, however, not large enough by itself to account for the data and is partially cancelled by the confinement spin-orbit component, which has the opposite sign, and by the negative spin-spin component. Coupling to inelastic channels likely contributes to the large experimental phase shift in this partial wave. The RGM phase shift is entirely negligible in this channel. Lemaire *et al.* [58] conclude that meson exchange effects cannot be neglected for higher-L waves.

Mukhopadhyay and Pirner [59] have calculated the P-wave phase shifts of the KN system in a nonrelativistic constituent quark model using the generator coordinate method (GCM) and find very similar results. They note that the antisymmetric parts of OGE and confinement spin-orbit potentials lead to unacceptably large splittings in the baryon spectra and so question their physical meaning. They therefore leave them out and keep only the symmetric parts, which almost totally cancel in the baryon spectra. They note, however, that there is no good theoretical reason to leave them out and that doing so leaves the $\Lambda_{1/2}(1405) - \Lambda_{3/2}(1520)$ splitting unexplained. They find that the OGE LS contribution by itself has the right sign and approximately the right magnitude in both isospins at low energies and note the especially large theoretical P_{01} wave. They doubt the inverted confinement contribution and so leave it out. Including spin-spin, Coulomb, Darwin terms makes both $I=1$ P-waves repulsive, just as we have found, and they conclude that the disagreement of the central potential indicates the existence of additional long range forces not included in the calculation. They conclude that there is an indication of the importance of quark-gluon degrees of freedom in low energy hadron scattering but that a better model of confinement is needed.

Bender *et al.* [61] found qualitatively good agreement for S-waves from qq forces variational with the GCM. They found excellent results for $I=0$ with OGE. In $I=1$ they find OGE is too small and concluded a Fermi statistics effect was dominant there. Campbell and Robson [62] found good results for S-waves in $I=0$ with the RGM, but their $I=1$ S-wave phase shift does not exhibit enough repulsion. The cloudy bag model calculation of Veit *et al.* [60] found poor agreement in channels where possible exotic resonances have been predicted (P_{01}, P_{13}, D_{03}). They predict a spin-orbit contribution that is too small to account for the data, and also find the wrong sign in the P_{13}

channel.

2.6 KN Conclusions and Extensions

It seems clear that quark-gluon forces are not large enough to explain the spin-orbit interaction in KN elastic scattering. The OGE spin-orbit contribution is only about one third the size required to account for the data and is partially cancelled by the confinement spin-orbit contribution. Coupling to inelastic channels is one reason to expect disagreement near the opening of the inelastic thresholds. It is possible for the rapid opening of an inelastic channel in a higher-L wave to induce a large phase shift and simulate a resonance. The contribution of inelastic effects to the elastic scattering phase shift needs to be included in a full analysis.

A second possible reason for the disagreement is the need for a better model of confinement. The confinement potential has traditionally been taken to be a Lorentz scalar, but this choice is not obvious, and in fact early models assumed a timelike vector form. The discovery of the 1P_1 h_c charmonium state had strongly ruled out vector confinement because of the near degeneracy with the $\{\chi_J\}$ 3P_J spin triplet states. Vector confinement predicts a splitting between the center of gravity of the $\{\chi_J\}$ and the h_c of ≈ 30 MeV because it includes a contact spin-spin term, whereas experimentally the splitting was only ≈ 1 MeV. Scalar confinement has no spin-spin term and so predicts a small 1^P_1 - 3P_J splitting. The experimental evidence for the h_c , however, is not conclusive, and recent experiments with better statistics may not support its existence [41]. Consequently, the case for scalar confinement is not as strong as previously thought.

The small spin-orbit splittings in meson spectroscopy also seemed to prefer scalar confinement because the confinement spin-orbit is inverted and therefore partially cancels the OGE spin-orbit, as in our scattering calculations. Vector confinement produces a normal spin-orbit that enhances the OGE spin-orbit. This would be a better arrangement in KN scattering, where a large spin-orbit effect is required. Even if the small spin-orbit splittings in meson spectroscopy could be explained by a scalar confinement, there is still the previously mentioned problem in baryon spectroscopy, notably in the P-waves, since there is no way to provide a cancellation for the three-body forces [44, 45].

The most general local confinement potential contains both vector and scalar components. Using an effective Dirac equation and describing the

QCD vacuum by bilocal gluonic correlators, Kalashnikova and Nefediev [46] find an effective interaction in the heavy quark limit that is $5/6$ scalar and $1/6$ vector. The QCD symmetry that Page, *et al.* [42] find for heavy-light systems emerges when the vector and scalar components differ by a constant. A more realistic model of confinement should simultaneously account for the baryon spectrum and the spin-orbit part of hadron-hadron scattering. Bender, *et al.* have also advocated the need for a better model of confinement [61], and their calculation of KN phase shifts leaves out the confinement contribution altogether. Blaschke has suggested putting in the confinement interaction only for the capture diagrams, i.e. only for those diagrams that are topologically confining [40], and this is an interesting idea for a future calculation.

It may be wondered whether t-channel meson exchange should be included as a separate effect in the calculation. Since our quark line diagrams are topologically $q\bar{q}$ exchanges in t-channel, they may implicitly incorporate t-channel meson exchange effects. The connection between the two pictures is a topic for further study.

3 DN Scattering

DN elastic scattering phase shifts are easily calculated in the Born order KN scattering model simply by replacing the s quark of the kaon with the c quark of the D -meson. The only new parameters are the charm quark mass, taken to be $m_c = 1.550$ GeV, and the D -meson mass. Knowledge of vacuum DN scattering amplitudes and observables is important for understanding the open-charm hadronic interactions in hot, dense media, as occur in relativistic heavy-ion collisions. Inelasticities may well be large in DN , as in KN scattering. In $I = 1$, the linear and spin-spin terms are roughly comparable and dominate scattering in the waves shown. The spin-orbit splitting is small in comparison. It is notable that in $I = 0$ the spin-independent terms (Coulomb and linear) are identically zero and the spin-orbit interactions dominate the scattering. The P_{01} and D_{03} channels are weakly attractive and the rest are repulsive. No bound states are found.

4 K^*N Elastic Scattering and $KN \rightarrow K^*N$ Inelastic Amplitudes

The S-matrix for K^*N elastic scattering is more complicated than for KN scattering because the former can have a total spin of $1/2$ or $3/2$ in the initial and final states, whereas the total spin of the KN system is just the nucleon spin. The development of the formalism for K^*N is important because it can be readily generalized to scattering of hadrons with arbitrary spins. This is evident in the Clebsch-Gordon expansion of the quark spin operators and in the general expressions for the T-matrix in terms of 6j-symbols, for instance. The phase shifts for elastic K^*N scattering are shown in Figs.(30)-(43) for $I=1,0$ and $S=1/2,3/2$.

A full analysis of KN elastic scattering must include coupling to inelastic channels, and requires further theoretical effort to apply consistently. KN elastic scattering through an intermediate K^*N state requires working to higher than Born order in our formalism, since $KN \rightarrow K^*N \rightarrow KN$ is clearly second order. This involves the general problem of how to correctly iterate the Born order T-matrix. At Born order, our amplitudes are real. Iterating the Born amplitude should allow the calculation of a complex and fully unitary T-matrix, which can then be parametrized in terms of the usual δ and η , but at present the procedure has not been worked out. In addition to the quark interchange mechanism, two-pion exchange is an important effect for this process. The calculation of the inelastic channel contributions to elastic KN scattering is an interesting topic for future research. As a first step, we compute the $KN \rightarrow K^*N$ amplitudes and calculate ϵ_{JLS} according to Eq.(90). The size of ϵ_{JLS} relative to the elastic δ_{JLS} should give some qualitative idea of the importance of inelastic coupling to K^*N in each of the channels.

5 J/ψ N Scattering Cross Sections

The size of the J/ψ -nucleon scattering cross section is relevant to the search for the quark-gluon plasma (QGP) in relativistic heavy-ion collisions because of the suggestion by Matsui and Satz [76] that a suppression in J/ψ production could be a signature for the creation of the QGP. They argued intuitively that the linear confining interaction should be screened in the QGP, so that a $c\bar{c}$ pair formed in the plasma is likely to dissociate into open-charm mesons. The competing process of direct charm production by scattering on light hadrons in the collision region must be understood in order to confirm a suppression due to plasma effects.

Experimentally, the J/ψ N total cross section must be inferred indirectly by, for example, assuming vector dominance in photoproduction, or from the background of drell-Yan lepton pairs produced with energy near those in the J/ψ peak in heavy-ion collisions. These estimates for $\sigma_{J/\psi+N}$ are poorly known and range from $\approx 1 - 10$ mb. There are now many theoretical calculations of these cross sections, with results differing over many orders of magnitude in the relevant energy range. Kharzeev, *et al.* [77, 78] found a very small $\sigma_{J/\psi+N} \approx 0.25 \mu\text{b}$ at $\sqrt{s} = 5$ GeV. in an early calculation using the parton model and perturbative QCD. The applicability of perturbative QCD in this low energy regime is questionable. See [79] for a summary of experimental information and theoretical calculations.

We can calculate the J/ψ N cross sections with the quark Born method. Despite the problems with interpreting the results for higher-L waves, the S-waves still have given good results where data exists, and we should therefore be able to make definite predictions for these cross sections. The new feature in our formalism is the appearance of charm baryons in the final state. These baryons have one heavy (charm) quark and two light quarks, and we must therefore allow for an asymmetry between the ρ and λ oscillators in the wave functions for these particles [38].

We have detailed the method below, and show results for three example reactions: $J/\psi p \rightarrow \bar{D}^0 \Sigma_c^+$, $\bar{D}^0 \Lambda_c^+$, and $D^{*-} \Sigma_c^{++}$. The largest cross section is ≈ 12 mb, with $\bar{D}^0 \Lambda_c^+$ in the final state. $\sigma_{J/\psi p \rightarrow \bar{D}^0 \Sigma_c^+}$ is approximately 100 times less because of the higher threshold and also because the spin-flavor factor for the confinement interaction favors $\bar{D}^0 \Lambda_c^+$ over $\bar{D}^0 \Sigma_c^+$ in the ratio 27:1. The cross sections calculated with $M_{\Sigma_c} = M_{\Lambda_c}$ are indeed in this ratio.

5.1 Parameters

$$M_\Psi = 3.097 \text{ GeV} \quad (105)$$

$$M_N = 0.939 \text{ GeV} \quad (106)$$

$$M_{\overline{D}} = 1.868 \text{ GeV} \quad (107)$$

$$M_{\overline{D}^*} = 2.008 \text{ GeV} \quad (108)$$

$$M_{\Sigma_c} = 2.453 \text{ GeV} \quad (109)$$

$$M_{\Lambda_c} = 2.285 \text{ GeV} \quad (110)$$

$$m_{u,d} = .330 \text{ GeV} \quad (111)$$

$$m_c = 1.600 \text{ GeV} \quad (112)$$

$$\alpha_s = 0.6 \quad (113)$$

$$b = 0.18 \text{ GeV}^2 \quad (114)$$

$$\alpha_\rho = 0.35 \text{ GeV} \quad (115)$$

$$\alpha_\lambda = \left(\frac{3 m_u m_c}{2 m_u + m_c} \right)^{1/4} \alpha_\rho = 0.32 \quad (116)$$

$$\beta = 0.4 \text{ GeV} \quad (117)$$

5.2 T-matrix

All observables can be computed from the T-matrix

$$T_{S',\lambda';S,\lambda}(\Omega', \Omega) = \langle (AB)_{S'\lambda'} | T_{fi}^{qq} | (CD)_{S\lambda} \rangle \delta(\mathbf{P}_f - \mathbf{P}_i). \quad (118)$$

There is an implicit sum over interactions between quarks in different interacting hadrons. Ω and Ω' are the directions of the incident and scattered mesons in the CM frame: $\mathbf{A} = \mathbf{A}(\Omega')$ and $\mathbf{C} = \mathbf{C}(\Omega)$.

5.3 Space Wave Functions

The harmonic oscillator Hamiltonian for a three light quark system

$$H = \sum_{i=1}^3 \frac{\mathbf{p}_i^2}{2m_i} + \sum_{i<j} \frac{K}{2} (\mathbf{r}_i - \mathbf{r}_j)^2 \quad (119)$$

separates in coordinates $\boldsymbol{\rho}, \boldsymbol{\lambda}, \mathbf{R}$, which are related to the quark position vectors $\mathbf{r}_1, \mathbf{r}_2, \mathbf{r}_3$ via

$$\boldsymbol{\rho} = \frac{\mathbf{r}_2 - \mathbf{r}_3}{\sqrt{2}} \quad (120)$$

$$\boldsymbol{\lambda} = \frac{\mathbf{r}_2 + \mathbf{r}_3 - 2\mathbf{r}_1}{\sqrt{6}} \quad (121)$$

$$\mathbf{R} = \frac{m_1 \mathbf{r}_1 + m_2 \mathbf{r}_2 + m_3 \mathbf{r}_3}{m_1 + m_2 + m_3}. \quad (122)$$

We use this choice in anticipation that m_1 will be the heavy quark in the charmed baryons.

The eigenfunctions of the transformed Hamiltonian

$$H = \sum_{i=1}^3 \frac{\mathbf{p}_i^2}{2m_i} + \sum_{i<j} \frac{3K}{2} (\boldsymbol{\rho}^2 + \boldsymbol{\lambda}^2) \quad (123)$$

are products of three dimensional harmonic oscillator eigenstates. For the S-wave baryons N and Δ the spatial wave function in coordinate space is

$$\Psi_{N,\Delta}(\boldsymbol{\rho}, \boldsymbol{\lambda}) = \frac{\alpha^3}{\pi^{3/2}} e^{-\alpha^2(\boldsymbol{\rho}^2 + \boldsymbol{\lambda}^2)}. \quad (124)$$

where $\alpha = (3Km_{u,d})^{1/4}$. For the Σ_c and Λ_c states we allow an asymmetry between the ρ and λ oscillators

$$\Psi_{\Sigma_c, \Lambda_c}(\boldsymbol{\rho}, \boldsymbol{\lambda}) = \frac{\alpha_\rho^{3/2} \alpha_\lambda^{3/2}}{\pi^{3/2}} e^{-(\alpha_\rho^2 \boldsymbol{\rho}^2 + \alpha_\lambda^2 \boldsymbol{\lambda}^2)/2}. \quad (125)$$

where $\alpha_\rho = (3Km_{u,d})^{1/4}$ and $\alpha_\lambda = (3Km_\lambda)^{1/4}$ with $m_\lambda = 3m_{u,d}m_c/(2m_{u,d} + m_c) = 3m_{u,d}/(2\rho_c + 1) > m_{u,d}$. We need to determine the momentum space wave function by Fourier transforming the coordinate space wave function.

$$\Phi_{\Sigma_c, \Lambda_c}(\mathbf{p}_1, \mathbf{p}_2, \mathbf{p}_3) = \iiint d^3r_1 d^3r_2 d^3r_3 e^{-i\mathbf{p}_1 \cdot \mathbf{r}_1} e^{-i\mathbf{p}_2 \cdot \mathbf{r}_2} e^{-i\mathbf{p}_3 \cdot \mathbf{r}_3} \Psi_{\Sigma_c, \Lambda_c}(\boldsymbol{\rho}, \boldsymbol{\lambda})$$

$$\begin{aligned}
&= \iiint 3^{3/2} d^3\rho d^3\lambda d^3R e^{-i(\tilde{\rho}\cdot\rho+\tilde{\lambda}\cdot\lambda+P\cdot R)} e^{-(\alpha_\rho^2\rho^2+\alpha_\lambda^2\lambda^2)/2} \\
&= (2\pi)^3 \delta^3(\mathbf{P}) 3^{3/2} \left(\frac{2\pi}{\alpha_\rho}\right)^{3/2} \left(\frac{2\pi}{\alpha_\lambda}\right)^{3/2} e^{-\tilde{\rho}^2/2\alpha_\rho^2} e^{-\tilde{\lambda}^2/2\alpha_\lambda^2}
\end{aligned} \tag{126}$$

where

$$\tilde{\rho} = \frac{\mathbf{p}_2 - \mathbf{p}_3}{\sqrt{2}} \tag{127}$$

$$\tilde{\lambda} = \sqrt{\frac{3}{2}} \left[\frac{-2\rho_c \mathbf{p}_1 + \mathbf{p}_2 + \mathbf{p}_3}{2\rho_c + 1} \right] \tag{128}$$

$$\mathbf{P} = \mathbf{p}_1 + \mathbf{p}_2 + \mathbf{p}_3 \tag{129}$$

and we have used $m_2 = m_3 = m_{u,d}$ and $m_1 = m_c$. Removing the total momentum conserving delta function and determining the normalization from

$$\iiint d^3p_1 d^3p_2 d^3p_3 |\Phi(\mathbf{p}_1, \mathbf{p}_2, \mathbf{p}_3)|^2 \delta^3(\mathbf{P}) = 1 \tag{130}$$

we find

$$\Phi_{\Sigma_c, \Lambda_c}(\mathbf{p}_1, \mathbf{p}_2, \mathbf{p}_3) = \frac{3^{3/4}}{\pi^{3/2} \alpha_\rho^{3/2} \alpha_\lambda^{3/2}} e^{-\tilde{\rho}^2/2\alpha_\rho^2} e^{-\tilde{\lambda}^2/2\alpha_\lambda^2}. \tag{131}$$

The remaining momentum space wave functions are the usual forms

$$\Phi_\Psi(\mathbf{p} - \bar{\mathbf{p}}) = \frac{1}{\pi^{3/4} \beta^{3/2}} e^{-(\mathbf{p} - \bar{\mathbf{p}})^2/8\beta^2} \tag{132}$$

$$\Phi_{\bar{D}}(\mathbf{p}_{rel}) = \frac{1}{\pi^{3/4} \beta^{3/2}} e^{-(\frac{2}{\rho_c+1})^2 (\mathbf{p} - \rho_c \bar{\mathbf{p}})^2/8\beta^2} \tag{133}$$

$$\Phi_N(\mathbf{p}_1, \mathbf{p}_2, \mathbf{p}_3) = \frac{3^{3/4}}{\pi^{3/2} \alpha_\rho^3} e^{-(\mathbf{p}_1^2 + \mathbf{p}_2^2 + \mathbf{p}_3^2 - \mathbf{p}_1 \cdot \mathbf{p}_2 - \mathbf{p}_1 \cdot \mathbf{p}_3 - \mathbf{p}_2 \cdot \mathbf{p}_3)/3\alpha_\rho^2} \tag{134}$$

where $\rho_c = m_{u,d}/m_c$.

5.4 Space Overlap

$$\begin{aligned}
T_{space}^{D_1} = & \int \dots d^3 a \, d^3 \bar{a} \, d^3 b_1 \, d^3 b_2 \, d^3 b_3 \, d^3 c \, d^3 \bar{c} \, d^3 d_1 \, d^3 d_2 \, d^3 d_3 \\
& \phi_A(a - \bar{a}) \, \phi_B(b_1, b_2, b_3) \, \phi_C(c - \bar{c}) \, \phi_D(d_1, d_2, d_3) \\
& T_{fi}^{qq} \left(d_1 - a, \frac{a + d_1}{2}, \frac{b_1 + c}{2} \right) \\
& \delta(\bar{a} - \bar{c}) \, \delta(b_2 - d_2) \, \delta(b_3 - d_3) \\
& \delta(A - a - \bar{a}) \, \delta(B - b_1 - b_2 - b_3) \\
& \delta(C - c - \bar{c}) \, \delta(D - d_1 - d_2 - d_3)
\end{aligned} \tag{135}$$

$$\begin{aligned}
T_{space}^{D_2} = & \int \dots d^3 a \, d^3 \bar{a} \, d^3 b_1 \, d^3 b_2 \, d^3 b_3 \, d^3 c \, d^3 \bar{c} \, d^3 d_1 \, d^3 d_2 \, d^3 d_3 \\
& \phi_A(a - \bar{a}) \, \phi_B(b_1, b_2, b_3) \, \phi_C(c - \bar{c}) \, \phi_D(d_1, d_2, d_3) \\
& T_{fi}^{qq} \left(d_1 - a, \frac{a + d_1}{2}, \frac{b_2 + d_2}{2} \right) \\
& \delta(\bar{a} - \bar{c}) \, \delta(b_1 - c) \, \delta(b_3 - d_3) \\
& \delta(A - a - \bar{a}) \, \delta(B - b_1 - b_2 - b_3) \\
& \delta(C - c - \bar{c}) \, \delta(D - d_1 - d_2 - d_3)
\end{aligned} \tag{136}$$

$$\begin{aligned}
T_{space}^{D_3} = & \int \dots d^3 a \, d^3 \bar{a} \, d^3 b_1 \, d^3 b_2 \, d^3 b_3 \, d^3 c \, d^3 \bar{c} \, d^3 d_1 \, d^3 d_2 \, d^3 d_3 \\
& \phi_A(a - \bar{a}) \, \phi_B(b_1, b_2, b_3) \, \phi_C(c - \bar{c}) \, \phi_D(d_1, d_2, d_3) \\
& T_{fi}^{qq} \left(\bar{c} - \bar{a}, \frac{\bar{a} + \bar{c}}{2}, \frac{b_1 + c}{2} \right) \\
& \delta(a - d_1) \, \delta(b_2 - d_2) \, \delta(b_3 - d_3) \\
& \delta(A - a - \bar{a}) \, \delta(B - b_1 - b_2 - b_3) \\
& \delta(C - c - \bar{c}) \, \delta(D - d_1 - d_2 - d_3)
\end{aligned} \tag{137}$$

$$\begin{aligned}
T_{space}^{D_4} = & \int \dots d^3 a \, d^3 \bar{a} \, d^3 b_1 \, d^3 b_2 \, d^3 b_3 \, d^3 c \, d^3 \bar{c} \, d^3 d_1 \, d^3 d_2 \, d^3 d_3 \\
& \phi_A(a - \bar{a}) \, \phi_B(b_1, b_2, b_3) \, \phi_C(c - \bar{c}) \, \phi_D(d_1, d_2, d_3)
\end{aligned}$$

$$\begin{aligned}
& T_{fi}^{qq} \left(\bar{c} - \bar{a}, \frac{\bar{a} + \bar{c}}{2}, \frac{b_2 + d_2}{2} \right) \\
& \delta(a - d_1) \delta(b_1 - c) \delta(b_3 - d_3) \\
& \delta(A - a - \bar{a}) \delta(B - b_1 - b_2 - b_3) \\
& \delta(C - c - \bar{c}) \delta(D - d_1 - d_2 - d_3)
\end{aligned} \tag{138}$$

After inserting the harmonic oscillator wave functions, these can be reduced to integrals over two (diagrams 1 and 3) or three (diagrams 2 and 4) momenta.

$$\begin{aligned}
T_{space}^{D_1} &= \eta e^{f(\mathbf{A}, \mathbf{C})} \int d^3 q \int d^3 P e^{-a_P(\mathbf{P} - \mathbf{P}_0)^2} e^{-a_q(\mathbf{q} - \mathbf{q}_0)^2} T_{fi}^{qq}(\mathbf{q}, \mathbf{P}, \mathbf{P} + \mathbf{C} - \mathbf{A}) \\
\eta &= \frac{3^{3/2}}{2^{3/2} \pi^3 \alpha_\rho^{3/2} \alpha_\lambda^{3/2} \beta^3}
\end{aligned}$$

$$\begin{aligned}
f(\mathbf{A}, \mathbf{C}) &= \left\{ - \left[(4\rho^4 + 12\rho^3 + 13\rho^2 + 6\rho + 1) (3\alpha_\rho^2 + 3\alpha_\lambda^2 + 16\beta^2) \right] \mathbf{A}^2 \right. \\
&+ \left[12(4\rho^3 + 8\rho^2 + 5\rho + 1) (\alpha_\rho^2 + \alpha_\lambda^2) + 96\rho(2\rho^3 + 5\rho^2 + 4\rho + 1)\beta^2 \right] \mathbf{A} \cdot \mathbf{C} \\
&- \left[12(4\rho^2 + 4\rho + 1) (\alpha_\rho^2 + \alpha_\lambda^2) + 144\rho^2(\rho^2 + 2\rho + 1)\beta^2 \right] \mathbf{C}^2 \Big\} \\
&\left\{ 48(\rho + 1)^2 (2\rho + 1)^2 (\alpha_\rho^2 + \alpha_\lambda^2) \beta^2 \right\}^{-1}
\end{aligned}$$

$$a_P = \frac{3}{4\alpha_\rho^2} + \frac{3}{4\alpha_\lambda^2} + \frac{1}{\beta^2}$$

$$a_q = \frac{3(\alpha_\rho^2 + \alpha_\lambda^2)}{3(\alpha_\rho^2 + \alpha_\lambda^2)\beta^2 + 4\alpha_\rho^2\alpha_\lambda^2}$$

$$\begin{aligned}
\mathbf{P}_0 &= \left\{ \left[(\rho + 1)(2\rho + 1)(6\alpha_\rho^2 + 4\beta^2)\alpha_\lambda^2 \right] \mathbf{A} \right. \\
&- \left[6(\rho + 1)\alpha_\rho^2\beta^2 + 6(\rho + 1)(2\rho + 1)\alpha_\lambda^2\beta^2 + 4(2\rho + 1)\alpha_\rho^2\alpha_\lambda^2 \right] \mathbf{C} \\
&+ (\rho + 1)(2\rho + 1) \left[-3(\alpha_\rho^2 + \alpha_\lambda^2)\beta^2 + 4\alpha_\rho^2\alpha_\lambda^2 \right] \mathbf{q} \Big\} \\
&\left\{ (\rho + 1)(2\rho + 1) \left[6(\alpha_\rho^2 + \alpha_\lambda^2)\beta^2 + 8\alpha_\rho^2\alpha_\lambda^2 \right] \right\}^{-1} \\
\mathbf{q}_0 &= - \frac{\left\{ \left[(\rho + 1)(2\rho + 1)(9\alpha_\rho^2 + \alpha_\lambda^2) \right] \mathbf{A} + \left[6\alpha_\rho^2 + 6(4\rho^2 + 4\rho + 1)\alpha_\lambda^2 \right] \mathbf{C} \right\}}{12(\rho + 1)(2\rho + 1)(\alpha_\rho^2 + \alpha_\lambda^2)}
\end{aligned}$$

$$T_{space}^{D_2} = \eta e^{f(\mathbf{A}, \mathbf{C})} \int d^3 q \int d^3 P \int d^3 P' e^{-a'_{P'}(\mathbf{P}' - \mathbf{P}'_0)^2} e^{-a_P(\mathbf{P} - \mathbf{P}_0)^2} e^{-a_q(\mathbf{q} - \mathbf{q}_0)^2} T_{fi}^{qq}(\mathbf{q}, \mathbf{P}, \mathbf{P}')$$

$$\eta = \frac{3^{3/2}}{\pi^{9/2} \alpha_\rho^{9/2} \alpha_\lambda^{3/2} \beta^3}$$

$$f(\mathbf{A}, \mathbf{C}) =$$

$$\begin{aligned} & \left\{ -(\rho+1)^2 (2\rho+1)^2 \left[36 \alpha_\rho^4 + 75 \alpha_\rho^2 \beta^2 + 5 \alpha_\lambda^2 \beta^2 + 24 \beta^4 + 6 \alpha_\rho^2 \alpha_\lambda^2 \right] \mathbf{A}^2 \right. \\ & + 12 (\rho+1) (2\rho+1) \left[-3 (\rho-1) (4\rho+1) \alpha_\rho^2 \beta^2 \right. \\ & - (\rho-1) (2\rho+1) \alpha_\lambda^2 \beta^2 + 12 \rho (\rho+1) \beta^4 \\ & + 2 (2\rho+1) \alpha_\rho^2 \alpha_\lambda^2 + 12 (2\rho+1) \alpha_\rho^4 \left. \right] \mathbf{A} \cdot \mathbf{C} \\ & - 12 \left[18 \rho^2 (\rho+1)^2 \beta^4 + 2 (2\rho+1)^2 \alpha_\rho^2 (6 \alpha_\rho^2 + \alpha_\lambda^2) \right. \\ & + 3 (24\rho^2 + 24\rho + 7) (2\rho^2 + 2\rho + 1) \alpha_\rho^2 \beta^2 \\ & + 3 (2\rho+1)^2 (2\rho^2 + 2\rho + 1) \alpha_\lambda^2 \beta^2 \left. \right] \mathbf{C}^2 \left. \right\} \\ & \left\{ 24 (\rho+1)^2 (2\rho+1)^2 \left[3 (7 \alpha_\rho^2 + \alpha_\lambda^2) \beta^2 + 4 (6 \alpha_\rho^2 + \alpha_\lambda^2) \alpha_\rho^2 \right] \beta^2 \right\}^{-1} \end{aligned}$$

$$a_P = \frac{3}{4 \alpha_\rho^2} + \frac{3}{4 \alpha_\lambda^2} + \frac{1}{\beta^2}$$

$$a_{P'} = \frac{2}{\alpha_\rho^2}$$

$$a_q = \frac{3 (7 \alpha_\rho^2 + \alpha_\lambda^2) \beta^2 + 4 \alpha_\rho^2 (6 \alpha_\rho^2 + \alpha_\lambda^2)}{8 \alpha_\rho^2 \left[3 (\alpha_\rho^2 + \alpha_\lambda^2) \beta^2 + 4 \alpha_\rho^2 \alpha_\lambda^2 \right]}$$

$$\begin{aligned} \mathbf{P}_0 = & \left\{ \left[(\rho+1) (2\rho+1) (6 \alpha_\rho^2 + 4 \beta^2) \alpha_\lambda^2 \right] \mathbf{A} \right. \\ & - \left[6 (\rho+1) \alpha_\rho^2 \beta^2 + 6 (\rho+1) (2\rho+1) \alpha_\lambda^2 \beta^2 + 4 (2\rho+1) \alpha_\rho^2 \alpha_\lambda^2 \right] \mathbf{C} \\ & + (\rho+1) (2\rho+1) \left[3 (-\alpha_\rho^2 + \alpha_\lambda^2) \beta^2 + 4 \alpha_\rho^2 \alpha_\lambda^2 \right] \mathbf{q} \left. \right\} \\ & \left\{ (\rho+1) (2\rho+1) \left[6 (\alpha_\rho^2 + \alpha_\lambda^2) \beta^2 + 8 \alpha_\rho^2 \alpha_\lambda^2 \right] \right\}^{-1} \end{aligned}$$

$$\mathbf{P}'_0 = -\frac{\mathbf{P}}{2} - \frac{\mathbf{C}}{2}$$

$$\mathbf{q}_0 = \left\{ - \left[(\rho+1) (2\rho+1) \alpha_\rho^2 (18 \alpha_\rho^2 + 12 \beta^2) \right] \mathbf{A} \right.$$

$$\begin{aligned}
& +12 \alpha_\rho^2 \left[3 \rho (\rho + 1) \beta^2 - \alpha_\rho^2 \right] \mathbf{C} \} \\
& \left\{ (\rho + 1) (2\rho + 1) \left[3 (7 \alpha_\rho^2 + \alpha_\lambda^2) \beta^2 + 4 \alpha_\rho^2 (6 \alpha_\rho^2 + \alpha_\lambda^2) \right] \right\}^{-1} \\
T_{space}^{D_3} &= \eta e^{f(\mathbf{A}, \mathbf{C})} \int d^3 q \int d^3 P e^{-a_P (\mathbf{P} - \mathbf{P}_0)^2} e^{-a_q (\mathbf{q} - \mathbf{q}_0)^2} T_{fi}^{qq}(\mathbf{q}, \mathbf{P}, -\mathbf{P} + \mathbf{C}) \\
\eta &= \frac{3^{3/2}}{2^{3/2} \pi^3 \alpha_\rho^{3/2} \alpha_\lambda^{3/2} \beta^3} \\
f(\mathbf{A}, \mathbf{C}) &= \left\{ -(4\rho^2 + 4\rho + 1) \left[9 \alpha_\rho^2 + \alpha_\lambda^2 + 24 \beta^2 \right] \mathbf{A}^2 \right. \\
&+ \left[36 (2\rho + 1) (-\alpha_\rho^2 + 4 \rho \beta^2) + 12 (4\rho^2 + 4\rho + 1) \alpha_\lambda^2 \right] \mathbf{A} \cdot \mathbf{C} \\
&- 36 \left[\alpha_\rho^2 + (4\rho^2 + 4\rho + 1) \alpha_\lambda^2 + 6 \rho^2 \beta^2 \right] \mathbf{C}^2 \} \\
&\left\{ 24 (2\rho + 1)^2 \left[3 (\alpha_\rho^2 + \alpha_\lambda^2) \beta^2 + 2 \alpha_\rho^2 \alpha_\lambda^2 \right] \right\}^{-1} \\
a_P &= \frac{3}{4 \alpha_\rho^2} + \frac{3}{4 \alpha_\lambda^2} + \frac{1}{\beta^2} \\
a_q &= \frac{3 (\alpha_\rho^2 + \alpha_\lambda^2) \beta^2 + 2 \alpha_\rho^2 \alpha_\lambda^2}{2 \beta^2 \left[3 (\alpha_\rho^2 + \alpha_\lambda^2) \beta^2 + 4 \alpha_\rho^2 \alpha_\lambda^2 \right]} \\
\mathbf{P}_0 &= \left\{ (\rho + 1) (2\rho + 1) \left[6 \alpha_\rho^2 \beta^2 + 2 \alpha_\lambda^2 \beta^2 + 2 \alpha_\rho^2 \alpha_\lambda^2 \right] \mathbf{A} \right. \\
&+ \left[6 (\rho + 1) \alpha_\rho^2 \beta^2 + 6 (\rho + 1) (2\rho + 1) \alpha_\lambda^2 \beta^2 + 4 (2\rho + 1) \alpha_\rho^2 \alpha_\lambda^2 \right] \mathbf{C} \\
&+ 3 (\rho + 1) (2\rho + 1) \left[\alpha_\rho^2 + \alpha_\lambda^2 \right] \beta^2 \mathbf{q} \} \\
&\left\{ (\rho + 1) (2\rho + 1) \left[6 (\alpha_\rho^2 + \alpha_\lambda^2) \beta^2 + 8 \alpha_\rho^2 \alpha_\lambda^2 \right] \right\}^{-1} \\
\mathbf{q}_0 &= \left\{ -(\rho + 1) (2\rho + 1) \left[3 \alpha_\rho^2 \beta^2 + \alpha_\lambda^2 \beta^2 + \alpha_\rho^2 \alpha_\lambda^2 \right] \mathbf{A} \right. \\
&+ \left[3 \rho \alpha_\rho^2 \beta^2 - 3 \rho (2\rho + 1) \alpha_\lambda^2 \beta^2 + 2 (2\rho + 1) \alpha_\rho^2 \alpha_\lambda^2 \right] \mathbf{C} \} \\
&\left\{ (\rho + 1) (2\rho + 1) \left[3 (\alpha_\rho^2 + \alpha_\lambda^2) \beta^2 + 2 \alpha_\rho^2 \alpha_\lambda^2 \right] \right\}^{-1} \\
T_{space}^{D_4} &= \eta e^{f(\mathbf{A}, \mathbf{C})} \int d^3 q \int d^3 P \int d^3 P' e^{-a'_P (\mathbf{P}' - \mathbf{P}'_0)^2} e^{-a_P (\mathbf{P} - \mathbf{P}_0)^2} \\
&e^{-a_q (\mathbf{q} - \mathbf{q}_0)^2} T_{fi}^{qq}(\mathbf{q}, \mathbf{P}, \mathbf{P}') \\
\eta &= \frac{3^{3/2}}{\pi^{9/2} \alpha_\rho^{9/2} \alpha_\lambda^{3/2} \beta^3}
\end{aligned}$$

$$\begin{aligned}
f(\mathbf{A}, \mathbf{C}) &= \left\{ -(\rho+1)^2 (2\rho+1)^2 \right. \\
&\quad \left[36 \alpha_\rho^4 + 123 \alpha_\rho^2 \beta^2 + 5 \alpha_\lambda^2 \beta^2 + 24 \beta^4 + 22 \alpha_\rho^2 \alpha_\lambda^2 \right] \mathbf{A}^2 \\
&\quad + (\rho+1) (2\rho+1) \left[-36 (8\rho^2 + 9\rho + 7) \alpha_\rho^2 \beta^2 \right. \\
&\quad \left. - 12 (\rho-1) (2\rho+1) \alpha_\lambda^2 \beta^2 + 144 \rho (\rho+1) \beta^4 \right. \\
&\quad \left. - 24 (2\rho+1) (4\rho-1) \alpha_\rho^2 \alpha_\lambda^2 - 144 (\rho+1) \alpha_\rho^4 \right] \mathbf{A} \cdot \mathbf{C} \\
&\quad - \left[216 \rho^2 (\rho+1)^2 \beta^4 + 24 (2\rho+1)^2 (6\rho+1)^2 \alpha_\rho^2 \alpha_\lambda^2 \right. \\
&\quad + 144 (\rho+1)^2 \alpha_\rho^4 + 36 (24\rho^4 + 24\rho^3 + 14\rho^2 + 14\rho + 7) \alpha_\rho^2 \beta^2 \\
&\quad \left. + 36 (2\rho+1)^2 (2\rho^2 + 2\rho + 1) \alpha_\lambda^2 \beta^2 \right] \mathbf{C}^2 \Big\} \\
&\quad \left\{ 24 (\rho+1)^2 (2\rho+1)^2 \right. \\
&\quad \left. \left[3 (7 \alpha_\rho^2 + \alpha_\lambda^2) \beta^4 + 4 (3 \alpha_\rho^2 + 4 \alpha_\lambda^2) \alpha_\rho^2 \beta^2 + 8 \alpha_\rho^4 \alpha_\lambda^2 \right] \right\}^{-1} \\
a_P &= \frac{3}{4 \alpha_\rho^2} + \frac{3}{4 \alpha_\lambda^2} + \frac{1}{\beta^2} \\
a_{P'} &= \frac{2}{\alpha_\rho^2} \\
a_q &= \frac{3 (7 \alpha_\rho^2 + \alpha_\lambda^2) \beta^4 + 4 \alpha_\rho^2 (3 \alpha_\rho^2 + 4 \alpha_\lambda^2) \beta^2 + 8 \alpha_\rho^4 \alpha_\lambda^2}{8 \alpha_\rho^2 \beta^2 \left[3 (\alpha_\rho^2 + \alpha_\lambda^2) \beta^2 + 4 \alpha_\rho^2 \alpha_\lambda^2 \right]} \\
\mathbf{P}_0 &= \left\{ (\rho+1) (2\rho+1) \left[(6 \alpha_\rho^2 + 2 \alpha_\lambda^2) \beta^2 + 2 \alpha_\rho^2 \alpha_\lambda^2 \right] \mathbf{A} \right. \\
&\quad + \left[6 (\rho+1) \alpha_\rho^2 \beta^2 + 6 (\rho+1) (2\rho+1) \alpha_\lambda^2 \beta^2 + 4 (2\rho+1) \alpha_\rho^2 \alpha_\lambda^2 \right] \mathbf{C} \\
&\quad + 3 (\rho+1) (2\rho+1) \left[\alpha_\rho^2 - \alpha_\lambda^2 \right] \beta^2 \mathbf{q} \Big\} \\
&\quad \left\{ (\rho+1) (2\rho+1) \left[6 (\alpha_\rho^2 + \alpha_\lambda^2) \beta^2 + 8 \alpha_\rho^2 \alpha_\lambda^2 \right] \right\}^{-1} \\
\mathbf{P}'_0 &= \frac{\mathbf{P}}{2} - \frac{(\mathbf{A} + \mathbf{C})}{2} \\
\mathbf{q}_0 &= \left\{ -(\rho+1) (2\rho+1) \alpha_\rho^2 \left[12 \beta^4 + 12 \alpha_\rho^2 \beta^2 + 2 \alpha_\lambda^2 \beta^2 + 4 \alpha_\rho^2 \alpha_\lambda^2 \right] \mathbf{A} \right. \\
&\quad + \alpha_\rho^2 \left[36 \rho (\rho+1) \beta^4 + 12 \rho \alpha_\rho^2 \beta^2 \right. \\
&\quad \left. + 12 (\rho+1) (2\rho+1) \alpha_\lambda^2 \beta^2 + 8 (2\rho+1) \alpha_\rho^2 \alpha_\lambda^2 \right] \mathbf{C} \Big\}
\end{aligned}$$

$$\left\{ (\rho + 1) (2\rho + 1) \left[3 (7 \alpha_\rho^2 + \alpha_\lambda^2) \beta^4 + 4 \alpha_\rho^2 (3 \alpha_\rho^2 + 4 \alpha_\lambda^2) \beta^2 + 8 \alpha_\rho^4 \alpha_\lambda^2 \right] \right\}^{-1}$$

The explicit scattering amplitudes are found by inserting the quark-quark interactions $T_{fi}^{qq}(\mathbf{q}, \mathbf{P}, \mathbf{P}')$ and performing the remaining integrations. The results are in App. D.

5.5 Spin-flavor Wave Functions

These use the phase conventions of Close. Apparently Le Yaouanc has the opposite sign for the Σ but the same sign for the N and Λ .

$$|\Sigma_c^+(+1/2)\rangle = \frac{1}{\sqrt{6}} \begin{vmatrix} c \\ u \\ d \end{vmatrix} \left(2 \begin{vmatrix} - \\ + \\ + \end{vmatrix} - \begin{vmatrix} + \\ - \\ + \end{vmatrix} - \begin{vmatrix} + \\ + \\ - \end{vmatrix} \right) \quad (139)$$

$$|\Sigma_c^+(-1/2)\rangle = -\frac{1}{\sqrt{6}} \begin{vmatrix} c \\ u \\ d \end{vmatrix} \left(2 \begin{vmatrix} + \\ - \\ - \end{vmatrix} - \begin{vmatrix} - \\ + \\ - \end{vmatrix} - \begin{vmatrix} - \\ - \\ + \end{vmatrix} \right) \quad (140)$$

$$|\Lambda_c^+(+1/2)\rangle = \frac{1}{\sqrt{2}} \begin{vmatrix} c \\ u \\ d \end{vmatrix} \left(\begin{vmatrix} + \\ + \\ - \end{vmatrix} - \begin{vmatrix} + \\ - \\ + \end{vmatrix} \right) \quad (141)$$

$$|\Lambda_c^+(-1/2)\rangle = -\frac{1}{\sqrt{2}} \begin{vmatrix} c \\ u \\ d \end{vmatrix} \left(\begin{vmatrix} - \\ - \\ + \end{vmatrix} - \begin{vmatrix} - \\ + \\ - \end{vmatrix} \right) \quad (142)$$

$$|\Sigma_c^{++}(+1/2)\rangle = \frac{1}{\sqrt{3}} \begin{vmatrix} c \\ u \\ u \end{vmatrix} \left(\begin{vmatrix} - \\ + \\ + \end{vmatrix} - \begin{vmatrix} + \\ - \\ + \end{vmatrix} \right) \quad (143)$$

$$|\Sigma_c^{++}(-1/2)\rangle = -\frac{1}{\sqrt{3}} \begin{vmatrix} c \\ u \\ u \end{vmatrix} \left(\begin{vmatrix} + \\ - \\ - \end{vmatrix} - \begin{vmatrix} - \\ + \\ - \end{vmatrix} \right) \quad (144)$$

$$|\Sigma_c^0(+1/2)\rangle = \frac{1}{\sqrt{3}} \begin{vmatrix} c \\ d \\ d \end{vmatrix} \left(\begin{vmatrix} - \\ + \\ + \end{vmatrix} - \begin{vmatrix} + \\ - \\ + \end{vmatrix} \right) \quad (145)$$

$$|\Sigma_c^0(-1/2)\rangle = -\frac{1}{\sqrt{3}} \begin{vmatrix} c \\ d \\ d \end{vmatrix} \left(\begin{vmatrix} + \\ - \\ - \end{vmatrix} - \begin{vmatrix} - \\ + \\ - \end{vmatrix} \right) \quad (146)$$

5.6 Spin-flavor Factors

		<i>hyperfinespin</i>	<i>confinement</i>
$\Psi \ p \rightarrow \overline{D}^0 \ \Sigma_c^+$	$D1$	$+\sqrt{6}/48$	$-1/2\sqrt{6}$
	$D2$	$+\sqrt{6}/12$	$-1/\sqrt{6}$
	$D3$	$+\sqrt{6}/16$	$-1/2\sqrt{6}$
	$D4$	$-\sqrt{6}/12$	$-1/\sqrt{6}$

		<i>hyperfinespin</i>	<i>confinement</i>
$\Psi \ p \rightarrow \overline{D}^0 \ \Lambda_c^+$	$D1$	$+3/8\sqrt{2}$	$-3/2\sqrt{2}$
	$D2$	0	$-3/\sqrt{2}$
	$D3$	$+9/8\sqrt{2}$	$-3/2\sqrt{2}$
	$D4$	0	$-3/\sqrt{2}$

		<i>hyperfinespin</i>	<i>confinement</i>
$\Psi \ p \rightarrow D^{*-} \ \Sigma_c^{++}(S=1/2)$	$D1$	$-7/24$	$-5/6$
	$D2$	$+5/6$	$-5/3$
	$D3$	$-5/24$	$-5/6$
	$D4$	$+1/2$	$-5/3$

		<i>hyperfinespin</i>	<i>confinement</i>
$\Psi \ p \rightarrow D^{*-} \ \Sigma_c^{++}(S=3/2)$	$D1$	$-5/12$	$-1/3$
	$D2$	$+1/3$	$-2/3$
	$D3$	$-1/12$	$-1/3$
	$D4$	0	$-2/3$

5.7 Cross Sections

The PDG formula

$$\frac{d\sigma}{dt} = \frac{|\mathcal{M}_{fi}|^2}{64 \pi s \mathbf{A}^2} \quad (147)$$

becomes

$$\frac{d\sigma}{dt} = \frac{E_A E_B E_C E_D}{4 \pi s \mathbf{A}^2} |T_{fi}|^2 \quad (148)$$

since our T_{fi} is related to \mathcal{M}_{fi} by

$$\mathcal{M}_{fi} = \sqrt{2E_A 2E_B 2E_C 2E_D} T_{fi}. \quad (149)$$

Therefore

$$\frac{d\sigma}{d\mu} = \frac{E_A E_B E_C E_D}{2 \pi s} \frac{|\mathbf{C}|}{|\mathbf{A}|} |T_{fi}(\mu)|^2 \quad (150)$$

where $\mathbf{A} \cdot \mathbf{C} = |\mathbf{A}| |\mathbf{C}| \mu$. The polarized cross section is

$$\sigma_{S'\lambda';S\lambda} = \frac{E_A E_B E_C E_D}{2 \pi s} \frac{|\mathbf{C}|}{|\mathbf{A}|} \int d\mu |T_{S'\lambda';S\lambda}(\mu)|^2 \quad (151)$$

where S', S are the initial and final total spins and λ', λ the z-components. The total unpolarized cross section is

$$\sigma_{tot} = \frac{1}{2S_A + 1} \frac{1}{2S_B + 1} \sum_{S'\lambda'S\lambda} \sigma_{S'\lambda';S\lambda}. \quad (152)$$

The channel cross section is defined as

$$\sigma_{S'S} = \frac{1}{2S' + 1} \frac{E_A E_B E_C E_D}{2 \pi s} \frac{|\mathbf{C}|}{|\mathbf{A}|} \sum_{\lambda'\lambda} \int d\mu |T_{S'\lambda';S\lambda}(\mu)|^2 \quad (153)$$

so that

$$\sigma_{tot} = \frac{1}{2S_A + 1} \frac{1}{2S_B + 1} \sum_{S'S} (2S' + 1) \sigma_{S'S}. \quad (154)$$

6 Conclusion

In this thesis we have applied the constituent quark model to meson baryon scattering. Specifically we have considered the problem of kaon-nucleon (KN) scattering, in channels which are free of $q\bar{q}$ valence annihilation. This is an interesting problem because KN is a model for NN , and there is a long-standing question in nuclear physics as to whether one can derive accurate spin-dependent NN forces in the quark model. It is especially interesting to determine if quark-gluon forces can explain the large spin-orbit interaction in KN scattering observed experimentally.

To treat this problem we have used the “quark Born diagram” formalism, including one gluon exchange forces linear scalar confinement, and Gaussian wavefunctions. We derived the meson-baryon scattering amplitudes analytically in this approach, and extracted elastic KN scattering phase shifts. We then compared these theoretical results to experimental data on KN scattering.

We find that the dominant S-waves are in reasonable agreement with data, but that the quark-gluon forces we assume are unable to reproduce the phase shifts in higher-L waves given standard quark model parameters. The experimental spin-orbit contribution to the P-wave phase shifts for example is approximately three times as large as the theoretical estimate. The reasons for this disagreement are unclear. The presence of inelastic channels, the effect of other forces such as meson exchange, and the need for a better model of confinement are possible reasons for this discrepancy.

DN phase shifts and $J/\psi N$ cross sections were also calculated using this approach. A knowledge of these cross sections is important for the search for a quark-gluon plasma in heavy ion collisions, for example at the RHIC facility at BNL. The work presented here is the first quark model calculation of DN and $J/\psi N$ scattering. We find that these cross sections are typically in the 1-10 mb range at the low energy scales relevant to QGP searches.

References

- [1] J. J. Aubert, *et al.*, *Phys. Rev. Lett.* **33** (1974) 1404
- [2] J. -E. Augustin, *et al.*, *Phys. Rev. Lett.* **33** (1974) 1406
- [3] E. Eichten and F. Feinberg, *Phys. Rev. Lett.* **43** (1979) 1205
- [4] E. Eichten and F. Feinberg, *Phys. Rev.* **D23** (1981) 2724
- [5] D. Gromes, *Z. Phys. C* **26** (1984) 401
- [6] D. Gromes, in *Proceedings of the Yukon Advanced Study Institute*, Whitehorse, Yukon, edited by N. Isgur, G. Karl, and P. J. O'Donnell, World Scientific, Singapore, (1984)
- [7] M. Fritzsch, M. Gell-Mann, and H. Leutwyler, *Phys. Lett.* **47B** (1971) 365
- [8] D. J. Gross and F. Wilczek *Phys. Rev.* **D8** (1973) 3497
- [9] S. Weinberg, *Phys. Rev. Lett.* **31** (1973) 494
- [10] J. D. Bjorken *Phys. Rev.* **179** (1969) 1547
- [11] K. Wilson, *Phys. Rev.* **D10** (1974) 2445
- [12] J. Kogut and L. Susskind, *Phys. Rev.* **D9** (1974) 3501
- [13] J. Kogut and L. Susskind, *Phys. Rev.* **D11** (1975) 395
- [14] L. Susskind, *Phys. Rev.* **D16** (1977) 3031
- [15] M. A. Shifman, A. I. Vainshtein, V. I. Zakharov, *Nucl. Phys.* **B147** (1979) 385,448
- [16] M. Gell-Mann, Caltech Report CTSL-20 (1961)
- [17] Y. Ne'eman, *Nucl. Phys.* **B26** (1961) 222
- [18] M. Gell-Mann, *Phys. Lett.* **8** (1964) 214
- [19] G. Zweig, CERN preprint 8419/TH.412; 8182/TH.401 (1964)
- [20] O. W. Greenberg, *Phys. Rev. Lett.* **13** (1964) 598

- [21] M. Han and Y. Nambu, *Phys. Rev.* **B139** (1965) 1006
- [22] R. H. Dalitz and D. G. Sutherland, *Phys. Rev.* **146** (1966) 1180
- [23] Morpurgo, *Physics* **2** (1965) 95
- [24] Morpurgo, In *Theory and Phenomenology in Particle Physics*, Part A, edited by A. Zichichi. New York:Academic Press (1969)
- [25] R. P. Feynman, M. Kislinger, and F. Ravndal *Phys. Rev.* **D3** (1971) 2706
- [26] J. J. Kokkedee, *The Quark Model*. Amsterdam: Benjamin (1969)
- [27] N. Isgur, *Int. J. Mod. Phys.* **E1** Vol.1, No.3 (1992) 465
- [28] A. De Rujula, H. Georgi, and S. L. Glashow, *Phys. Rev.* **D12** (1975) 147
- [29] T. Appelquist, A. De Rujula, and H. D. Politzer, *Phys. Rev. Lett.* **34** (1975) 365
- [30] T. Appelquist and H. D. Politzer, *Phys. Rev. Lett.* **34** (1975) 43
- [31] T. Appelquist and H. D. Politzer, *Phys. Rev.* **D12** (1975) 1404
- [32] E. Eichten *et al.* *Phys. Rev. Lett.* **34** (1975) 369
- [33] N. Isgur and G. Karl, *Phys. Lett.* **72B** (1977) 109
- [34] N. Isgur and G. Karl, *Phys. Rev.* **D18** (1978) 4187
- [35]] N. Isgur and G. Karl, *Phys. Rev.* **D19** (1979) 2653
- [36] S. Godfrey and N. Isgur, *Phys. Rev.* **D32** (1985) 189
- [37] S. Capstick and N. Isgur, *Phys. Rev.* **D34** (1986) 2809
- [38] S. Capstick and W. Roberts, (2000) nucl-th/0008028
- [39] S. Godfrey and J. Napolitano, *Rev. Mod. Phys.* **71** (1999) 1411
- [40] D. Blaschke, personal communication.

- [41] K. Seth, personal communication.
- [42] P. R. Page, T. Goldman, and J. N. Ginocchio, *Phys. Rev. Lett.* **86** (2001) 204
- [43] G. Bali, K. Schilling, A. Wachter, *Phys. Rev. bf D56* (1997) 2566
- [44] N. Isgur, *Phys. Rev. bf D62* (2000) 014025
- [45] N. Isgur, *Phys. Rev. bf D62* (2000) 054026
- [46] Yu. S. Kalashnikova and A. V. Nefediev, *Phys. Lett.* **414B** (1997) 149
- [47] N. Isgur and H. B. Thacker, *Phys. Rev. bf D64* (2001) 094507
- [48] A. LeYaouanc, L. Oliver, O. Pene, J.-C. Raynal, "Hadron Transitions in the Quark Model", Gordon and Breach Science Publishers, Amsterdam, 1988, ISBN 2-88124-214-6
- [49] S. Okubo *Phys. Lett.* **5** (1963) 165
- [50] G. Zweig (1964) *op. cit.*
- [51] J. Iizuka *prog. Theor. Phys. Suppl.* **37,38** (1966) 21
- [52] K. Hashimoto, *Phys. Rev.* **C29** (1984) 1377
- [53] C. B. Dover and G. E. Walker, *Phys. Rep.* **89** (1982) 1
- [54] Hyslop, Arndt, Roper, and Workman *Phys. Rev.* **D46** (1992) 961
- [55] J. Watts *et al.*, *Phys. Lett.* **95B** (1980) 323
- [56] K. Nakajima *et al.*, *Phys. Lett.* **112B** (1982) 80
- [57] B. Martin and G. C. Oades, contributed paper IVth Int. Conf. on Baryon Resonances (Toronto, 1980)
- [58] S. Lemaire, J. Labarsouque, B. and Silvestre-Brac, *Nucl. Phys.* **A696** (2001) 497
- [59] D. Mukhopadhyay and H. J. Pirner, *Nucl. Phys.* **A442** (1985) 605

- [60] E. A. Veit, A. W. Thomas, and B. K. Jennings, *Phys. Rev.* **D31** (1985) 2242
- [61] I. Bender, H. G. Dosch, H. J. Pirner, and H. G. Kruse, *Nucl. Phys.* **A414** (1984) 359
- [62] R. K. Campbell and D. Robson, *Phys. Rev.* **D36** (1987) 2682
- [63] M. Oka and K. Yazaki *Phys. Lett.* **90B** (1980) 41
- [64] K. Yazaki, *Nucl. Phys.* **A416** (1984) 87C
- [65] Particle Data Group, *Eur. Phys. J.* **C15** (2000) 1
- [66] C. Amsler and F. Close, *Phys. Rev.* **D53** 295
- [67] T. Barnes and E. S. Swanson, *Phys. Rev.* **D46** (1992) 131
- [68] T. Barnes, E. S. Swanson, and J. Weinstein, *Phys. Rev.* **D46** (1992) 4868
- [69] T. Barnes and E. S. Swanson *Phys. Rev.* **C49** (1994) 1166
- [70] T. Barnes, S. Capstick, M. D. Kovarik, and E. S. Swanson *Phys. Rev.* **C48** (1993) 539
- [71] T. Barnes, N. Black, and E. S. Swanson, *Phys. Rev.* **C63** (2001) 025204
- [72] A. Valcarce, A. Buchmann, F. Fernández, and A. Faessler, *Phys. Rev.* **C51** (1995) 1480
- [73] A. Faessler, *J. Phys.* **G27** (2001) 1851
- [74] A. R. Edmonds, "Angular Momentum in Quantum Mechanics", Princeton Univ. Press (1957)
- [75] D. A. Varshalovich, A. N. Moskalev, and V. K. Khersonskii, "Quantum Theory of Angular Momentum", World Scientific (1988)
- [76] T. Matsui and H. Satz, *Phys. Lett.* **178B** (1986) 416

- [77] D. Kharzeev and H. Satz, *Phys. Lett.* **334B** (1994) 155
- [78] D. Kharzeev, H. Satz, A. Syamtomov, and G. Zinovjev, *Phys. Lett.* **389B** (1996) 595
- [79] T. Barnes, E. S. Swanson, and C. Y. Wong, in *Proceedings of Heavy Quark Physics 5*, Dubna, Russia (2000)
- [80] Gupta *et al.* [81] have calculated the $\pi - \pi$ scattering amplitude at threshold, which is related by means of the Luscher formula [82, 83] to the volume dependence of the energy levels of two pions confined in a large box.
- [81] R. Gupta, A. Patel, and S. R. Sharpe, *Nucl. Phys. Proc. Suppl.* **34** (1994) 335
- [82] M. Luscher, *Commun. Math. Phys.* **104** (1986) 177; **105** (1986) 153
- [83] M. Luscher, *Nucl. Phys.* **354** (1991) 531
- [84] For a review see J. I. Friedman, H. W. Kendall, and R. E. Taylor, *Rev. Mod. Phys.* **63** (1991) 573
- [85] J. D. Bjorken and E. A. Paschos, *Phys. Rev.* **185** (1969) 1975
- [86] For discussions of the development of the parton model see F. E. Close, *An Introduction to Quarks and Partons*, Academic, New York, 1979, and R. P. Feynman, *Photon-Hadron Interactions*, Benjamin, Reading, Massachusetts, 1972.
- [87] N. Isgur and J. Paton, *Phys. Lett.* **124B** (1983) 247
- [88] N. Isgur and J. Paton, *Phys. Rev.* **D31** (1985) 2910
- [89] N. Isgur, R. Kokoski, and J. Paton, *Phys. Rev. Lett.* **54** (1985) 869

Appendix

A Vectors and Spherical Tensors

A physical vector \vec{S} may be expanded in terms of its spherical components S_μ and the spherical basis vectors $\hat{\mathbf{e}}_\mu$:

$$\vec{S} = \sum_{\mu} (-)^{\mu} S_{\mu} \hat{\mathbf{e}}_{\mu} \quad (155)$$

$$S_{\mu} = \vec{S} \cdot \hat{\mathbf{e}}_{\mu}. \quad (156)$$

The $\hat{\mathbf{e}}_{\mu}$ obey the orthonormality condition

$$\hat{\mathbf{e}}_{\mu} \cdot \hat{\mathbf{e}}_{-\nu} = (-)^{\mu} \delta_{\mu\nu}. \quad (157)$$

The matrix elements of the spin operators are related to the CG coefficients by

$$(S_{\mu})_{\lambda'\lambda} = \sqrt{S(S+1)} C_{S\lambda 1\mu}^{S\lambda'}. \quad (158)$$

It is convenient to have the cartesian components of the T^{LM} . Note that the cartesian indices serve only to keep track of the quarks (i for quark 1, j for quark 2); we could equally well rely on the ordering of the spherical basis vectors in the following expressions. Explicitly, we have for $L = 0, 1$, and 2

$$\hat{T}_{ij}^{00} = - \frac{\hat{\mathbf{z}}_i \hat{\mathbf{z}}_j - \hat{\mathbf{p}}_i \hat{\mathbf{m}}_j - \hat{\mathbf{m}}_i \hat{\mathbf{p}}_j}{\sqrt{3}} = - \frac{1}{\sqrt{3}} \delta_{ij} \quad (159)$$

$$\hat{T}_{ij}^{11} = \frac{\hat{\mathbf{z}}_i \hat{\mathbf{m}}_j - \hat{\mathbf{m}}_i \hat{\mathbf{z}}_j}{\sqrt{2}} \quad (160)$$

$$\hat{T}_{ij}^{10} = \frac{\hat{\mathbf{m}}_i \hat{\mathbf{p}}_j - \hat{\mathbf{p}}_i \hat{\mathbf{m}}_j}{\sqrt{2}} \quad (161)$$

$$\hat{T}_{ij}^{1-1} = \frac{\hat{\mathbf{p}}_i \hat{\mathbf{z}}_j - \hat{\mathbf{z}}_i \hat{\mathbf{p}}_j}{\sqrt{2}} \quad (162)$$

$$\hat{T}_{ij}^{22} = \hat{\mathbf{m}}_i \hat{\mathbf{m}}_j \quad (163)$$

$$\hat{T}_{ij}^{21} = - \frac{\hat{\mathbf{z}}_i \hat{\mathbf{m}}_j + \hat{\mathbf{m}}_i \hat{\mathbf{z}}_j}{\sqrt{2}} \quad (164)$$

$$\hat{T}_{ij}^{20} = \frac{2 \hat{\mathbf{z}}_i \hat{\mathbf{z}}_j + \hat{\mathbf{m}}_i \hat{\mathbf{p}}_j + \hat{\mathbf{p}}_i \hat{\mathbf{m}}_j}{\sqrt{6}} \quad (165)$$

$$\hat{T}_{ij}^{2-1} = - \frac{\hat{\mathbf{p}}_i \hat{\mathbf{z}}_j + \hat{\mathbf{z}}_i \hat{\mathbf{p}}_j}{\sqrt{2}} \quad (166)$$

$$\hat{T}_{ij}^{2-2} = \hat{\mathbf{p}}_i \hat{\mathbf{p}}_j. \quad (167)$$

B Integrals

$$\int d^3p \mathbf{p} e^{-a(\mathbf{p}-\mathbf{p}_0)^2} = \mathbf{p}_0 \left(\frac{\pi}{a} \right)^{3/2} \quad (168)$$

$$\int d^3p p^2 e^{-a(\mathbf{p}-\mathbf{p}_0)^2} = \left(\frac{\pi}{a} \right)^{3/2} \left[\frac{3}{2a} + p_0^2 \right] \quad (169)$$

$$\int d^3p p_i p_j e^{-a(\mathbf{p}-\mathbf{p}_0)^2} = \left(\frac{\pi}{a} \right)^{3/2} \left[p_{0i} p_{0j} + \frac{\delta_{ij}}{2a} \right] \quad (170)$$

$$\int d^3q e^{-a(\mathbf{q}-\mathbf{q}_0)^2} \cdot \frac{1}{q^2} = 2 \frac{\pi^{3/2}}{a^{1/2}} f_{\frac{1}{2}, \frac{3}{2}}(aq_0^2) e^{-aq_0^2} \quad (171)$$

$$\int d^3q e^{-a(\mathbf{q}-\mathbf{q}_0)^2} \cdot \frac{q_i}{q^2} = \frac{2}{3} \frac{\pi^{3/2}}{a^{1/2}} q_{0i} f_{\frac{3}{2}, \frac{5}{2}}(aq_0^2) e^{-aq_0^2} \quad (172)$$

$$\int d^3q e^{-a(\mathbf{q}-\mathbf{q}_0)^2} \cdot \frac{q_i q_j}{q^2} = \frac{\pi^{3/2}}{a^{1/2}} \left[\frac{1}{3a} \delta_{ij} f_{\frac{3}{2}, \frac{5}{2}}(aq_0^2) + \frac{2}{5} q_{0i} q_{0j} f_{\frac{5}{2}, \frac{7}{2}}(aq_0^2) \right] e^{-aq_0^2} \quad (173)$$

$$\int d^3q e^{-a(\mathbf{q}-\mathbf{q}_0)^2} \cdot \frac{1}{q^4} = -4 a^{1/2} \pi^{3/2} f_{-\frac{1}{2}, \frac{3}{2}}(aq_0^2) e^{-aq_0^2} \quad (174)$$

$$\int d^3q e^{-a(\mathbf{q}-\mathbf{q}_0)^2} \cdot \frac{q_i}{q^4} = \frac{4}{3} a^{1/2} \pi^{3/2} q_{0i} f_{\frac{1}{2}, \frac{5}{2}}(aq_0^2) e^{-aq_0^2} \quad (175)$$

$$\int d^3q e^{-a(\mathbf{q}-\mathbf{q}_0)^2} \cdot \frac{q_i q_j}{q^4} = \frac{\pi^{3/2}}{a^{1/2}} \left[\frac{2}{3} \delta_{ij} f_{\frac{1}{2}, \frac{5}{2}}(aq_0^2) + \frac{4}{15} a q_{0i} q_{0j} f_{\frac{3}{2}, \frac{7}{2}}(aq_0^2) \right] e^{-aq_0^2} \quad (176)$$

C KN, K^*N Space Amplitudes

C.1 Reduced Forms

$$T_{space}^{D_1} = \eta e^{f(\mathbf{A}, \mathbf{C})} \int d^3 q \int d^3 P e^{-a_P(\mathbf{P}-\mathbf{P}_0)^2} e^{-a_q(\mathbf{q}-\mathbf{q}_0)^2} T_{fi}^{qq}(\mathbf{q}, \mathbf{P}, \mathbf{P} + \mathbf{C} - \mathbf{A})$$

$$\eta = \frac{3^{3/2}}{2^{3/2} \pi^3 \beta^3 \alpha_\rho^3}$$

$$f(\mathbf{A}, \mathbf{C}) = - \left[\frac{2 (\rho + 1)^2 \beta^2 + 3 \alpha_\rho^2}{12 (\rho + 1)^2 \beta^2 \alpha_\rho^2} \right] (\mathbf{A} - \mathbf{C})^2$$

$$a_P = \frac{3}{2 \alpha_\rho^2} + \frac{1}{\beta^2}$$

$$a_q = \frac{3}{2 \alpha_\rho^2 + 3 \beta^2}$$

$$\begin{aligned} \mathbf{P}_0 = & \left\{ \left[2 (\rho + 1) \beta^2 + 2 (2\rho + 1) \alpha_\rho^2 \right] \mathbf{A} \right. \\ & - \left[4 (\rho + 1) \beta^2 + 2 \alpha_\rho^2 \right] \mathbf{C} \\ & + (\rho + 1) \left[-3 \beta^2 + 2 \alpha_\rho^2 \right] \mathbf{q} \left. \right\} \\ & \left\{ (\rho + 1) \left[6 \beta^2 + 4 \alpha_\rho^2 \right] \right\}^{-1} \end{aligned}$$

$$\mathbf{q}_0 = - \frac{(4\rho + 1)}{6(\rho + 1)} (\mathbf{A} + \mathbf{C}) \quad (177)$$

$$\begin{aligned} T_{space}^{D_2} = & \eta e^{f(\mathbf{A}, \mathbf{C})} \int d^3 q \int d^3 P \int d^3 P' e^{-a'_P(\mathbf{P}'-\mathbf{P}'_0)^2} e^{-a_P(\mathbf{P}-\mathbf{P}_0)^2} \\ & e^{-a_q(\mathbf{q}-\mathbf{q}_0)^2} T_{fi}^{qq}(\mathbf{q}, \mathbf{P}, \mathbf{P}') \end{aligned}$$

$$\eta = \frac{3^{3/2}}{\pi^{9/2} \beta^3 \alpha_\rho^6}$$

$$\begin{aligned} f(\mathbf{A}, \mathbf{C}) = & \left\{ - \left[21 \alpha_\rho^4 + 2 (8\rho^2 + \rho + 11) \alpha_\rho^2 \beta^2 + 3 (\rho + 1)^2 \beta^4 \right] \mathbf{A}^2 \right. \\ & + \left[42 \alpha_\rho^4 - 48 (\rho^2 - 1) \alpha_\rho^2 \beta^2 + 6 (\rho + 1)^2 \beta^4 \right] \mathbf{A} \cdot \mathbf{C} \\ & - \left[21 \alpha_\rho^4 + 2 (32\rho^2 + 31 \rho + 17) \alpha_\rho^2 \beta^2 + 3 (\rho + 1)^2 \beta^4 \right] \mathbf{C}^2 \Big\} \\ & \left\{ 12 (\rho + 1)^2 \alpha_\rho^2 \beta^2 \left[6 \beta^2 + 7 \alpha_\rho^2 \right] \right\}^{-1} \end{aligned}$$

$$a_P = \frac{3}{2 \alpha_\rho^2} + \frac{1}{\beta^2}$$

$$a_{P'} = \frac{2}{\alpha_\rho^2}$$

$$a_q = \frac{7 \alpha_\rho^2 + 6 \beta^2}{4 \alpha_\rho^2 (2 \alpha_\rho^2 + 3 \beta^2)}$$

$$\begin{aligned} \mathbf{P}_0 = & \left\{ \left[(\rho + 1) \beta^2 + (2\rho + 1) \alpha_\rho^2 \right] \mathbf{A} \right. \\ & - \left[2 (\rho + 1) \beta^2 + \alpha_\rho^2 \right] \mathbf{C} \\ & + (\rho + 1) \alpha_\rho^2 \mathbf{q} \Big\} \\ & \left\{ (\rho + 1) \left[3 \beta^2 + 2 \alpha_\rho^2 \right] \right\}^{-1} \end{aligned}$$

$$\mathbf{P}'_0 = - \frac{\mathbf{P} + \mathbf{C}}{2}$$

$$\begin{aligned} \mathbf{q}_0 = & \left\{ -3 \left[(\rho + 1) \beta^2 + (2\rho + 1) \alpha_\rho^2 \right] \mathbf{A} \right. \\ & + \left[3 (\rho + 1) \beta^2 + (-2\rho + 1) \alpha_\rho^2 \right] \mathbf{C} \Big\} \\ & \left\{ (\rho + 1) \left[6 \beta^2 + 7 \alpha_\rho^2 \right] \right\}^{-1} \end{aligned} \tag{178}$$

$$T_{space}^{D_3} = \eta e^{f(\mathbf{A}, \mathbf{C})} \int d^3 q \int d^3 P e^{-a_P (\mathbf{P} - \mathbf{P}_0)^2} e^{-a_q (\mathbf{q} - \mathbf{q}_0)^2} T_{fi}^{qq}(\mathbf{q}, \mathbf{P}, \mathbf{C} - \mathbf{P})$$

$$\eta = \frac{3^{3/2}}{2^{3/2} \pi^3 \beta^3 \alpha_\rho^3}$$

$$\begin{aligned} f(\mathbf{A}, \mathbf{C}) = & \left\{ - \left[(5\rho^2 - 2\rho + 2) \alpha_\rho^2 + 3 (\rho + 1)^2 \beta^2 \right] \mathbf{A}^2 \right. \\ & + \left[-6 (\rho^2 - 1) \alpha_\rho^2 + 6 (\rho + 1)^2 \beta^2 \right] \mathbf{A} \cdot \mathbf{C} \\ & - (\rho + 1)^2 \left[5 \alpha_\rho^2 + 3 \beta^2 \right] \mathbf{C}^2 \Big\} \\ & \left\{ 6 (\rho + 1)^2 \alpha_\rho^2 \left[3 \beta^2 + \alpha_\rho^2 \right] \right\}^{-1} \end{aligned}$$

$$a_P = \frac{3}{2 \alpha_\rho^2} + \frac{1}{\beta^2}$$

$$a_q = \frac{3\beta^2 + \alpha_\rho^2}{2 \beta^2 (2 \alpha_\rho^2 + 3 \beta^2)}$$

$$\begin{aligned} \mathbf{P}_0 = & \left\{ \left[4 (\rho + 1) \beta^2 + 2 \alpha_\rho^2 \right] (\mathbf{A} + \mathbf{C}) \right. \\ & + 3 (\rho + 1) \beta^2 \mathbf{q} \Big\} \\ & \left\{ (\rho + 1) \left[6 \beta^2 + 4 \alpha_\rho^2 \right] \right\}^{-1} \end{aligned}$$

$$\begin{aligned} \mathbf{q}_0 = & \left\{ - \left[2 (\rho + 1) \beta^2 + \alpha_\rho^2 \right] \mathbf{A} \right. \\ & + \left[(-2\rho + 1) \beta^2 + \alpha_\rho^2 \right] \mathbf{C} \Big\} \\ & \left\{ (\rho + 1) \left[3 \beta^2 + \alpha_\rho^2 \right] \right\}^{-1} \end{aligned} \tag{179}$$

$$T_{space}^{D_4} = \eta e^{f(\mathbf{A}, \mathbf{C})} \int d^3 q \int d^3 P \int d^3 P' e^{-a'_{P'}(\mathbf{P}' - \mathbf{P}'_0)^2} e^{-a_P(\mathbf{P} - \mathbf{P}_0)^2} e^{-a_q(\mathbf{q} - \mathbf{q}_0)^2} T_{fi}^{qq}(\mathbf{q}, \mathbf{P}, \mathbf{P}')$$

$$\eta = \frac{3^{3/2}}{\pi^{9/2} \beta^3 \alpha_\rho^6}$$

$$\begin{aligned} f(\mathbf{A}, \mathbf{C}) = & \left\{ - \left[(20\rho^2 + 4\rho + 5) \alpha_\rho^4 + 2 (20\rho^2 + 7\rho + 5) \alpha_\rho^2 \beta^2 \right. \right. \\ & + 3 (\rho + 1)^2 \beta^4 \left. \right] (\mathbf{A}^2 + \mathbf{C}^2) \\ & + \left[-6 (4\rho^2 + 4\rho - 1) \alpha_\rho^4 - 12 (\rho + 1) (4\rho - 1) \alpha_\rho^2 \beta^2 \right. \\ & + 6 (\rho + 1)^2 \beta^4 \left. \right] \mathbf{A} \cdot \mathbf{C} \left. \right\} \\ & \left\{ 12 (\rho + 1)^2 \alpha_\rho^2 \left[6 \beta^4 + 7 \alpha_\rho^2 \beta^2 + 2 \alpha_\rho^4 \right] \right\}^{-1} \end{aligned}$$

$$a_P = \frac{3}{2 \alpha_\rho^2} + \frac{1}{\beta^2}$$

$$a_{P'} = \frac{2}{\alpha_\rho^2}$$

$$a_q = \frac{1}{2 \alpha_\rho^2} + \frac{1}{4 \beta^2}$$

$$\mathbf{P}_0 = \frac{\left[2 (\rho + 1) \beta^2 + \alpha_\rho^2 \right]}{(\rho + 1) \left[3 \beta^2 + 2 \alpha_\rho^2 \right]} (\mathbf{A} + \mathbf{C})$$

$$\mathbf{P}'_0 = \frac{\mathbf{P} - \mathbf{A} - \mathbf{C}}{2}$$

$$\mathbf{q}_0 = \frac{\left[(\rho + 1) \beta^2 + \alpha_\rho^2 \right]}{(\rho + 1) \left[2 \beta^2 + \alpha_\rho^2 \right]} (\mathbf{C} - \mathbf{A}) \quad (180)$$

C.2 Explicit Amplitudes

C.2.1 Spin-spin

$$T_{space}^{(D1)}(\text{hfs}) = -\frac{2^3}{3} \frac{\pi \alpha_s}{m^2} \exp \left\{ -\frac{[3 \alpha_\rho^2 + 2 (\rho+1)^2 \beta^2] (\mathbf{A} - \mathbf{C})^2}{12 (\rho+1)^2 \alpha_\rho^2 \beta^2} \right\} \quad (181)$$

$$T_{space}^{(D2)}(\text{hfs}) = -\frac{2^6 3^{1/2} \pi \alpha_s}{m^2} \frac{\alpha_\rho^3}{(7 \alpha_\rho^2 + 6 \beta^2)^{3/2}} \exp \left\{ \begin{aligned} & - [21 \alpha_\rho^4 + (16\rho^2 + 2\rho + 22) \alpha_\rho^2 \beta^2 + 3 (\rho+1)^2 \beta^4] \mathbf{A}^2 \\ & + 6 [7 \alpha_\rho^4 - 8 (\rho^2 - 1) \alpha_\rho^2 \beta^2 + (\rho+1)^2 \beta^4] \mathbf{A} \cdot \mathbf{C} \\ & - [21 \alpha_\rho^4 + (64\rho^2 + 62\rho + 34) \alpha_\rho^2 \beta^2 + 3 (\rho+1)^2 \beta^4] \mathbf{C}^2 \end{aligned} \right\} \\ \left\{ 12 (\rho+1)^2 (7 \alpha_\rho^2 + 6 \beta^2) \alpha_\rho^2 \beta^2 \right\}^{-1} \quad (182)$$

$$T_{space}^{(D3)}(\text{hfs}) = -\frac{2^{9/2} 3^{1/2} \pi \alpha_s \rho}{m^2} \frac{\beta^3}{(\alpha_\rho^2 + 3 \beta^2)^{3/2}} \exp \left\{ \begin{aligned} & - [(5\rho^2 - 2\rho + 2) \alpha_\rho^2 + 3 (\rho+1)^2 \beta^2] \mathbf{A}^2 \\ & - 6 [(\rho^2 - 1) \alpha_\rho^2 - (\rho+1)^2 \beta^2] \mathbf{A} \cdot \mathbf{C} \\ & - (\rho+1)^2 [5 \alpha_\rho^2 + 3 \beta^2] \mathbf{C}^2 \end{aligned} \right\} \\ \left\{ 6 (\rho+1)^2 (\alpha_\rho^2 + 3 \beta^2) \alpha_\rho^2 \right\}^{-1} \quad (183)$$

$$T_{space}^{(D4)}(\text{hfs}) = -\frac{2^6 3^{1/2} \pi \alpha_s \rho}{m^2} \frac{\alpha_\rho^3 \beta^3}{(2 \alpha_\rho^2 + 3 \beta^2)^{3/2} (\alpha_\rho^2 + 2 \beta^2)^{3/2}} \exp \left\{ \begin{aligned} & - [(20\rho^2 + 4\rho + 5) \alpha_\rho^4 + (40\rho^2 + 14\rho + 10) \alpha_\rho^2 \beta^2 \\ & + 3 (\rho+1)^2 \beta^4] (\mathbf{A}^2 + \mathbf{C}^2) \\ & - 6 [(4\rho^2 + 4\rho - 1) \alpha_\rho^4 + 2 (\rho+1) (4\rho - 1) \alpha_\rho^2 \beta^2 \\ & - (\rho+1)^2 \beta^4] \mathbf{A} \cdot \mathbf{C} \end{aligned} \right\} \\ \left\{ 12 (\rho+1)^2 (\alpha_\rho^2 + 2 \beta^2) (2 \alpha_\rho^2 + 3 \beta^2) \alpha_\rho^2 \right\}^{-1} \quad (184)$$

C.2.2 Coulomb

$$\begin{aligned}
T_{space}^{(D1)}(\text{coul}) &= \frac{2^3 3 \pi \alpha_s}{(2 \alpha_\rho^2 + 3 \beta^2)} \\
f_{1/2,3/2} &\left\{ \frac{(4\rho + 1)^2 (\mathbf{A} + \mathbf{C})^2}{12 (\rho + 1)^2 (2 \alpha_\rho^2 + 3 \beta^2)} \right\} \\
&\exp\left\{ \left\{ - \left[3 \alpha_\rho^4 + (10\rho^2 + 8\rho + 7) \alpha_\rho^2 \beta^2 + 3 (\rho + 1)^2 \beta^4 \right] (\mathbf{A}^2 + \mathbf{C}^2) \right. \right. \\
&\quad \left. \left. + \left[-6 \alpha_\rho^4 + 12 (\rho^2 - 1) \alpha_\rho^2 \beta^2 - 6 (\rho + 1)^2 \beta^4 \right] \mathbf{A} \cdot \mathbf{C} \right\} \right. \\
&\quad \left. \left\{ 6 (\rho + 1)^2 (2 \alpha_\rho^2 + 3 \beta^2) \alpha_\rho^2 \beta^2 \right\}^{-1} \right\} \tag{185}
\end{aligned}$$

$$\begin{aligned}
T_{space}^{(D2)}(\text{coul}) &= \frac{2^4 3^{3/2} \pi \alpha_s \alpha_\rho}{(2 \alpha_\rho^2 + 3 \beta^2) (7 \alpha_\rho^2 + 6 \beta^2)^{1/2}} \\
f_{1/2,3/2} &\left\{ \left\{ 3 \left[(2\rho + 1) \alpha_\rho^2 + (\rho + 1) \beta^2 \right] \mathbf{A} \right. \right. \\
&\quad \left. \left. + \left[(2\rho - 1) \alpha_\rho^2 - 3 (\rho + 1) \beta^2 \right] \mathbf{C} \right\}^2 \right. \\
&\quad \left. \left\{ 4 (\rho + 1)^2 (7 \alpha_\rho^2 + 6 \beta^2) (2 \alpha_\rho^2 + 3 \beta^2) \alpha_\rho^2 \right\}^{-1} \right\} \\
&\exp\left\{ \left\{ - \left[3 \alpha_\rho^4 + (10\rho^2 + 8\rho + 7) \alpha_\rho^2 \beta^2 + 3 (\rho + 1)^2 \beta^4 \right] (\mathbf{A}^2 + \mathbf{C}^2) \right. \right. \\
&\quad \left. \left. + \left[-6 \alpha_\rho^4 + 12 (\rho^2 - 1) \alpha_\rho^2 \beta^2 - 6 (\rho + 1)^2 \beta^4 \right] \mathbf{A} \cdot \mathbf{C} \right\} \right. \\
&\quad \left. \left\{ 6 (\rho + 1)^2 (2 \alpha_\rho^2 + 3 \beta^2) \alpha_\rho^2 \beta^2 \right\}^{-1} \right\} \tag{186}
\end{aligned}$$

$$\begin{aligned}
T_{space}^{(D3)}(\text{coul}) &= \frac{2^{7/2} 3^{3/2} \pi \alpha_s \beta}{(2 \alpha_\rho^2 + 3 \beta^2) (\alpha_\rho^2 + 3 \beta^2)^{1/2}} \\
f_{1/2,3/2} &\left\{ \frac{\left(\left[\alpha_\rho^2 + 2 (\rho + 1) \beta^2 \right] \mathbf{A} + \left[-\alpha_\rho^2 + (2\rho - 1) \beta^2 \right] \mathbf{C} \right)^2}{2 (\rho + 1)^2 (\alpha_\rho^2 + 3 \beta^2) (2 \alpha_\rho^2 + 3 \beta^2) \beta^2} \right\} \\
&\exp\left\{ \left\{ - \left[3 \alpha_\rho^4 + (10\rho^2 + 8\rho + 7) \alpha_\rho^2 \beta^2 + 3 (\rho + 1)^2 \beta^4 \right] (\mathbf{A}^2 + \mathbf{C}^2) \right. \right. \\
&\quad \left. \left. + \left[-6 \alpha_\rho^4 + 12 (\rho^2 - 1) \alpha_\rho^2 \beta^2 - 6 (\rho + 1)^2 \beta^4 \right] \mathbf{A} \cdot \mathbf{C} \right\} \right. \\
&\quad \left. \left\{ 6 (\rho + 1)^2 (2 \alpha_\rho^2 + 3 \beta^2) \alpha_\rho^2 \beta^2 \right\}^{-1} \right\} \tag{187}
\end{aligned}$$

$$\begin{aligned}
T_{space}^{(D4)}(\text{coul}) &= \frac{2^4 3^{3/2} \pi \alpha_s \alpha_\rho \beta}{(2 \alpha_\rho^2 + 3 \beta^2)^{3/2} (\alpha_\rho^2 + 2 \beta^2)^{1/2}} \\
& f_{1/2,3/2} \left\{ \frac{[\alpha_\rho^2 + (\rho + 1) \beta^2]^2 (\mathbf{A} - \mathbf{C})^2}{4 (\rho + 1)^2 (\alpha_\rho^2 + 2 \beta^2) \alpha_\rho^2 \beta^2} \right\} \\
& \exp \left\{ \left\{ - \left[3 \alpha_\rho^4 + (10\rho^2 + 8\rho + 7) \alpha_\rho^2 \beta^2 + 3 (\rho + 1)^2 \beta^4 \right] (\mathbf{A}^2 + \mathbf{C}^2) \right. \right. \\
& \quad \left. \left. + \left[-6 \alpha_\rho^4 + 12 (\rho^2 - 1) \alpha_\rho^2 \beta^2 - 6 (\rho + 1)^2 \beta^4 \right] \mathbf{A} \cdot \mathbf{C} \right\} \right. \\
& \quad \left. \left\{ 6 (\rho + 1)^2 (2 \alpha_\rho^2 + 3 \beta^2) \alpha_\rho^2 \beta^2 \right\}^{-1} \right\} \quad (188)
\end{aligned}$$

C.2.3 Linear

$$\begin{aligned}
T_{space}^{(D1)}(\text{lin}) &= - \frac{2^3 3^3 \pi b}{(2 \alpha_\rho^2 + 3 \beta^2)^2} \\
& f_{-1/2,3/2} \left\{ \frac{(4\rho + 1)^2 (\mathbf{A} + \mathbf{C})^2}{12 (\rho + 1)^2 (2 \alpha_\rho^2 + 3 \beta^2)} \right\} \\
& \exp \left\{ \left\{ - \left[3 \alpha_\rho^4 + (10\rho^2 + 8\rho + 7) \alpha_\rho^2 \beta^2 + 3 (\rho + 1)^2 \beta^4 \right] (\mathbf{A}^2 + \mathbf{C}^2) \right. \right. \\
& \quad \left. \left. + \left[-6 \alpha_\rho^4 + 12 (\rho^2 - 1) \alpha_\rho^2 \beta^2 - 6 (\rho + 1)^2 \beta^4 \right] \mathbf{A} \cdot \mathbf{C} \right\} \right. \\
& \quad \left. \left\{ 6 (\rho + 1)^2 (2 \alpha_\rho^2 + 3 \beta^2) \alpha_\rho^2 \beta^2 \right\}^{-1} \right\} \quad (189)
\end{aligned}$$

$$\begin{aligned}
T_{space}^{(D2)}(\text{lin}) &= - 2^2 3^{5/2} \pi b \frac{(7 \alpha_\rho^2 + 6 \beta^2)^{1/2}}{\alpha_\rho (2 \alpha_\rho^2 + 3 \beta^2)^2} \\
& f_{-1/2,3/2} \left\{ \left\{ 3 \left[(2\rho + 1) \alpha_\rho^2 + (\rho + 1) \beta^2 \right] \mathbf{A} \right. \right. \\
& \quad \left. \left. + \left[(2\rho - 1) \alpha_\rho^2 - 3 (\rho + 1) \beta^2 \right] \mathbf{C} \right\}^2 \right. \\
& \quad \left. \left\{ 4 (\rho + 1)^2 (7 \alpha_\rho^2 + 6 \beta^2) (2 \alpha_\rho^2 + 3 \beta^2) \alpha_\rho^2 \right\}^{-1} \right\} \\
& \exp \left\{ \left\{ - \left[3 \alpha_\rho^4 + (10\rho^2 + 8\rho + 7) \alpha_\rho^2 \beta^2 + 3 (\rho + 1)^2 \beta^4 \right] (\mathbf{A}^2 + \mathbf{C}^2) \right. \right. \\
& \quad \left. \left. + \left[-6 \alpha_\rho^4 + 12 (\rho^2 - 1) \alpha_\rho^2 \beta^2 - 6 (\rho + 1)^2 \beta^4 \right] \mathbf{A} \cdot \mathbf{C} \right\} \right. \\
& \quad \left. \left\{ 6 (\rho + 1)^2 (2 \alpha_\rho^2 + 3 \beta^2) \alpha_\rho^2 \beta^2 \right\}^{-1} \right\} \quad (190)
\end{aligned}$$

$$\begin{aligned}
T_{space}^{(D3)}(\text{lin}) = & - 2^{5/2} 3^{5/2} \pi \text{ b } \frac{(\alpha_\rho^2 + 3 \beta^2)^{1/2}}{\beta (2 \alpha_\rho^2 + 3 \beta^2)^2} \\
& f_{-1/2,3/2} \left\{ \frac{\left(\left[\alpha_\rho^2 + 2 (\rho + 1) \beta^2 \right] \mathbf{A} + \left[-\alpha_\rho^2 + (2\rho - 1) \beta^2 \right] \mathbf{C} \right)^2}{2 (\rho + 1)^2 (\alpha_\rho^2 + 3 \beta^2) (2 \alpha_\rho^2 + 3 \beta^2) \beta^2} \right\} \\
& \exp \left\{ \left\{ - \left[3 \alpha_\rho^4 + (10\rho^2 + 8\rho + 7) \alpha_\rho^2 \beta^2 + 3 (\rho + 1)^2 \beta^4 \right] (\mathbf{A}^2 + \mathbf{C}^2) \right. \right. \\
& \quad \left. \left. + \left[-6 \alpha_\rho^4 + 12 (\rho^2 - 1) \alpha_\rho^2 \beta^2 - 6 (\rho + 1)^2 \beta^4 \right] \mathbf{A} \cdot \mathbf{C} \right\} \right. \\
& \quad \left. \left\{ 6 (\rho + 1)^2 (2 \alpha_\rho^2 + 3 \beta^2) \alpha_\rho^2 \beta^2 \right\}^{-1} \right\} \quad (191)
\end{aligned}$$

$$\begin{aligned}
T_{space}^{(D4)}(\text{lin}) = & - 2^2 3^{5/2} \pi \text{ b } \frac{(\alpha_\rho^2 + 2 \beta^2)^{1/2}}{\alpha_\rho \beta (2 \alpha_\rho^2 + 3 \beta^2)^{3/2}} \\
& f_{-1/2,3/2} \left\{ \frac{\left[\alpha_\rho^2 + (\rho + 1) \beta^2 \right]^2 (\mathbf{A} - \mathbf{C})^2}{4 (\rho + 1)^2 (\alpha_\rho^2 + 2 \beta^2) \alpha_\rho^2 \beta^2} \right\} \\
& \exp \left\{ \left\{ - \left[3 \alpha_\rho^4 + (10\rho^2 + 8\rho + 7) \alpha_\rho^2 \beta^2 + 3 (\rho + 1)^2 \beta^4 \right] (\mathbf{A}^2 + \mathbf{C}^2) \right. \right. \\
& \quad \left. \left. + \left[-6 \alpha_\rho^4 + 12 (\rho^2 - 1) \alpha_\rho^2 \beta^2 - 6 (\rho + 1)^2 \beta^4 \right] \mathbf{A} \cdot \mathbf{C} \right\} \right. \\
& \quad \left. \left\{ 6 (\rho + 1)^2 (2 \alpha_\rho^2 + 3 \beta^2) \alpha_\rho^2 \beta^2 \right\}^{-1} \right\} \quad (192)
\end{aligned}$$

C.2.4 OGE Spin-orbit

$$\begin{aligned}
T_{space}^{(D1)}(\text{OGE } \mathbf{L} \cdot \mathbf{S}) = & + \frac{2 \pi \alpha_s}{m^2} \frac{(4\rho + 1)}{(\rho + 1)} \frac{1}{(2 \alpha_\rho^2 + 3 \beta^2)^2} \\
& (\mathbf{s}_1 + \mathbf{s}_2) \cdot i(\mathbf{A} \times \mathbf{C}) \\
& f_{3/2,5/2} \left\{ \frac{(4\rho + 1)^2 (\mathbf{A} + \mathbf{C})^2}{12 (\rho + 1)^2 (2 \alpha_\rho^2 + 3 \beta^2)} \right\} \\
& \exp \left\{ \left\{ - \left[3 \alpha_\rho^4 + (10\rho^2 + 8\rho + 7) \alpha_\rho^2 \beta^2 + 3 (\rho + 1)^2 \beta^4 \right] (\mathbf{A}^2 + \mathbf{C}^2) \right. \right. \\
& \quad \left. \left. + \left[-6 \alpha_\rho^4 + 12 (\rho^2 - 1) \alpha_\rho^2 \beta^2 - 6 (\rho + 1)^2 \beta^4 \right] \mathbf{A} \cdot \mathbf{C} \right\} \right. \\
& \quad \left. \left\{ 6 (\rho + 1)^2 (2 \alpha_\rho^2 + 3 \beta^2) \alpha_\rho^2 \beta^2 \right\}^{-1} \right\} \quad (193)
\end{aligned}$$

$$T_{space}^{(D2)}(\text{OGE } \mathbf{L} \cdot \mathbf{S}) =$$

$$\begin{aligned}
& - \frac{2^3 3^{1/2} \pi \alpha_s}{m^2 (\rho + 1) (7 \alpha_\rho^2 + 6 \beta^2)^{3/2} (2 \alpha_\rho^2 + 3 \beta^2)} \\
& \left[(2\rho + 1) \alpha_\rho^2 + (\rho + 1) \beta^2 \right] (\mathbf{s}_1 - \mathbf{s}_2) \cdot i(\mathbf{A} \times \mathbf{C}) \\
& f_{3/2,5/2} \left\{ \left\{ 3 \left[(2\rho + 1) \alpha_\rho^2 + (\rho + 1) \beta^2 \right] \mathbf{A} \right. \right. \\
& \left. \left. + \left[(2\rho - 1) \alpha_\rho^2 - 3 (\rho + 1) \beta^2 \right] \mathbf{C} \right\}^2 \right. \\
& \left. \left\{ 4 (\rho + 1)^2 (7 \alpha_\rho^2 + 6 \beta^2) (2 \alpha_\rho^2 + 3 \beta^2) \alpha_\rho^2 \right\}^{-1} \right\} \\
& \exp \left\{ \left\{ - \left[3 \alpha_\rho^4 + (10\rho^2 + 8\rho + 7) \alpha_\rho^2 \beta^2 + 3 (\rho + 1)^2 \beta^4 \right] (\mathbf{A}^2 + \mathbf{C}^2) \right. \right. \\
& \left. \left. + \left[-6 \alpha_\rho^4 + 12 (\rho^2 - 1) \alpha_\rho^2 \beta^2 - 6 (\rho + 1)^2 \beta^4 \right] \mathbf{A} \cdot \mathbf{C} \right\} \right. \\
& \left. \left\{ 6 (\rho + 1)^2 (2 \alpha_\rho^2 + 3 \beta^2) \alpha_\rho^2 \beta^2 \right\}^{-1} \right\} \quad (194)
\end{aligned}$$

$$\begin{aligned}
T_{space}^{(D3)}(\text{OGE } \mathbf{L} \cdot \mathbf{S}) & = + \frac{2^{5/2} 3^{1/2} \pi \alpha_s \rho \beta i}{m^2} (\rho + 1)^{-2} \\
& (\alpha_\rho^2 + 3 \beta^2)^{-3/2} (2 \alpha_\rho^2 + 3 \beta^2)^{-1} \\
& \left[\alpha_\rho^2 + 2 (\rho + 1) \beta^2 \right] (\rho \mathbf{s}_1 - \mathbf{s}_2) \cdot i(\mathbf{A} \times \mathbf{C}) \\
& f_{3/2,5/2} \left\{ \frac{\left(\left[\alpha_\rho^2 + 2 (\rho + 1) \beta^2 \right] \mathbf{A} + \left[-\alpha_\rho^2 + (2\rho - 1) \beta^2 \right] \mathbf{C} \right)^2}{2 (\rho + 1)^2 (\alpha_\rho^2 + 3 \beta^2) (2 \alpha_\rho^2 + 3 \beta^2) \beta^2} \right\} \\
& \exp \left\{ \left\{ - \left[3 \alpha_\rho^4 + (10\rho^2 + 8\rho + 7) \alpha_\rho^2 \beta^2 + 3 (\rho + 1)^2 \beta^4 \right] (\mathbf{A}^2 + \mathbf{C}^2) \right. \right. \\
& \left. \left. + \left[-6 \alpha_\rho^4 + 12 (\rho^2 - 1) \alpha_\rho^2 \beta^2 - 6 (\rho + 1)^2 \beta^4 \right] \mathbf{A} \cdot \mathbf{C} \right\} \right. \\
& \left. \left\{ 6 (\rho + 1)^2 (2 \alpha_\rho^2 + 3 \beta^2) \alpha_\rho^2 \beta^2 \right\}^{-1} \right\} \quad (195)
\end{aligned}$$

$$\begin{aligned}
T_{space}^{(D4)}(\text{OGE } \mathbf{L} \cdot \mathbf{S}) & = - \frac{2^3 3^{1/2} \pi \alpha_s \alpha_\rho \beta}{m^2} \\
& (\rho + 1)^{-2} (2 \alpha_\rho^2 + 3 \beta^2)^{-5/2} (\alpha_\rho^2 + 2 \beta^2)^{-3/2} \\
& \left[\alpha_\rho^2 + (\rho + 1) \beta^2 \right] \\
& \left(\left[2\rho (3\rho + 1) \alpha_\rho^2 + 2\rho (\rho + 1) (2\rho + 1) \beta^2 \right] \mathbf{s}_1 \right. \\
& \left. + \left[(6\rho + 1) \alpha_\rho^2 + (\rho + 1) (8\rho + 1) \beta^2 \right] \mathbf{s}_2 \right) \cdot i(\mathbf{A} \times \mathbf{C})
\end{aligned}$$

$$\begin{aligned}
& f_{3/2,5/2} \left\{ \frac{[\alpha_\rho^2 + (\rho+1)\beta^2]^2 (\mathbf{A} - \mathbf{C})^2}{4(\rho+1)^2 (\alpha_\rho^2 + 2\beta^2) \alpha_\rho^2 \beta^2} \right\} \\
& \exp \left\{ \left[-3\alpha_\rho^4 + (10\rho^2 + 8\rho + 7)\alpha_\rho^2 \beta^2 + 3(\rho+1)^2 \beta^4 \right] (\mathbf{A}^2 + \mathbf{C}^2) \right. \\
& \quad \left. + \left[-6\alpha_\rho^4 + 12(\rho^2 - 1)\alpha_\rho^2 \beta^2 - 6(\rho+1)^2 \beta^4 \right] \mathbf{A} \cdot \mathbf{C} \right\} \\
& \left\{ 6(\rho+1)^2 (2\alpha_\rho^2 + 3\beta^2) \alpha_\rho^2 \beta^2 \right\}^{-1} \Big\} \tag{196}
\end{aligned}$$

C.2.5 Confinement Spin-orbit

$$\begin{aligned}
& T_{space}^{(D1)}(\text{lin } \mathbf{L} \cdot \mathbf{S}) = \\
& - \frac{2 \cdot 3 \pi b}{m^2} \frac{(4\rho+1)}{(\rho+1)} \frac{1}{(2\alpha_\rho^2 + 3\beta^2)^2} \\
& (\mathbf{s}_1 + \mathbf{s}_2) \cdot i(\mathbf{A} \times \mathbf{C}) \\
& f_{1/2,5/2} \left\{ \frac{(4\rho+1)^2 (\mathbf{A} + \mathbf{C})^2}{12(\rho+1)^2 (2\alpha_\rho^2 + 3\beta^2)} \right\} \\
& \exp \left\{ \left[-3\alpha_\rho^4 + (10\rho^2 + 8\rho + 7)\alpha_\rho^2 \beta^2 + 3(\rho+1)^2 \beta^4 \right] (\mathbf{A}^2 + \mathbf{C}^2) \right. \\
& \quad \left. + \left[-6\alpha_\rho^4 + 12(\rho^2 - 1)\alpha_\rho^2 \beta^2 - 6(\rho+1)^2 \beta^4 \right] \mathbf{A} \cdot \mathbf{C} \right\} \\
& \left\{ 6(\rho+1)^2 (2\alpha_\rho^2 + 3\beta^2) \alpha_\rho^2 \beta^2 \right\}^{-1} \Big\} \tag{197}
\end{aligned}$$

$$\begin{aligned}
& T_{space}^{(D2)}(\text{lin } \mathbf{L} \cdot \mathbf{S}) = - \frac{2 \cdot 3^{3/2} \pi b}{m^2} \\
& \frac{1}{(\rho+1) \alpha_\rho (7\alpha_\rho^2 + 6\beta^2)^{1/2} (2\alpha_\rho^2 + 3\beta^2)^2} \\
& \left[(2\rho+1) \alpha_\rho^2 + (\rho+1) \beta^2 \right] (\mathbf{s}_1 - \mathbf{s}_2) \cdot i(\mathbf{A} \times \mathbf{C}) \\
& f_{1/2,5/2} \left\{ \left\{ 3 \left[(2\rho+1) \alpha_\rho^2 + (\rho+1) \beta^2 \right] \mathbf{A} \right. \right. \\
& \quad \left. \left. + \left[(2\rho-1) \alpha_\rho^2 - 3(\rho+1) \beta^2 \right] \mathbf{C} \right\}^2 \right. \\
& \quad \left. \left\{ 4(\rho+1)^2 (7\alpha_\rho^2 + 6\beta^2) (2\alpha_\rho^2 + 3\beta^2) \alpha_\rho^2 \right\}^{-1} \right\} \\
& \exp \left\{ \left[-3\alpha_\rho^4 + (10\rho^2 + 8\rho + 7)\alpha_\rho^2 \beta^2 + 3(\rho+1)^2 \beta^4 \right] (\mathbf{A}^2 + \mathbf{C}^2) \right. \\
& \quad \left. + \left[-6\alpha_\rho^4 + 12(\rho^2 - 1)\alpha_\rho^2 \beta^2 - 6(\rho+1)^2 \beta^4 \right] \mathbf{A} \cdot \mathbf{C} \right\}
\end{aligned}$$

$$\left\{6 (\rho + 1)^2 (2 \alpha_\rho^2 + 3 \beta^2) \alpha_\rho^2 \beta^2\right\}^{-1}\} \quad (198)$$

$$\begin{aligned} T_{space}^{(D3)}(\text{lin } \mathbf{L} \cdot \mathbf{S}) = & \\ & + \frac{2^{3/2} 3^{3/2} \pi b}{m^2} \frac{\rho}{(\rho + 1)^2} \frac{1}{\beta (\alpha_\rho^2 + 3 \beta^2)^{1/2} (2 \alpha_\rho^2 + 3 \beta^2)^2} \\ & [\alpha_\rho^2 + 2 (\rho + 1) \beta^2] (\rho \mathbf{s}_1 - \mathbf{s}_2) \cdot i(\mathbf{A} \times \mathbf{C}) \\ & f_{1/2,5/2} \left\{ \frac{\left([\alpha_\rho^2 + 2 (\rho + 1) \beta^2] \mathbf{A} + [-\alpha_\rho^2 + (2\rho - 1) \beta^2] \mathbf{C} \right)^2}{2 (\rho + 1)^2 (\alpha_\rho^2 + 3 \beta^2) (2 \alpha_\rho^2 + 3 \beta^2) \beta^2} \right\} \\ & exp\left\{ \left\{ - \left[3 \alpha_\rho^4 + (10\rho^2 + 8\rho + 7) \alpha_\rho^2 \beta^2 + 3 (\rho + 1)^2 \beta^4 \right] (\mathbf{A}^2 + \mathbf{C}^2) \right. \right. \\ & + \left. \left[-6 \alpha_\rho^4 + 12 (\rho^2 - 1) \alpha_\rho^2 \beta^2 - 6 (\rho + 1)^2 \beta^4 \right] \mathbf{A} \cdot \mathbf{C} \right\} \\ & \left. \left\{ 6 (\rho + 1)^2 (2 \alpha_\rho^2 + 3 \beta^2) \alpha_\rho^2 \beta^2 \right\}^{-1} \right\} \quad (199) \end{aligned}$$

$$\begin{aligned} T_{space}^{(D4)}(\text{lin } \mathbf{L} \cdot \mathbf{S}) = & + \frac{2 \cdot 3^{3/2} \pi b}{m^2} \frac{1}{(\rho + 1)^2} \\ & \frac{[\alpha_\rho^2 + (\rho + 1) \beta^2]}{\alpha_\rho \beta (\alpha_\rho^2 + 2 \beta^2)^{1/2} (2 \alpha_\rho^2 + 3 \beta^2)^{5/2}} \\ & (2 \rho^2 [\alpha_\rho^2 + 2 (\rho + 1) \beta^2] \mathbf{s}_1 \\ & + [(2\rho + 1) \alpha_\rho^2 + (\rho + 1) \beta^2] \mathbf{s}_2) \cdot i(\mathbf{A} \times \mathbf{C}) \\ & f_{1/2,5/2} \left\{ \frac{[\alpha_\rho^2 + (\rho + 1) \beta^2]^2 (\mathbf{A} - \mathbf{C})^2}{4 (\rho + 1)^2 (\alpha_\rho^2 + 2 \beta^2) \alpha_\rho^2 \beta^2} \right\} \\ & exp\left\{ \left\{ - \left[3 \alpha_\rho^4 + (10\rho^2 + 8\rho + 7) \alpha_\rho^2 \beta^2 + 3 (\rho + 1)^2 \beta^4 \right] (\mathbf{A}^2 + \mathbf{C}^2) \right. \right. \\ & + \left. \left[-6 \alpha_\rho^4 + 12 (\rho^2 - 1) \alpha_\rho^2 \beta^2 - 6 (\rho + 1)^2 \beta^4 \right] \mathbf{A} \cdot \mathbf{C} \right\} \\ & \left. \left\{ 6 (\rho + 1)^2 (2 \alpha_\rho^2 + 3 \beta^2) \alpha_\rho^2 \beta^2 \right\}^{-1} \right\} \quad (200) \end{aligned}$$

D J/ψ N Space Amplitudes

D.1 Spin-spin

$$\begin{aligned}
T_{space}^{D1}(hfs) = & - \frac{16 \pi \sqrt{2} \rho_c \alpha_s \alpha_\rho^{3/2} \alpha_\lambda^{3/2}}{3 (\alpha_\rho^2 + \alpha_\lambda^2)^{3/2} m^2} \\
& exp \left\{ + 1/48 \left\{ \left[+(-12 \rho_c^4 - 36 \rho_c^3 - 39 \rho_c^2 - 18 \rho_c - 3) \alpha_\rho^2 \right. \right. \right. \\
& + (-12 \rho_c^4 - 36 \rho_c^3 - 39 \rho_c^2 - 18 \rho_c - 3) \alpha_\lambda^2 \\
& + (-64 \rho_c^4 - 192 \rho_c^3 - 208 \rho_c^2 - 96 \rho_c - 16) \beta^2 \left. \right] \mathbf{A}^2 \\
& + \left[+(+48 \rho_c^3 + 96 \rho_c^2 + 60 \rho_c) + 12 \alpha_\rho^2 \right. \\
& + (+48 \rho_c^3 + 96 \rho_c^2 + 60 \rho_c + 12) \alpha_\lambda^2 \\
& + (+192 \rho_c^4 + 480 \rho_c^3 + 384 \rho_c^2 + 96 \rho_c) \beta^2 \left. \right] \mathbf{A} \cdot \mathbf{C} \\
& + \left[+(-48 \rho_c^2 - 48 \rho_c - 12) \alpha_\rho^2 \right. \\
& + (-144 \rho_c^4 - 288 \rho_c^3 - 144 \rho_c^2) \beta^2 \left. \right] \mathbf{C}^2 \left. \right\} \\
& \left\{ (\rho_c + 1)^2 (2 \rho_c + 1)^2 (\alpha_\rho^2 + \alpha_\lambda^2) \beta^2 \right\}^{-1} \left. \right\} \quad (201)
\end{aligned}$$

$$\begin{aligned}
T_{space}^{D2}(hfs) = & - \frac{512 \pi \sqrt{3} \rho_c \alpha_s \alpha_\rho^{9/2} \alpha_\lambda^{3/2}}{(24 \alpha_\rho^4 + 4 \alpha_\rho^2 \alpha_\lambda^2 + 21 \alpha_\rho^2 \beta^2 + 3 \alpha_\lambda^2 \beta^2)^{3/2} m^2} \\
& exp \left\{ + 1/24 \left\{ \left[+(-144 \rho_c^4 - 432 \rho_c^3 - 468 \rho_c^2 - 216 \rho_c - 36) \alpha_\rho^4 \right. \right. \right. \\
& + (-24 \rho_c^4 - 72 \rho_c^3 - 78 \rho_c^2 - 36 \rho_c - 6) \alpha_\rho^2 \alpha_\lambda^2 \\
& + (-300 \rho_c^4 - 900 \rho_c^3 - 975 \rho_c^2 - 450 \rho_c - 75) \alpha_\rho^2 \beta^2 \\
& + (-20 \rho_c^4 - 60 \rho_c^3 - 65 \rho_c^2 - 30 \rho_c - 5) \alpha_\lambda^2 \beta^2 \\
& + (-96 \rho_c^4 - 288 \rho_c^3 - 312 \rho_c^2 - 144 \rho_c - 24) \beta^4 \left. \right] \mathbf{A}^2 \\
& + \left[+(+576 \rho_c^3 + 1152 \rho_c^2 + 720 \rho_c + 144) \alpha_\rho^4 \right. \\
& + (+96 \rho_c^3 + 192 \rho_c^2 + 120 \rho_c + 24) \alpha_\rho^2 \alpha_\lambda^2 \\
& + (-288 \rho_c^4 - 216 \rho_c^3 + 252 \rho_c^2 + 216 \rho_c + 36) \alpha_\rho^2 \beta^2 \\
& + (-48 \rho_c^4 - 48 \rho_c^3 + 36 \rho_c^2 + 48 \rho_c + 12) \alpha_\lambda^2 \beta^2 \\
& + (+288 \rho_c^4 + 720 \rho_c^3 + 576 \rho_c^2 + 144 \rho_c) \beta^4 \left. \right] \mathbf{A} \cdot \mathbf{C}
\end{aligned}$$

$$\begin{aligned}
& \left[+(-576 \rho_c^2 - 576 \rho_c - 144) \alpha_\rho^4 \right. \\
& +(-96 \rho_c^2 - 96 \rho_c - 24) \alpha_\rho^2 \alpha_\lambda^2 \\
& +(-1728 \rho_c^4 - 3456 \rho_c^3 - 3096 \rho_c^2 - 1368 \rho_c - 252) \alpha_\rho^2 \beta^2 \\
& +(-288 \rho_c^4 - 576 \rho_c^3 - 504 \rho_c^2 - 216 \rho_c) \alpha_\lambda^2 \beta^2 - 36 \alpha_\lambda^2 \beta^2 \\
& \left. +(-216 \rho_c^4 - 432 \rho_c^3 - 216 \rho_c^2) \beta^4 \right] \mathbf{C}^2 \}^{-1} \\
& \left\{ (\rho_c + 1)^2 \beta^2 \right. \\
& \left. (2 \rho_c + 1)^2 (24 \alpha_\rho^4 + 4 \alpha_\rho^2 \alpha_\lambda^2 + 21 \alpha_\rho^2 \beta^2 + 3 \alpha_\lambda^2 \beta^2) \right\}^{-1} \} \quad (202)
\end{aligned}$$

$$\begin{aligned}
T_{space}^{D3}(hfs) = & - \frac{64 \pi \sqrt{3} \rho_c \alpha_s \alpha_\rho^{3/2} \alpha_\lambda^{3/2} \beta^3}{(2 \alpha_\rho^2 \alpha_\lambda^2 + 3 \alpha_\rho^2 \beta^2 + 3 \alpha_\lambda^2 \beta^2)^{3/2} m^2} \\
& \exp \left\{ - \frac{1}{24} \left\{ \left[+(+36 \rho_c^2 + 36 \rho_c + 9) \alpha_\rho^2 \right. \right. \right. \\
& +(+4 \rho_c^2 + 4 \rho_c + 1) \alpha_\lambda^2 \\
& \left. \left. +(+96 \rho_c^2 + 96 \rho_c + 24) \beta^2 \right] \mathbf{A}^2 \right. \right. \\
& \left[+(+72 \rho_c + 36) \alpha_\rho^2 \right. \\
& +(-48 \rho_c^2 - 48 \rho_c - 12) \alpha_\lambda^2 \\
& \left. \left. +(-288 \rho_c^2 - 144 \rho_c) \beta^2 \right] \mathbf{A} \cdot \mathbf{C} \right. \\
& \left[+36 \alpha_\rho^2 \right. \\
& +(+144 \rho_c^2 + 144 \rho_c + 36) \alpha_\lambda^2 \\
& \left. \left. +216 \rho_c^2 \beta^2 \right] \mathbf{C}^2 \right\} \\
& \left\{ (2 \rho_c + 1)^2 (2 \alpha_\rho^2 \alpha_\lambda^2 + 3 \alpha_\rho^2 \beta^2 + 3 \alpha_\lambda^2 \beta^2) \right\}^{-1} \} \quad (203)
\end{aligned}$$

$$\begin{aligned}
T_{space}^{D4}(hfs) = & - 512 \pi \sqrt{3} \rho_c \alpha_s \alpha_\rho^{9/2} \alpha_\lambda^{3/2} \beta^3 \\
& (8 \alpha_\rho^4 \alpha_\lambda^2 + 12 \alpha_\rho^4 \beta^2 + 16 \alpha_\rho^2 \alpha_\lambda^2 \beta^2 + 21 \alpha_\rho^2 \beta^4 + 3 \alpha_\lambda^2 \beta^4)^{-3/2} m^{-2} \\
& \exp \left\{ - \frac{1}{24} \left\{ \left[+(+144 \rho_c^4 + 432 \rho_c^3 + 468 \rho_c^2 + 216 \rho_c + 36) \alpha_\rho^4 \right. \right. \right. \\
& +(+88 \rho_c^4 + 264 \rho_c^3 + 286 \rho_c^2 + 132 \rho_c + 22) \alpha_\rho^2 \alpha_\lambda^2 \\
& \left. \left. +(+492 \rho_c^4 + 1476 \rho_c^3 + 1599 \rho_c^2 + 738 \rho_c + 123) \alpha_\rho^2 \beta^2 \right. \right.
\end{aligned}$$

$$\begin{aligned}
& +(+20 \rho_c^4 + 60 \rho_c^3 + 65 \rho_c^2 + 30 \rho_c + 5) \alpha_\lambda^2 \beta^2 \\
& +96 \rho_c^4 \beta^4 + 288 \rho_c^3 \beta^4 + 312 \rho_c^2 \beta^4 + 144 \rho_c \beta^4 + 24 \beta^4] \mathbf{A}^2 \\
& \left[(+288 \rho_c^3 + 720 \rho_c^2 + 576 \rho_c + 144) \alpha_\rho^4 \right. \\
& +(+576 \rho_c^4 + 1512 \rho_c^3 + 1764 \rho_c^2 + 1080 \rho_c + 252) \alpha_\rho^2 \beta^2 \\
& +(+384 \rho_c^4 + 672 \rho_c^3 + 288 \rho_c^2 - 24 \rho_c - 24) \alpha_\rho^2 \alpha_\lambda^2 \\
& +(+48 \rho_c^4 + 48 \rho_c^3 - 36 \rho_c^2 - 48 \rho_c - 12) \alpha_\lambda^2 \beta^2 \\
& +(-288 \rho_c^4 - 720 \rho_c^3 - 576 \rho_c^2 - 144 \rho_c) \beta^4] \mathbf{A} \cdot \mathbf{C} \\
& \left[(+144 \rho_c^2 + 288 \rho_c + 144) \alpha_\rho^4 \right. \\
& +(+576 \rho_c^4 + 576 \rho_c^3 + 240 \rho_c^2 + 96 \rho_c + 24) \alpha_\rho^2 \alpha_\lambda^2 \\
& +(+864 \rho_c^4 + 504 \rho_c^2 + 864 \rho_c^3 + 504 \rho_c + 252) \alpha_\rho^2 \beta^2 \\
& +(+288 \rho_c^4 + 576 \rho_c^3 + 504 \rho_c^2 + 216 \rho_c + 36) \alpha_\lambda^2 \beta^2 \\
& \left. +(+216 \rho_c^4 + 432 \rho_c^3 + 216 \rho_c^2) \beta^4 \right] \mathbf{C}^2 \} \\
& \left\{ (\rho_c + 1)^2 (2 \rho_c + 1)^2 \right. \\
& \left. (8 \alpha_\rho^4 \alpha_\lambda^2 + 12 \alpha_\rho^4 \beta^2 + 16 \alpha_\rho^2 \alpha_\lambda^2 \beta^2 + 21 \alpha_\rho^2 \beta^4 + 3 \alpha_\lambda^2 \beta^4) \right\}^{-1} \} \quad (204)
\end{aligned}$$

D.2 Coulomb

$$\begin{aligned}
T_{space}^{D1}(coul) &= \frac{48 \pi \sqrt{2} \alpha_s \alpha_\rho^{3/2} \alpha_\lambda^{3/2}}{(3 \alpha_\lambda^2 \beta^2 + (4 \alpha_\lambda^2 + 3 \beta^2) \alpha_\rho^2) \sqrt{\alpha_\rho^2 + \alpha_\lambda^2}} \\
& f_{1/2,3/2} \left(\frac{1}{48} \left\{ \left[(+18 \rho_c^2 + 27 \rho_c + 9) \alpha_\rho^2 + (+2 \rho_c^2 + 3 \rho_c + 1) \alpha_\lambda^2 \right] \mathbf{A} \right. \right. \\
& \left. \left. + \left[+6 \alpha_\rho^2 + (+24 \rho_c^2 + 24 \rho_c + 6) \alpha_\lambda^2 \right] \mathbf{C} \right\}^2 \right. \\
& \left. \left\{ (\alpha_\rho^2 + \alpha_\lambda^2) (2 \rho_c^2 + 3 \rho_c + 1)^2 (4 \alpha_\rho^2 \alpha_\lambda^2 + 3 \alpha_\rho^2 \beta^2 + 3 \alpha_\lambda^2 \beta^2) \right\}^{-1} \right) \\
& \exp \left\{ +1/24 \left\{ \left[+(-24 \rho_c^4 - 72 \rho_c^3 - 78 \rho_c^2 - 36 \rho_c - 6) \alpha_\rho^2 \alpha_\lambda^2 \right. \right. \right. \\
& +(-180 \rho_c^4 - 540 \rho_c^3 - 585 \rho_c^2 - 270 \rho_c - 45) \alpha_\rho^2 \beta^2 \\
& +(-20 \rho_c^4 - 60 \rho_c^3 - 65 \rho_c^2 - 30 \rho_c - 5) \alpha_\lambda^2 \beta^2 \\
& \left. \left. +(-96 \rho_c^4 - 288 \rho_c^3 - 312 \rho_c^2 - 144 \rho_c - 24) \beta^4 \right] \mathbf{A}^2 \right. \right. \\
& \left. \left. + \left[(+96 \rho_c^3 + 192 \rho_c^2 + 120 \rho_c + 24) \alpha_\rho^2 \alpha_\lambda^2 \right. \right. \right.
\end{aligned}$$

$$\begin{aligned}
& +(+72 \rho_c^3 + 36 \rho_c^2 - 72 \rho_c - 36) \alpha_\rho^2 \beta^2 \\
& +(-48 \rho_c^4 - 48 \rho_c^3 + 36 \rho_c^2 + 48 \rho_c + 12) \alpha_\lambda^2 \beta^2 \\
& +(+288 \rho_c^4 + 720 \rho_c^3 + 576 \rho_c^2 + 144 \rho_c) \beta^4 \Big] \mathbf{A} \cdot \mathbf{C} \\
& + \Big[+(-96 \rho_c^2 - 96 \rho_c - 24) \alpha_\rho^2 \alpha_\lambda^2 \\
& +(-72 \rho_c^2 - 72 \rho_c - 36) \alpha_\rho^2 \beta^2 \\
& +(-288 \rho_c^4 - 576 \rho_c^3 - 504 \rho_c^2 - 216 \rho_c - 36) \alpha_\lambda^2 \beta^2 \\
& +(-216 \rho_c^4 - 432 \rho_c^3 - 216 \rho_c^2) \beta^4 \Big] \mathbf{C}^2 \Big\} \\
& \Big\{ \left(4 \alpha_\rho^2 \alpha_\lambda^2 + 3 \alpha_\rho^2 \beta^2 + 3 \alpha_\lambda^2 \beta^2 \right) (2 \rho_c + 1)^2 (\rho_c + 1)^2 \beta^2 \Big\}^{-1} \Big\} \quad (205)
\end{aligned}$$

$$\begin{aligned}
T_{space}^{D2}(coul) &= \frac{192 \pi \sqrt{3} \alpha_s \alpha_\rho^{5/2} \alpha_\lambda^{3/2}}{(3 \alpha_\lambda^2 \beta^2 + (4 \alpha_\lambda^2 + 3 \beta^2) \alpha_\rho^2)} \\
& \quad (24 \alpha_\rho^4 + 4 \alpha_\rho^2 \alpha_\lambda^2 + 21 \alpha_\rho^2 \beta^2 + 3 \alpha_\lambda^2 \beta^2)^{-1/2} \\
& \quad f_{1/1,3/2} \Big(9/2 \Big\{ \Big[(+6 \rho_c^2 + 9 \rho_c + 3) \alpha_\rho^2 \\
& \quad +(+4 \rho_c^2 + 6 \rho_c + 2) \beta^2 \Big] \mathbf{A} \\
& \quad \Big[+2 \alpha_\rho^2 + (-6 \rho_c - 6 \rho_c^2) \beta^2 \Big] \mathbf{C} \Big\}^2 \\
& \quad \Big\{ \alpha_\rho^2 (2 \rho_c^2 + 3 \rho_c + 1) \\
& \quad \Big(+ (48 \rho_c^2 + 72 \rho_c + 24) \alpha_\rho^4 \\
& \quad + (+8 \rho_c^2 + 12 \rho_c + 4) \alpha_\rho^2 \alpha_\lambda^2 \\
& \quad + (+42 \rho_c^2 + 63 \rho_c + 21) \alpha_\rho^2 \beta^2 \\
& \quad + (+6 \rho_c^2 + 9 \rho_c + 3) \alpha_\lambda^2 \beta^2 \Big) \\
& \quad \Big(4 \alpha_\rho^2 \alpha_\lambda^2 + 3 \alpha_\rho^2 \beta^2 + 3 \alpha_\lambda^2 \beta^2 \Big) \Big\}^{-1} \Big) \\
& \quad exp \Big\{ +1/24 \Big[\Big(+(-24 \rho_c^4 - 72 \rho_c^3 - 78 \rho_c^2 - 36 \rho_c - 6) \alpha_\rho^2 \alpha_\lambda^2 \\
& \quad +(-180 \rho_c^4 - 540 \rho_c^3 - 585 \rho_c^2 - 270 \rho_c - 45) \alpha_\rho^2 \beta^2 \\
& \quad +(-20 \rho_c^4 - 60 \rho_c^3 - 65 \rho_c^2 - 30 \rho_c - 5) \alpha_\lambda^2 \beta^2 \\
& \quad +(-96 \rho_c^4 - 288 \rho_c^3 - 312 \rho_c^2 - 144 \rho_c - 24) \beta^4 \Big] \mathbf{A}^2 \\
& \quad \Big[+(+96 \rho_c^3 + 192 \rho_c^2 + 120 \rho_c + 24) \alpha_\rho^2 \alpha_\lambda^2
\end{aligned}$$

$$\begin{aligned}
& +(+36 \rho_c^2 + 72 \rho_c^3 - 72 \rho_c - 36) \alpha_\rho^2 \beta^2 \\
& +(-48 \rho_c^4 - 48 \rho_c^3 + 36 \rho_c^2 + 48 \rho_c + 12) \alpha_\lambda^2 \beta^2 \\
& +(+288 \rho_c^4 + 720 \rho_c^3 + 576 \rho_c^2 + 144 \rho_c) \beta^4 \Big] \mathbf{A} \cdot \mathbf{C} \\
& \Big[+(-96 \rho_c^2 - 96 \rho_c - 24) \alpha_\rho^2 \alpha_\lambda^2 \\
& +(-72 \rho_c^2 - 72 \rho_c - 36) \alpha_\rho^2 \beta^2 \\
& +(-288 \rho_c^4 - 576 \rho_c^3 - 504 \rho_c^2 - 216 \rho_c - 36) \alpha_\lambda^2 \beta^2 \\
& +(-216 \rho_c^4 - 432 \rho_c^3 - 216 \rho_c^2) \beta^4 \Big] \mathbf{C}^2 \Big\} \\
& \Big\{ (\rho_c + 1)^2 (2 \rho_c + 1)^2 \left(4 \alpha_\rho^2 \alpha_\lambda^2 + 3 \alpha_\rho^2 \beta^2 + 3 \alpha_\lambda^2 \beta^2 \right) \beta^2 \Big\}^{-1} \Big\} \quad (206)
\end{aligned}$$

$$\begin{aligned}
T_{space}^{D3}(coul) &= \frac{96 \pi \sqrt{3} \alpha_s \alpha_\rho^{3/2} \alpha_\lambda^{3/2} \beta}{(3 \alpha_\lambda^2 \beta^2 + (4 \alpha_\lambda^2 + 3 \beta^2) \alpha_\rho^2)} \\
& \left(2 \alpha_\rho^2 \alpha_\lambda^2 + 3 \alpha_\rho^2 \beta^2 + 3 \alpha_\lambda^2 \beta^2 \right)^{-1/2} \\
& f_{1/2,3/2} \left(1/2 \left\{ \left[(+3 \rho_c + 2 \rho_c^2 + 1) \alpha_\rho^2 \alpha_\lambda^2 \right. \right. \right. \\
& \left. \left. \left. +(+6 \rho_c^2 + 9 \rho_c + 3) \alpha_\rho^2 \beta^2 \right. \right. \right. \\
& \left. \left. \left. +(+2 \rho_c^2 + 3 \rho_c + 1) \alpha_\lambda^2 \beta^2 \right] \mathbf{A} \right. \right. \\
& \left. \left. \left[+(-4 \rho_c - 2) \alpha_\rho^2 \alpha_\lambda^2 \right. \right. \right. \\
& \left. \left. \left. -3 \rho_c \alpha_\rho^2 \beta^2 \right. \right. \right. \\
& \left. \left. \left. +(+6 \rho_c^2 + 3 \rho_c) \alpha_\lambda^2 \beta^2 \right] \mathbf{C} \right\}^2 \right. \\
& \left. \left\{ (2 \rho_c^2 + 3 \rho_c + 1) \right. \right. \\
& \left. \left. (+(+4 \rho_c^2 + 6 \rho_c + 2) \alpha_\rho^2 \alpha_\lambda^2 \right. \right. \\
& \left. \left. +(+6 \rho_c^2 + 9 \rho_c + 3) \alpha_\rho^2 \beta^2 \right. \right. \\
& \left. \left. +(+6 \rho_c^2 + 9 \rho_c + 3) \alpha_\lambda^2 \beta^2 \right) \right. \\
& \left. \left. \left(4 \alpha_\rho^2 \alpha_\lambda^2 + 3 \alpha_\rho^2 \beta^2 + 3 \alpha_\lambda^2 \beta^2 \right) \beta^2 \right\}^{-1} \right) \\
& exp \left\{ +1/24 \left\{ \left[+(-24 \rho_c^4 - 72 \rho_c^3 - 78 \rho_c^2 - 36 \rho_c - 6) \alpha_\rho^2 \alpha_\lambda^2 \right. \right. \right. \right. \\
& \left. \left. \left. +(-180 \rho_c^4 - 540 \rho_c^3 - 585 \rho_c^2 - 270 \rho_c - 45) \alpha_\rho^2 \beta^2 \right. \right. \right. \\
& \left. \left. \left. +(-20 \rho_c^4 - 60 \rho_c^3 - 65 \rho_c^2 - 30 \rho_c - 5) \alpha_\lambda^2 \beta^2 \right. \right. \right.
\end{aligned}$$

$$\begin{aligned}
& +(-96 \rho_c^4 - 288 \rho_c^3 - 312 \rho_c^2 - 144 \rho_c - 24) \beta^4] \mathbf{A}^2 \\
& + \left[(+96 \rho_c^3 + 192 \rho_c^2 + 120 \rho_c + 24) \alpha_\rho^2 \alpha_\lambda^2 \right. \\
& + (+72 \rho_c^3 + 36 \rho_c^2 - 72 \rho_c - 36) \alpha_\rho^2 \beta^2 \\
& + (-48 \rho_c^4 - 48 \rho_c^3 + 36 \rho_c^2 + 48 \rho_c + 12) \alpha_\lambda^2 \beta^2 \\
& \left. + (+288 \rho_c^4 + 720 \rho_c^3 + 576 \rho_c^2 + 144 \rho_c) \beta^4 \right] \mathbf{A} \cdot \mathbf{C} \\
& + \left[(-96 \rho_c^2 - 96 \rho_c - 24) \alpha_\rho^2 \alpha_\lambda^2 \right. \\
& + (-72 \rho_c^2 - 72 \rho_c - 36) \alpha_\rho^2 \beta^2 \\
& + (-288 \rho_c^4 - 576 \rho_c^3 - 504 \rho_c^2 - 216 \rho_c - 36) \alpha_\lambda^2 \beta^2 \\
& \left. + (-216 \rho_c^4 - 432 \rho_c^3 - 216 \rho_c^2) \beta^4 \right] \mathbf{C}^2 \} \\
& \left\{ \left(4 \alpha_\rho^2 \alpha_\lambda^2 + 3 \alpha_\rho^2 \beta^2 + 3 \alpha_\lambda^2 \beta^2 \right) (2 \rho_c + 1)^2 (\rho_c + 1)^2 \beta^2 \right\}^{-1} \} \quad (207)
\end{aligned}$$

$$\begin{aligned}
T_{space}^{D4}(coul) &= 192 \sqrt{3} \pi \alpha_s ar^{5/2} al^{3/2} \beta \left(3 al^2 \beta^2 + (4 al^2 + 3 \beta^2) ar^2 \right)^{-1} \\
& \left(8 ar^4 al^2 + 12 ar^4 \beta^2 + 16 ar^2 al^2 \beta^2 + 21 ar^2 \beta^4 + 3 al^2 \beta^4 \right)^{-1/2} \\
& f_{1/2,3/2} \left(1/2 \left\{ \left[+4 \rho_c^2 \alpha_\rho^2 \alpha_\lambda^2 + 6 \rho_c \alpha_\rho^2 \alpha_\lambda^2 + 2 \alpha_\rho^2 \alpha_\lambda^2 \right. \right. \right. \\
& + 12 \rho_c^2 \alpha_\rho^2 \beta^2 + 18 \rho_c \alpha_\rho^2 \beta^2 + 6 \alpha_\rho^2 \beta^2 \\
& + 2 \rho_c^2 \alpha_\lambda^2 \beta^2 + 3 \rho_c \alpha_\lambda^2 \beta^2 + \alpha_\lambda^2 \beta^2 \\
& \left. + 12 \rho_c^2 \beta^4 + 18 \rho_c \beta^4 + 6 \beta^4 \right] \mathbf{A} \\
& \left[+(-8 \rho_c - 4) \alpha_\rho^2 \alpha_\lambda^2 \right. \\
& - 6 \rho_c \alpha_\rho^2 \beta^2 \\
& + (-12 \rho_c^2 - 18 \rho_c - 6) \alpha_\lambda^2 \beta^2 \\
& \left. + (-18 \rho_c^2 - 18 \rho_c) \beta^4 \right] \mathbf{C} \}^2 \\
& \left\{ \alpha_\rho^2 (2 \rho_c^2 + 3 \rho_c + 1) \right. \\
& \left(+(+16 \rho_c^2 + 24 \rho_c + 8) \alpha_\rho^4 \alpha_\lambda^2 \right. \\
& + (+24 \rho_c^2 + 36 \rho_c + 12) \alpha_\rho^4 \beta^2 \\
& + (+32 \rho_c^2 + 48 \rho_c + 16) \alpha_\rho^2 \alpha_\lambda^2 \beta^2 \\
& + (+42 \rho_c^2 + 63 \rho_c + 21) \alpha_\rho^2 \beta^4 \\
& \left. \left. + (+6 \rho_c^2 + 9 \rho_c + 3) \alpha_\lambda^2 \beta^4 \right) \right\}
\end{aligned}$$

$$\begin{aligned}
& \left(4 \alpha_\rho^2 \alpha_\lambda^2 + 3 \alpha_\rho^2 \beta^2 + 3 \alpha_\lambda^2 \beta^2 \right) \beta^2 \}^{-1} \Big) \\
& \exp \left\{ + 1/24 \left\{ \left[+ (-24 \rho_c^4 - 72 \rho_c^3 - 78 \rho_c^2 - 36 \rho_c - 6) \alpha_\rho^2 \alpha_\lambda^2 \right. \right. \right. \\
& + (-180 \rho_c^4 - 540 \rho_c^3 - 585 \rho_c^2 - 270 \rho_c - 45) \alpha_\rho^2 \beta^2 \\
& + (-20 \rho_c^4 - 60 \rho_c^3 - 65 \rho_c^2 - 30 \rho_c - 5) \alpha_\lambda^2 \beta^2 \\
& + (-96 \rho_c^4 - 288 \rho_c^3 - 312 \rho_c^2 - 144 \rho_c - 24) \beta^4 \Big] \mathbf{A}^2 \\
& + \left[+ (+96 \rho_c^3 + 192 \rho_c^2 + 120 \rho_c + 24) \alpha_\rho^2 \alpha_\lambda^2 \right. \\
& + (+72 \rho_c^3 + 36 \rho_c^2 - 72 \rho_c - 36) \alpha_\rho^2 \beta^2 \\
& + (-48 \rho_c^4 - 48 \rho_c^3 + 36 \rho_c^2 + 48 \rho_c + 12) \alpha_\lambda^2 \beta^2 \\
& + (+288 \rho_c^4 + 720 \rho_c^3 + 576 \rho_c^2 + 144 \rho_c) \beta^4 \Big] \mathbf{A} \cdot \mathbf{C} \\
& + \left[+ (-96 \rho_c^2 - 96 \rho_c - 24) \alpha_\rho^2 \alpha_\lambda^2 \right. \\
& + (-72 \rho_c^2 - 72 \rho_c - 36) \alpha_\rho^2 \beta^2 \\
& + (-288 \rho_c^4 - 576 \rho_c^3 - 504 \rho_c^2 - 216 \rho_c - 36) \alpha_\lambda^2 \beta^2 \\
& + (-216 \rho_c^4 - 432 \rho_c^3 - 216 \rho_c^2) \beta^4 \Big] \mathbf{C}^2 \Big\} \\
& \left. \left\{ \left(4 \alpha_\rho^2 \alpha_\lambda^2 + 3 \alpha_\rho^2 \beta^2 + 3 \alpha_\lambda^2 \beta^2 \right) (2 \rho_c + 1)^2 (\rho_c + 1)^2 \beta^2 \right\}^{-1} \right\} \quad (208)
\end{aligned}$$

D.3 Linear

$$\begin{aligned}
T_{space}^{D1}(lin) &= - \frac{432 \pi \sqrt{2} \sqrt{\alpha_\rho^2 + \alpha_\lambda^2} \alpha_\rho^{3/2} \alpha_\lambda^{3/2} b}{(3 \alpha_\lambda^2 \beta^2 + (4 \alpha_\lambda^2 + 3 \beta^2) \alpha_\rho^2)^2} \\
& f_{-1/2,3/2} \left(1/48 \left\{ \left[+ (+18 \rho_c^2 + 27 \rho_c + 9) \alpha_\rho^2 + (+2 \rho_c^2 + 3 \rho_c + 1) \alpha_\lambda^2 \right] \mathbf{A} \right. \right. \\
& + \left. \left[+6 \alpha_\rho^2 + (+24 \rho_c^2 + 24 \rho_c + 6) \alpha_\lambda^2 \right] \mathbf{C} \right\}^2 \\
& \left. \left\{ \left(\alpha_\rho^2 + \alpha_\lambda^2 \right) \left(2 \rho_c^2 + 3 \rho_c + 1 \right)^2 \left(4 \alpha_\rho^2 \alpha_\lambda^2 + 3 \alpha_\rho^2 \beta^2 + 3 \alpha_\lambda^2 \beta^2 \right) \right\}^{-1} \right) \\
& \exp \left\{ + 1/24 \left\{ \left[+ (-24 \rho_c^4 - 72 \rho_c^3 - 78 \rho_c^2 - 36 \rho_c - 6) \alpha_\rho^2 \alpha_\lambda^2 \right. \right. \right. \\
& + (-180 \rho_c^4 - 540 \rho_c^3 - 585 \rho_c^2 - 270 \rho_c - 45) \alpha_\rho^2 \beta^2 \\
& + (-20 \rho_c^4 - 60 \rho_c^3 - 65 \rho_c^2 - 30 \rho_c - 5) \alpha_\lambda^2 \beta^2 \\
& + (-96 \rho_c^4 - 288 \rho_c^3 - 312 \rho_c^2 - 144 \rho_c - 24) \beta^4 \Big] \mathbf{A}^2 \\
& + \left. \left[+ (+96 \rho_c^3 + 192 \rho_c^2 + 120 \rho_c + 24) \alpha_\rho^2 \alpha_\lambda^2 \right. \right.
\end{aligned}$$

$$\begin{aligned}
& +(+72 \rho_c^3 + 36 \rho_c^2 - 72 \rho_c - 36) \alpha_\rho^2 \beta^2 \\
& +(-48 \rho_c^4 - 48 \rho_c^3 + 36 \rho_c^2 + 48 \rho_c + 12) \alpha_\lambda^2 \beta^2 \\
& +(+288 \rho_c^4 + 720 \rho_c^3 + 576 \rho_c^2 + 144 \rho_c) \beta^4 \Big] \mathbf{A} \cdot \mathbf{C} \\
& \Big[+(-96 \rho_c^2 - 96 \rho_c - 24) \alpha_\rho^2 \alpha_\lambda^2 \\
& +(-72 \rho_c^2 - 72 \rho_c - 36) \alpha_\rho^2 \beta^2 \\
& +(-288 \rho_c^4 - 576 \rho_c^3 - 504 \rho_c^2 - 216 \rho_c - 36) \alpha_\lambda^2 \beta^2 \\
& +(-216 \rho_c^4 - 432 \rho_c^3 - 216 \rho_c^2) \beta^4 \Big] \mathbf{C}^2 \Big\} \\
& \Big\{ (4 \alpha_\rho^2 \alpha_\lambda^2 + 3 \alpha_\rho^2 \beta^2 + 3 \alpha_\lambda^2 \beta^2) (2 \rho_c + 1)^2 (\rho_c + 1)^2 \beta^2 \Big\}^{-1} \Big\} \quad (209)
\end{aligned}$$

$$\begin{aligned}
T_{space}^{D2}(lin) = & -72 \sqrt{3} \pi b \sqrt{\alpha_\rho} \alpha_\lambda^{3/2} \\
& \sqrt{24 \alpha_\rho^4 + 4 \alpha_\rho^2 \alpha_\lambda^2 + 21 \alpha_\rho^2 \beta^2 + 3 \alpha_\lambda^2 \beta^2} \\
& (3 \alpha_\lambda^2 \beta^2 + (4 \alpha_\lambda^2 + 3 \beta^2) \alpha_\rho^2)^{-2} \\
& f_{-1/2,3/2} \Big(9/2 \Big\{ \Big[(+6 \rho_c^2 + 9 \rho_c + 3) \alpha_\rho^2 \\
& +(+4 \rho_c^2 + 6 \rho_c + 2) \beta^2 \Big] \mathbf{A} \\
& \Big[+2 \alpha_\rho^2 + (-6 \rho_c - 6 \rho_c^2) \beta^2 \Big] \mathbf{C} \Big\}^2 \\
& \Big\{ \alpha_\rho^2 (2 \rho_c^2 + 3 \rho_c + 1) \\
& (+48 \rho_c^2 + 72 \rho_c \alpha_\rho^4 + 24) \alpha_\rho^4 \\
& (+8 \rho_c^2 + 12 \rho_c + 4) \alpha_\rho^2 \alpha_\lambda^2 \\
& (+42 \rho_c^2 + 63 \rho_c + 21) \alpha_\rho^2 \beta^2 \\
& (+6 \rho_c^2 + 9 \rho_c + 3) \alpha_\lambda^2 \beta^2 \Big\} \\
& (4 \alpha_\rho^2 \alpha_\lambda^2 + 3 \alpha_\rho^2 \beta^2 + 3 \alpha_\lambda^2 \beta^2) \Big\}^{-1} \Big) \\
& exp \Big\{ +1/24 \Big\{ \Big[+(-24 \rho_c^4 - 72 \rho_c^3 - 78 \rho_c^2 - 36 \rho_c - 6) \alpha_\rho^2 \alpha_\lambda^2 \\
& +(-180 \rho_c^4 - 540 \rho_c^3 - 585 \rho_c^2 - 270 \rho_c - 45) \alpha_\rho^2 \beta^2 \\
& +(-20 \rho_c^4 - 60 \rho_c^3 - 65 \rho_c^2 - 30 \rho_c - 5) \alpha_\lambda^2 \beta^2 \\
& +(-96 \rho_c^4 - 288 \rho_c^3 - 312 \rho_c^2 - 144 \rho_c - 24) \beta^4 \Big] \mathbf{A}^2 \\
& + \Big[(+96 \rho_c^3 + 192 \rho_c^2 + 120 \rho_c + 24) \alpha_\rho^2 \alpha_\lambda^2
\end{aligned}$$

$$\begin{aligned}
& +(+72 \rho_c^3 + 36 \rho_c^2 - 72 \rho_c - 36) \alpha_\rho^2 \beta^2 \\
& +(-48 \rho_c^4 - 48 \rho_c^3 + 36 \rho_c^2 + 48 \rho_c + 12) \alpha_\lambda^2 \beta^2 \\
& +(+288 \rho_c^4 + 720 \rho_c^3 + 576 \rho_c^2 + 144 \rho_c) \beta^4 \Big] \mathbf{A} \cdot \mathbf{C} \\
& + \Big[+(-96 \rho_c^2 - 96 \rho_c - 24) \alpha_\rho^2 \alpha_\lambda^2 \\
& +(-72 \rho_c^2 - 72 \rho_c - 36) \alpha_\rho^2 \beta^2 \\
& +(-288 \rho_c^4 - 576 \rho_c^3 - 504 \rho_c^2 - 216 \rho_c - 36) \alpha_\lambda^2 \beta^2 \\
& +(-216 \rho_c^4 - 432 \rho_c^3 - 216 \rho_c^2) \beta^4 \Big] \mathbf{C}^2 \Big\} \\
& \Big\{ \left(4 \alpha_\rho^2 \alpha_\lambda^2 + 3 \alpha_\rho^2 \beta^2 + 3 \alpha_\lambda^2 \beta^2 \right) (2 \rho_c + 1)^2 (\rho_c + 1)^2 \beta^2 \Big\}^{-1} \Big\} \quad (210)
\end{aligned}$$

$$\begin{aligned}
T_{space}^{D3}(lin) = & -144 \sqrt{3} \pi b \alpha_\rho^{3/2} \alpha_\lambda^{3/2} \\
& \sqrt{2 \alpha_\rho^2 \alpha_\lambda^2 + 3 \alpha_\rho^2 \beta^2 + 3 \alpha_\lambda^2 \beta^2} \\
& \left(3 \alpha_\lambda^2 \beta^2 + (4 \alpha_\lambda^2 + 3 \beta^2) \alpha_\rho^2 \right)^{-2} \beta^{-1} \\
& f_{-1/2,3/2} \left(1/2 \left\{ \left[(+2 \rho_c^2 + 3 \rho_c + 1) \alpha_\rho^2 \alpha_\lambda^2 \right. \right. \right. \\
& \left. \left. \left. +(+6 \rho_c^2 + 9 \rho_c + 3) \alpha_\rho^2 \beta^2 \right. \right. \right. \\
& \left. \left. \left. +(+2 \rho_c^2 + 3 \rho_c + 1) \alpha_\lambda^2 \beta^2 \right] \mathbf{A} \right. \right. \\
& \left. \left. \left[+(-4 \rho_c - 2) \alpha_\rho^2 \alpha_\lambda^2 \right. \right. \right. \\
& \left. \left. \left. -3 \rho_c \alpha_\rho^2 \beta^2 \right. \right. \right. \\
& \left. \left. \left. +(+6 \rho_c^2 + 3 \rho_c) \alpha_\lambda^2 \beta^2 \right] \mathbf{C} \right\}^2 \right. \\
& \left. \left\{ (2 \rho_c^2 + 3 \rho_c + 1) \right. \right. \\
& \left. \left. \left(+(+4 \rho_c^2 6 \rho_c + 2) \alpha_\rho^2 \alpha_\lambda^2 \right. \right. \right. \\
& \left. \left. \left. +(+6 \rho_c^2 + 9 \rho_c + 3) \alpha_\rho^2 \beta^2 \right. \right. \right. \\
& \left. \left. \left. +(+6 \rho_c^2 + 9 \rho_c + 3) \alpha_\lambda^2 \beta^2 \right) \right. \right. \\
& \left. \left. \left(4 \alpha_\rho^2 \alpha_\lambda^2 + 3 \alpha_\rho^2 \beta^2 + 3 \alpha_\lambda^2 \beta^2 \right) \beta^2 \right\}^{-1} \right) \\
& exp \Big\{ +1/24 \left\{ \left[+(-24 \rho_c^4 - 72 \rho_c^3 - 78 \rho_c^2 - 36 \rho_c - 6) \alpha_\rho^2 \alpha_\lambda^2 \right. \right. \right. \\
& \left. \left. \left. +(-180 \rho_c^4 - 540 \rho_c^3 - 585 \rho_c^2 - 270 \rho_c - 45) \alpha_\rho^2 \beta^2 \right. \right. \right. \\
& \left. \left. \left. +(-20 \rho_c^4 - 60 \rho_c^3 - 65 \rho_c^2 - 30 \rho_c - 5) \alpha_\lambda^2 \beta^2 \right. \right. \right.
\end{aligned}$$

$$\begin{aligned}
& +(-96\rho_c^4 - 288\rho_c^3 - 312\rho_c^2 - 144\rho_c - 24)\beta^4] \mathbf{A}^2 \\
& + \left[(+96\rho_c^3 + 192\rho_c^2 + 120\rho_c + 24)\alpha_\rho^2\alpha_\lambda^2 \right. \\
& + (+72\rho_c^3 + 36\rho_c^2 - 72\rho_c - 36)\alpha_\rho^2\beta^2 \\
& + (-48\rho_c^4 - 48\rho_c^3 + 36\rho_c^2 + 48\rho_c + 12)\alpha_\lambda^2\beta^2 \\
& \left. + (+288\rho_c^4 + 720\rho_c^3 + 576\rho_c^2 + 144\rho_c)\beta^4 \right] \mathbf{A} \cdot \mathbf{C} \\
& + \left[+(-96\rho_c^2 - 96\rho_c - 24)\alpha_\rho^2\alpha_\lambda^2 \right. \\
& + (-72\rho_c^2 - 72\rho_c - 36)\alpha_\rho^2\beta^2 \\
& + (-288\rho_c^4 - 576\rho_c^3 - 504\rho_c^2 - 216\rho_c - 36)\alpha_\lambda^2\beta^2 \\
& \left. + (-216\rho_c^4 - 432\rho_c^3 - 216\rho_c^2)\beta^4 \right] \mathbf{C}^2 \} \\
& \left\{ \left(4\alpha_\rho^2\alpha_\lambda^2 + 3\alpha_\rho^2\beta^2 + 3\alpha_\lambda^2\beta^2 \right) (2\rho_c + 1)^2 (\rho_c + 1)^2 \beta^2 \right\}^{-1} \} \quad (211)
\end{aligned}$$

$$\begin{aligned}
T_{space}^{D4}(lin) = & -72\sqrt{3}\pi\sqrt{\alpha_\rho}\alpha_\lambda^{3/2} \\
& \sqrt{8\alpha_\rho^4\alpha_\lambda^2 + 12\alpha_\rho^4\beta^2 + 16\alpha_\rho^2\alpha_\lambda^2\beta^2 + 21\alpha_\rho^2\beta^4 + 3\alpha_\lambda^2\beta^4} \\
& \left(3\alpha_\lambda^2\beta^2 + (4\alpha_\lambda^2 + 3\beta^2)\alpha_\rho^2 \right)^{-2} \beta^{-1}b \\
& f_{-1/2,3/2} \left(\frac{1}{2} \left\{ \left[(+4\rho_c^2 + 6\rho_c + 2)\alpha_\rho^2\alpha_\lambda^2 \right. \right. \right. \\
& + (+12\rho_c^2 + 18\rho_c + 6)\alpha_\rho^2\beta^2 \\
& + (+2\rho_c^2 + 3\rho_c + 1)\alpha_\lambda^2\beta^2 \\
& \left. \left. + (+12\rho_c^2 + 18\rho_c + 6)\beta^4 \right] \mathbf{A} \right. \right. \\
& \left. \left[+(-8\rho_c - 4)\alpha_\rho^2\alpha_\lambda^2 \right. \right. \\
& - 6\rho_c\alpha_\rho^2\beta^2 \\
& + (-12\rho_c^2 - 18\rho_c - 6)\alpha_\lambda^2\beta^2 \\
& \left. \left. + (-18\rho_c^2 - 18\rho_c)\beta^4 \right] \mathbf{C} \right\}^2 \\
& \left\{ \alpha_\rho^2 (2\rho_c^2 + 3\rho_c + 1) \right. \\
& \left. (+16\rho_c^2 + 24\rho_c + 8)\alpha_\rho^4\alpha_\lambda^2 \right. \\
& + (+24\rho_c^2 + 36\rho_c + 12)\alpha_\rho^4\beta^2 \\
& + (+32\rho_c^2 + 48\rho_c + 16)\alpha_\rho^2\alpha_\lambda^2\beta^2 \\
& \left. \left. + (+42\rho_c^2 + 63\rho_c + 21)\alpha_\rho^2\beta^4 \right. \right.
\end{aligned}$$

$$\begin{aligned}
& +(+6\rho_c^2 + 9\rho_c + 3)\alpha_\lambda^2\beta^4) \\
& (4\alpha_\rho^2\alpha_\lambda^2 + 3\alpha_\rho^2\beta^2 + 3\alpha_\lambda^2\beta^2)\beta^2\}^{-1}) \\
& \exp\left\{+1/24\left\{\left[+(-24\rho_c^4 - 72\rho_c^3 - 78\rho_c^2 - 36\rho_c - 6)\alpha_\rho^2\alpha_\lambda^2\right.\right.\right. \\
& +(-180\rho_c^4 - 540\rho_c^3 - 585\rho_c^2 - 270\rho_c - 45)\alpha_\rho^2\beta^2 \\
& +(-20\rho_c^4 - 60\rho_c^3 - 65\rho_c^2 - 30\rho_c - 5)\alpha_\lambda^2\beta^2 \\
& +(-96\rho_c^4 - 288\rho_c^3 - 312\rho_c^2 - 144\rho_c - 24)\beta^4\left.\right]\mathbf{A}^2 \\
& +\left[+(+96\rho_c^3 + 192\rho_c^2 + 120\rho_c + 24)\alpha_\rho^2\alpha_\lambda^2\right. \\
& +(+72\rho_c^3 + 36\rho_c^2 - 72\rho_c - 36)\alpha_\rho^2\beta^2 \\
& +(-48\rho_c^4 - 48\rho_c^3 + 36\rho_c^2 + 48\rho_c + 12)\alpha_\lambda^2\beta^2 \\
& +(+288\rho_c^4 + 720\rho_c^3 + 576\rho_c^2 + 144\rho_c)\beta^4\left.\right]\mathbf{A} \cdot \mathbf{C} \\
& +\left[+(-96\rho_c^2 - 96\rho_c - 24)\alpha_\rho^2\alpha_\lambda^2\right. \\
& +(-72\rho_c^2 - 72\rho_c - 36)\alpha_\rho^2\beta^2 \\
& +(-288\rho_c^4 - 576\rho_c^3 - 504\rho_c^2 - 216\rho_c - 36)\alpha_\lambda^2\beta^2 \\
& +(-216\rho_c^4 - 432\rho_c^3 - 216\rho_c^2)\beta^4\left.\right]\mathbf{C}^2\left.\right\} \\
& \left\{(4\alpha_\rho^2\alpha_\lambda^2 + 3\alpha_\rho^2\beta^2 + 3\alpha_\lambda^2\beta^2)(2\rho_c + 1)^2(\rho_c + 1)^2\beta^2\}^{-1}\right\} \quad (212)
\end{aligned}$$

E Figures

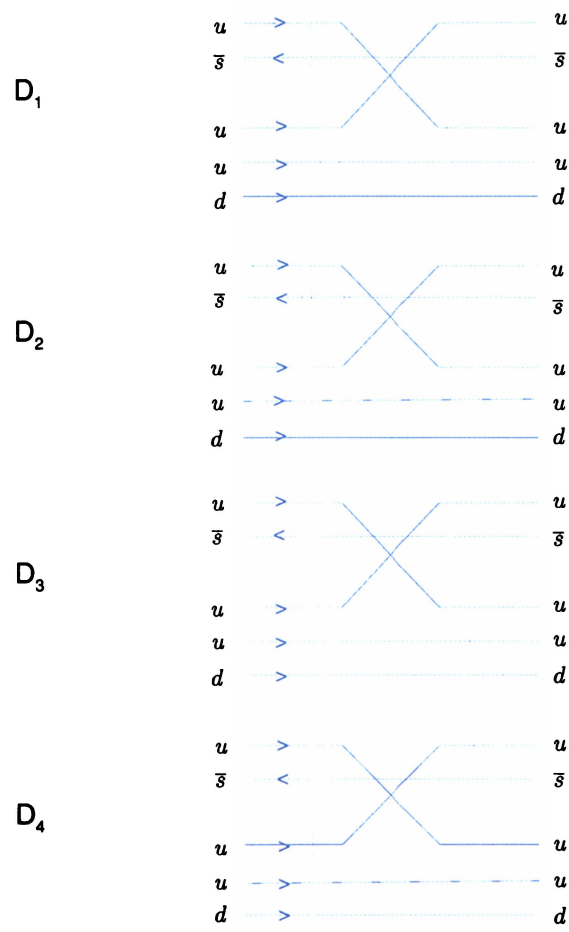


Figure 1: Quark line diagrams.

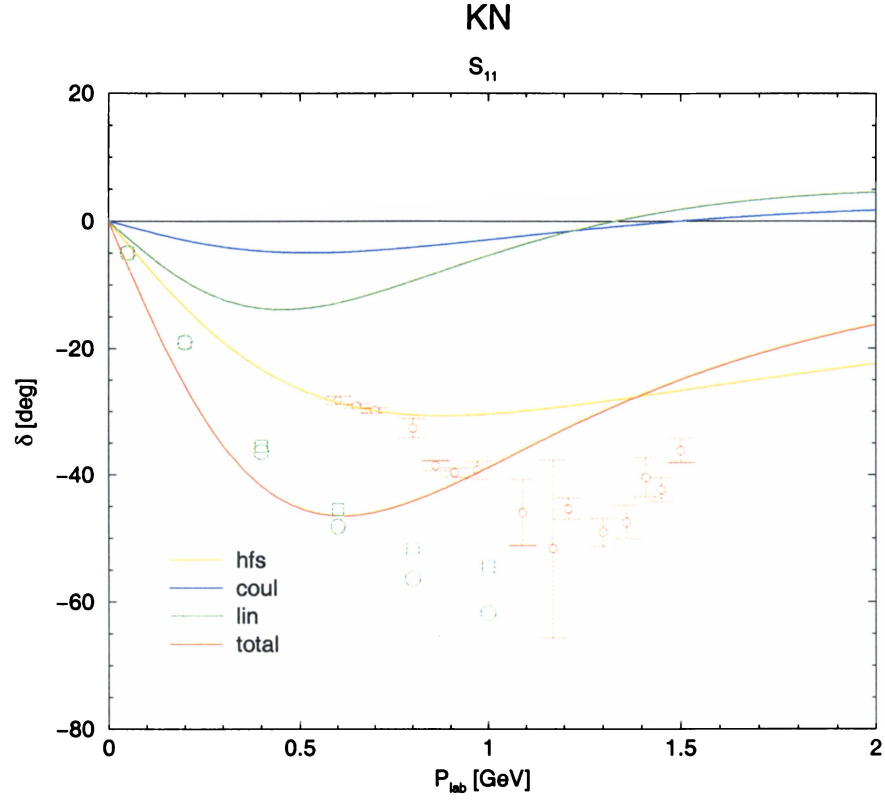


Figure 2: Theoretical S_{11} KN phase shift. The experimental phase shifts of Hashimoto (triangles with error bars) and the RGM theoretical phase shifts of Lemaire, *et al.* (circles and squares, two wave functions) are shown.

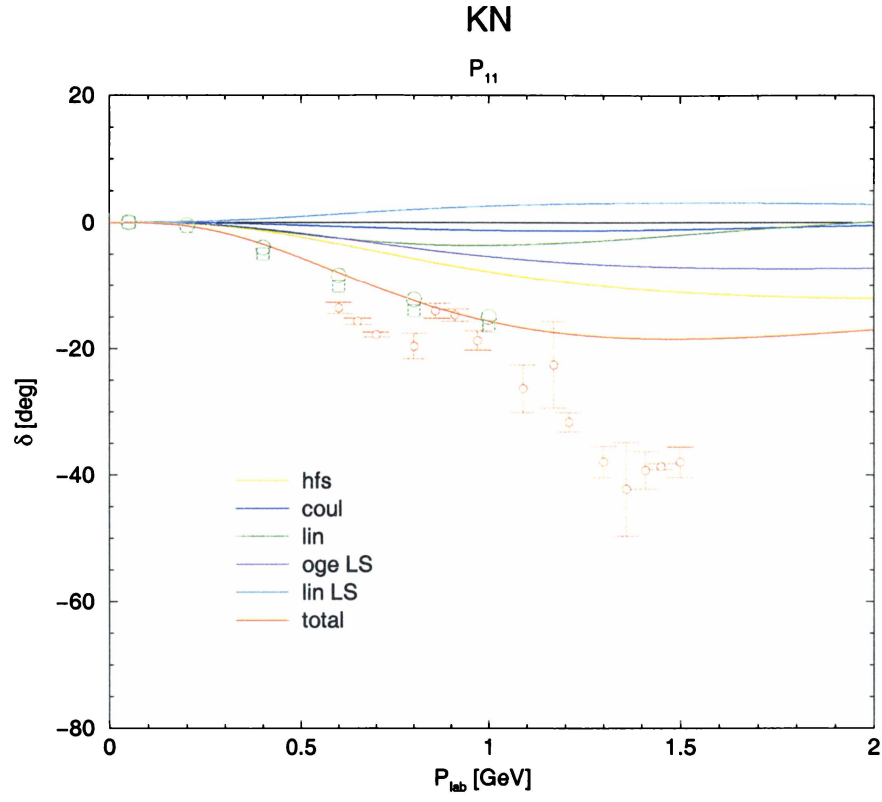


Figure 3: Theoretical P_{11} KN phase shift. The symbols are as in Fig. 1.

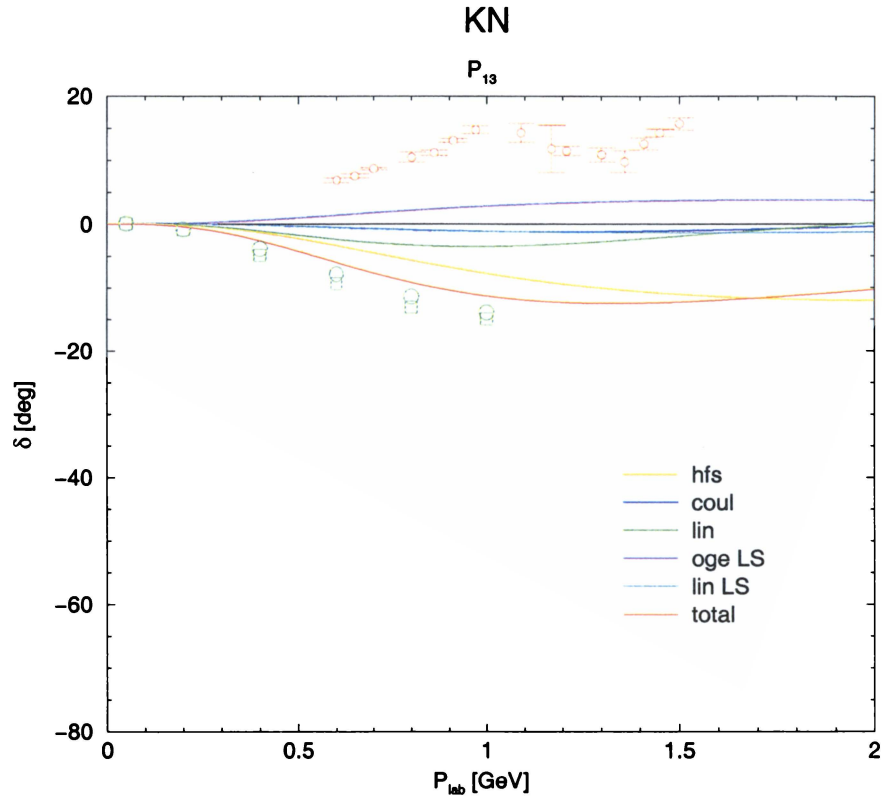


Figure 4: Theoretical P_{13} KN phase shift. The symbols are as in Fig. 1.

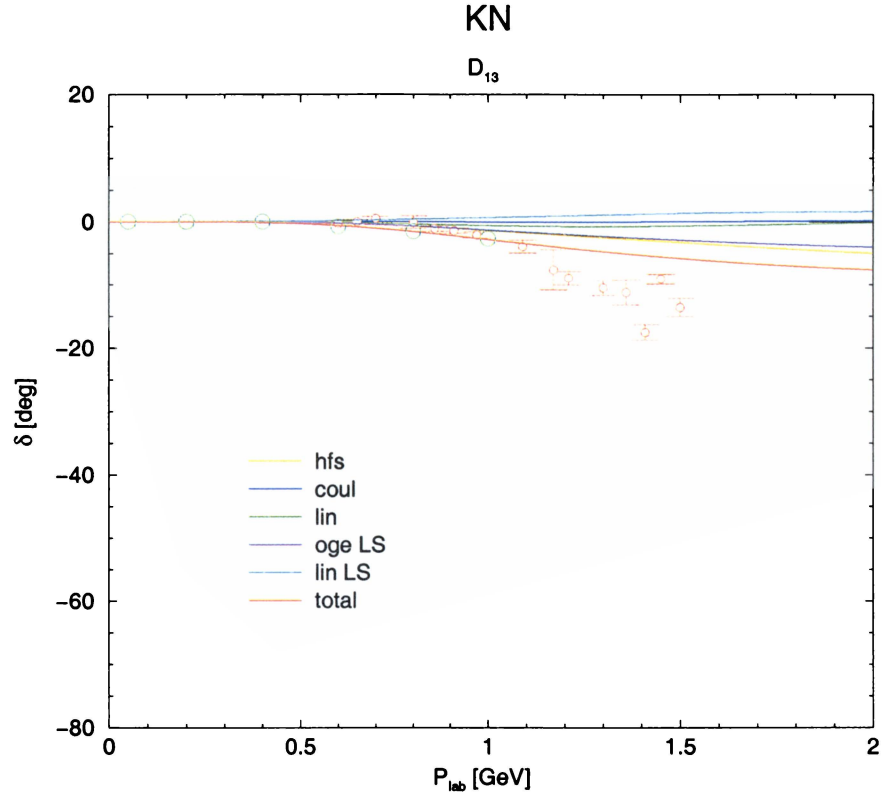


Figure 5: Theoretical D_{13} KN phase shift. The symbols are as in Fig. 1.

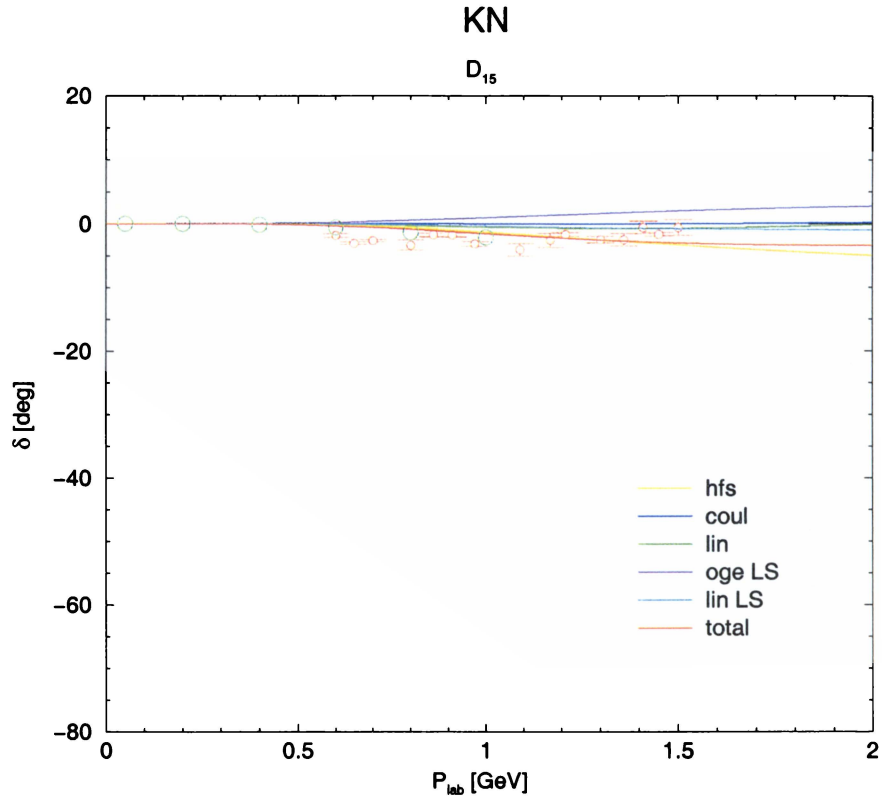


Figure 6: Theoretical D_{15} KN phase shift. The symbols are as in Fig. 1.

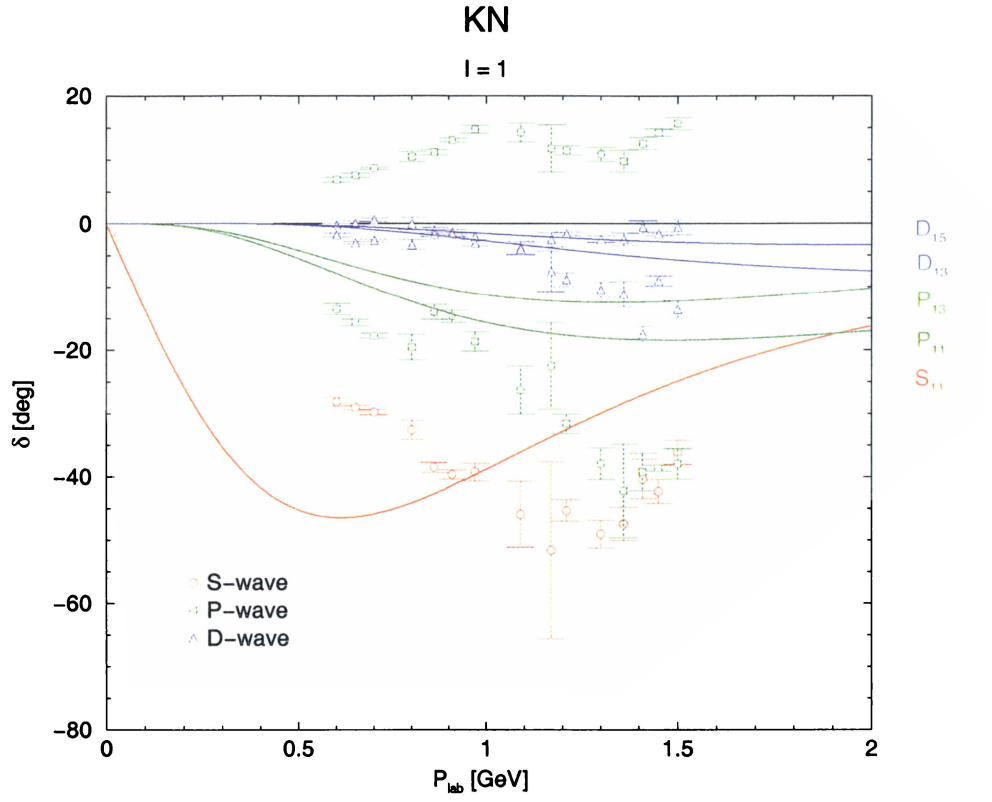


Figure 7: Theoretical I=1 KN total phase shifts. The data points are from Hashimoto .

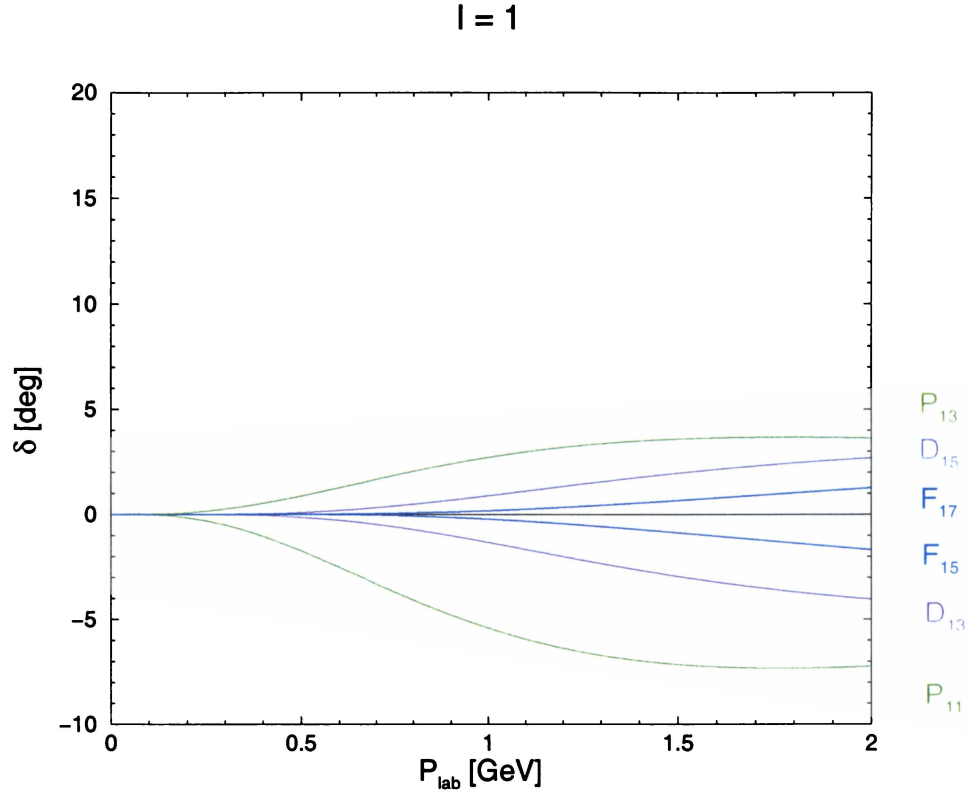


Figure 8: Theoretical $I=1$ KN OGE spin-orbit phase shifts. The data points are from Hashimoto .

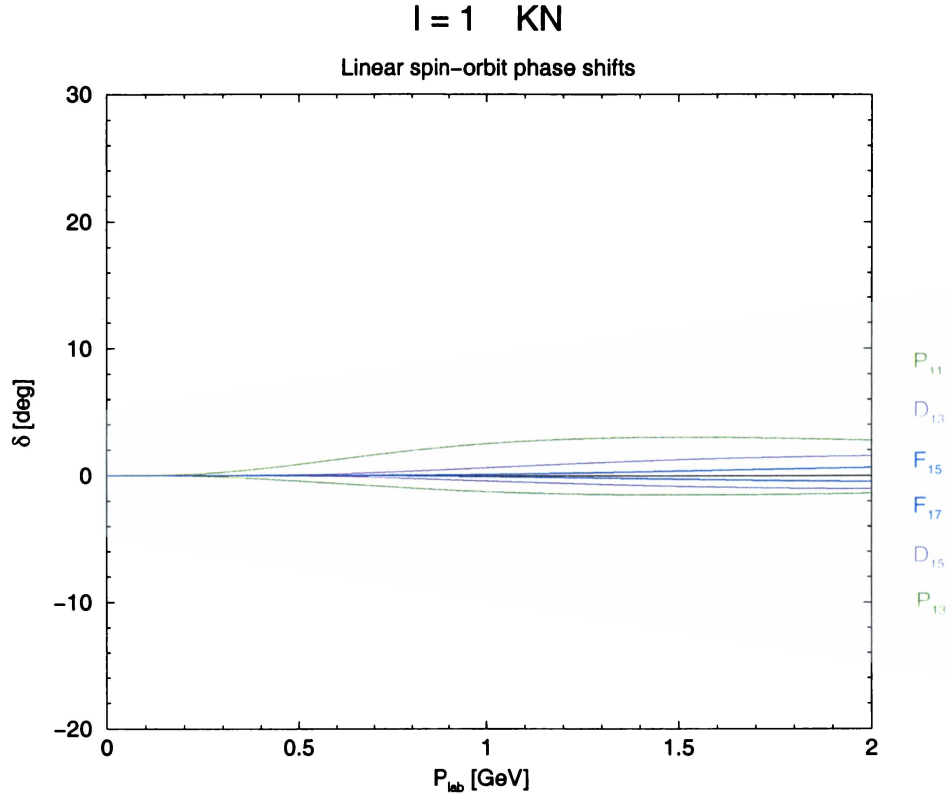


Figure 9: Theoretical $I=1$ KN confinement spin-orbit phase shifts. The data points are from Hashimoto .

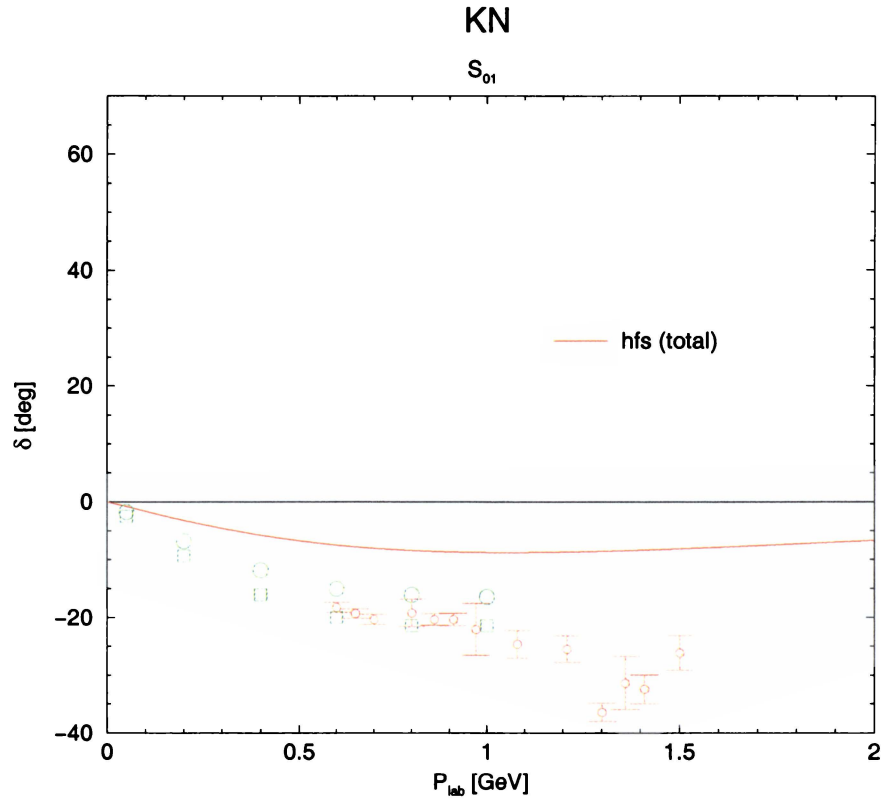


Figure 10: Theoretical S_{01} KN phase shift. The symbols are as in Fig. 1.

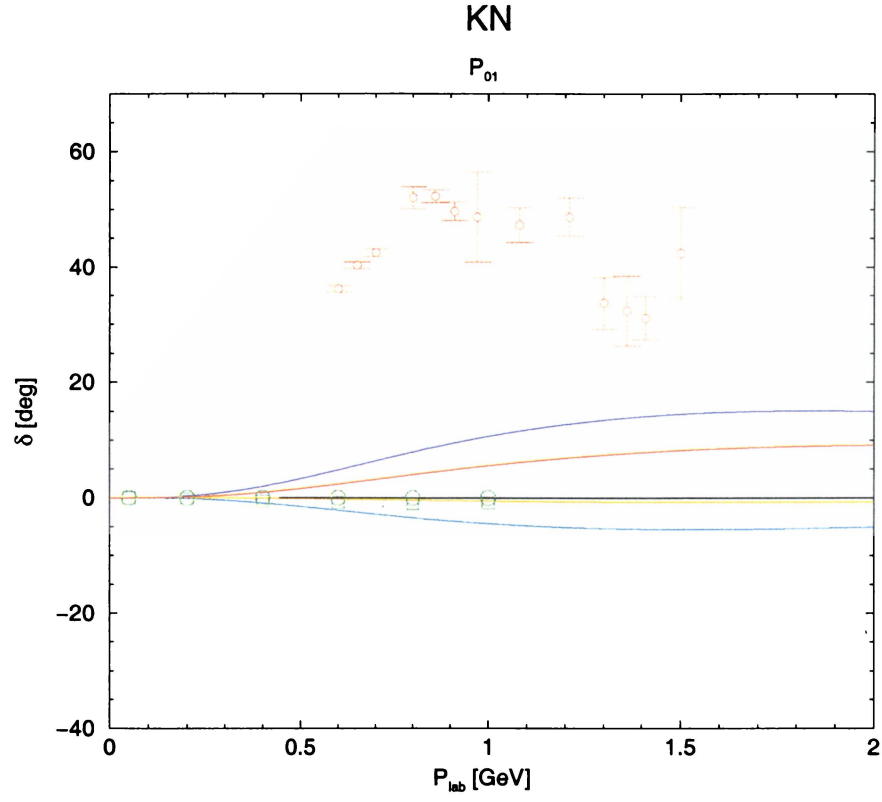


Figure 11: Theoretical P_{01} KN phase shift. The symbols are as in Fig. 1.

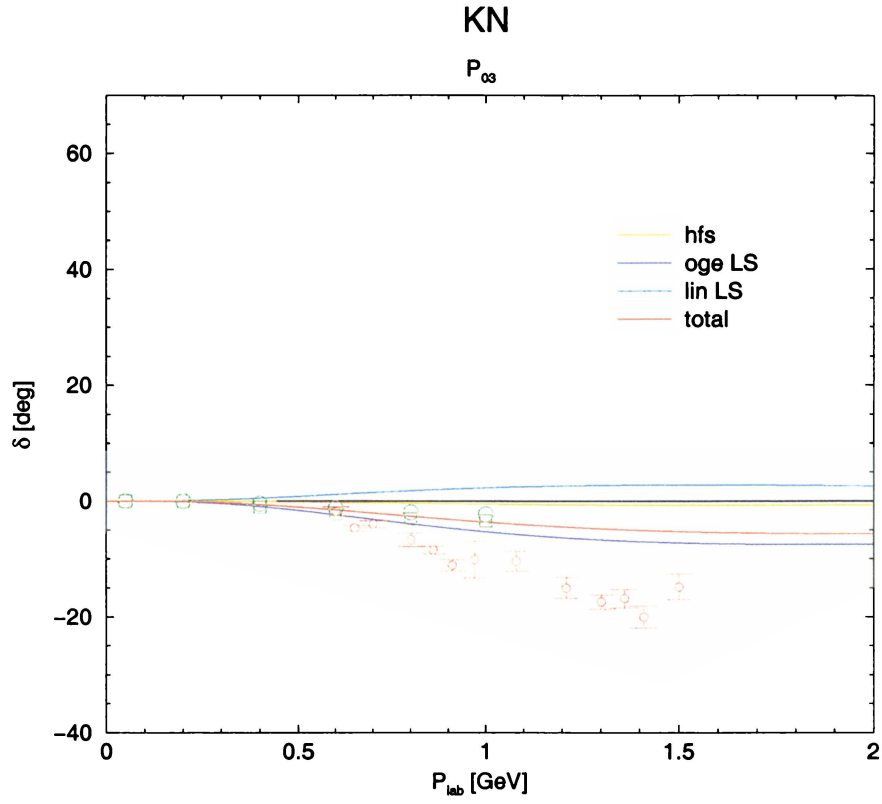


Figure 12: Theoretical P_{03} KN phase shift. The symbols are as in Fig. 1.

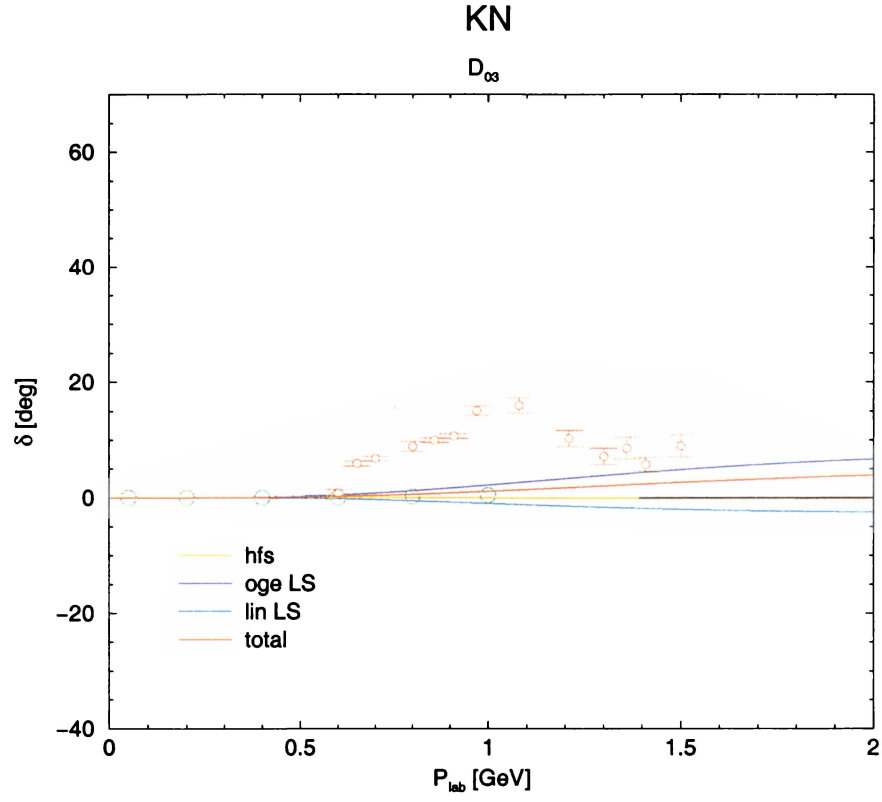


Figure 13: Theoretical D_{03} KN phase shift. The symbols are as in Fig. 1.

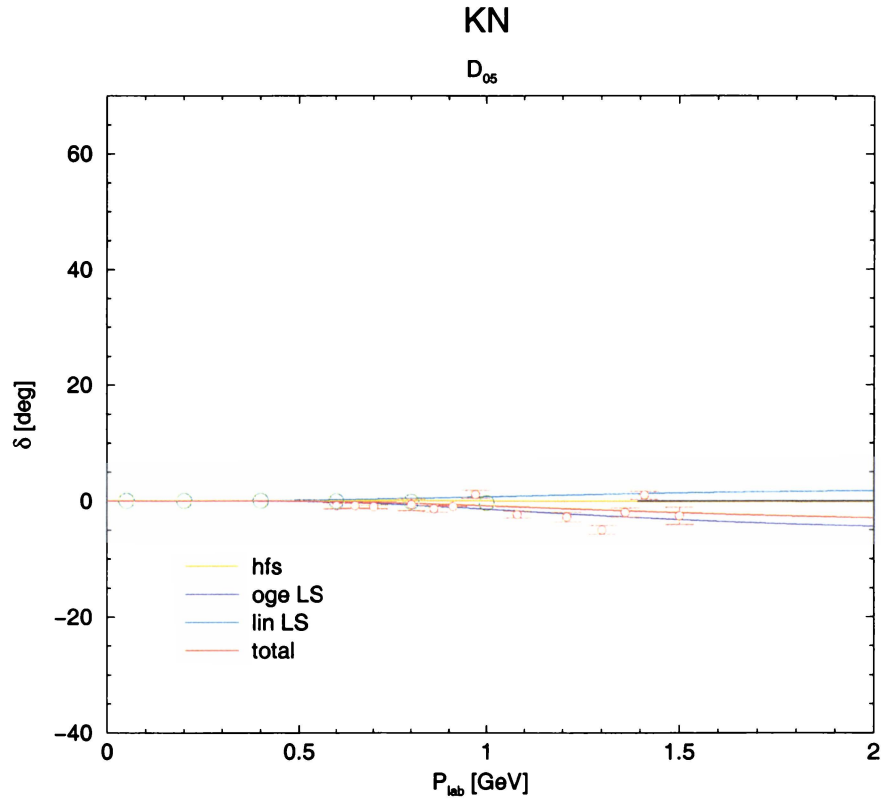


Figure 14: Theoretical D_{05} KN phase shift. The symbols are as in Fig. 1.

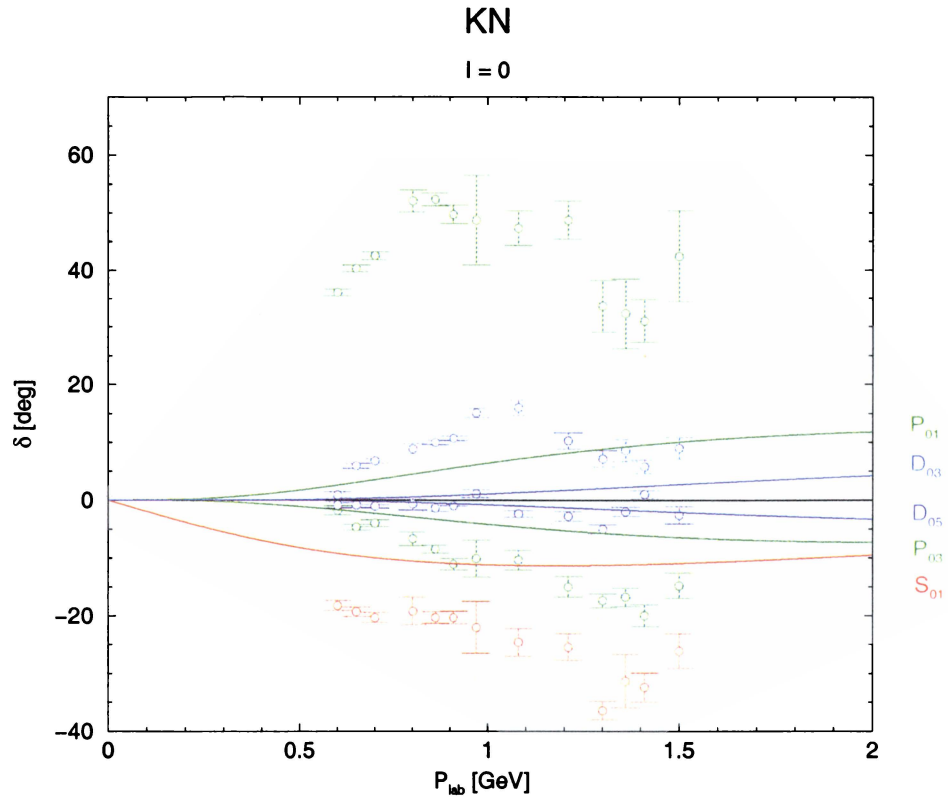


Figure 15: Theoretical I=0 KN total phase shifts. The data points are from Hashimoto .

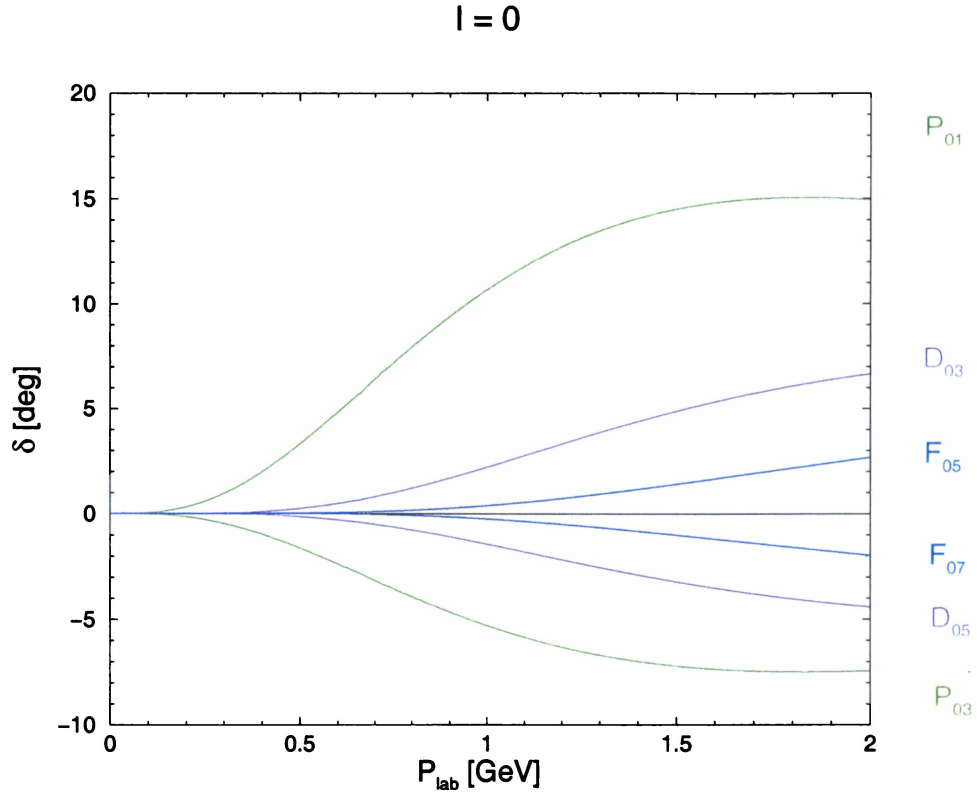


Figure 16: Theoretical $I=0$ KN OGE spin-orbit phase shifts. The data points are from Hashimoto .

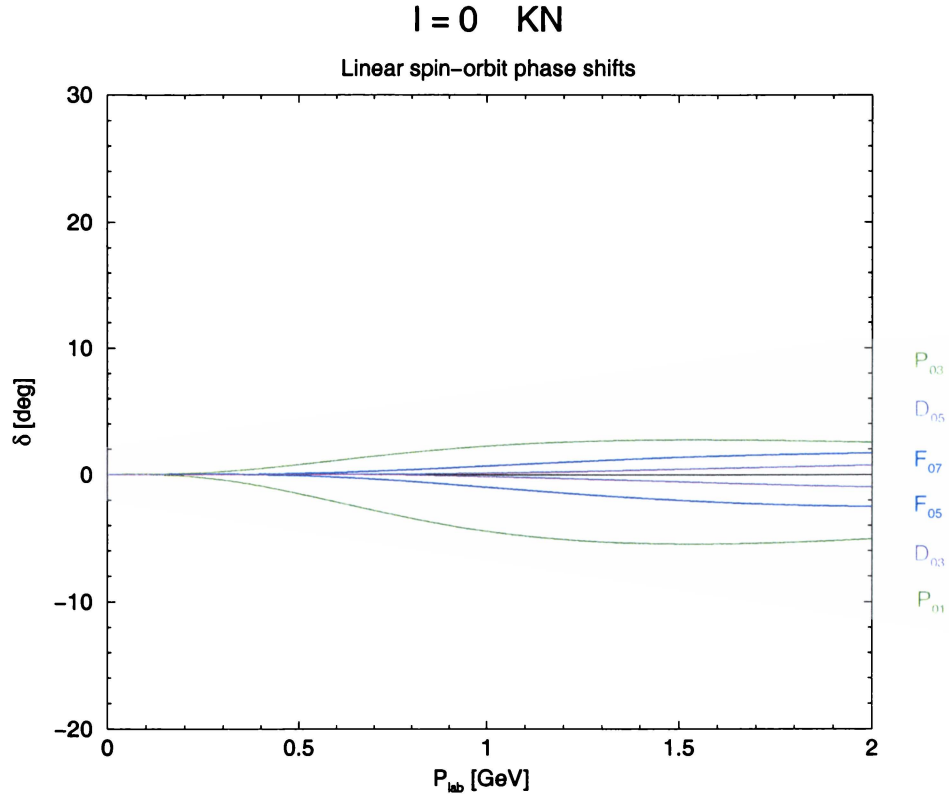


Figure 17: Theoretical $I=0$ KN confinement spin-orbit phase shifts. The data points are from Hashimoto .

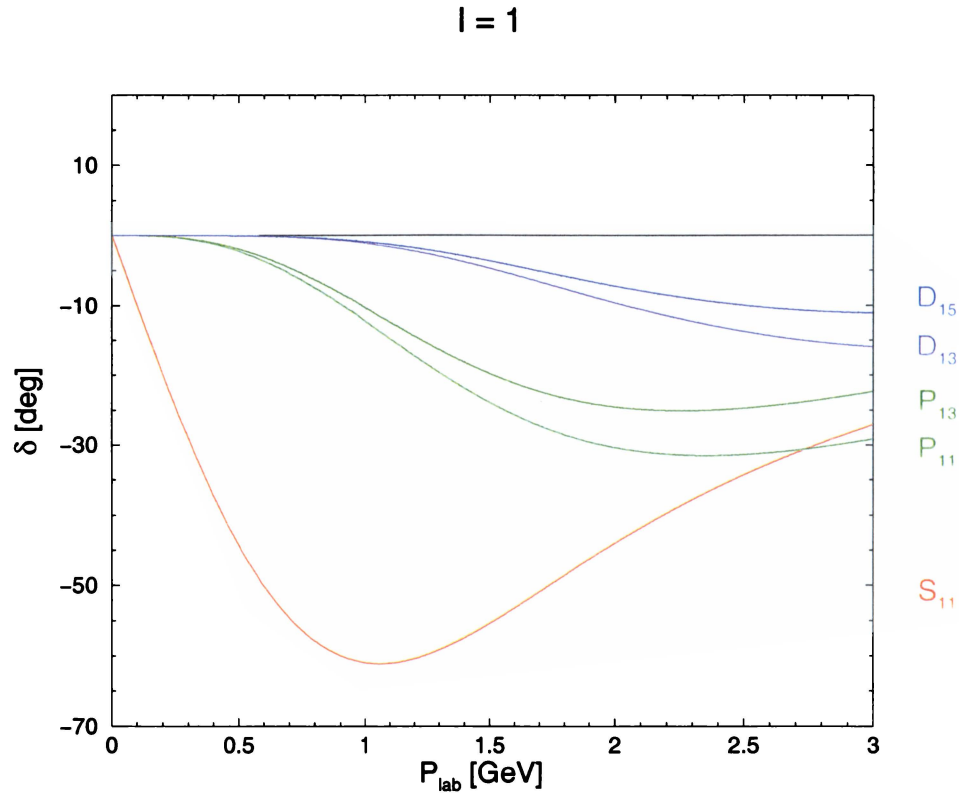


Figure 18: Theoretical $I=1$ DN phase shifts.

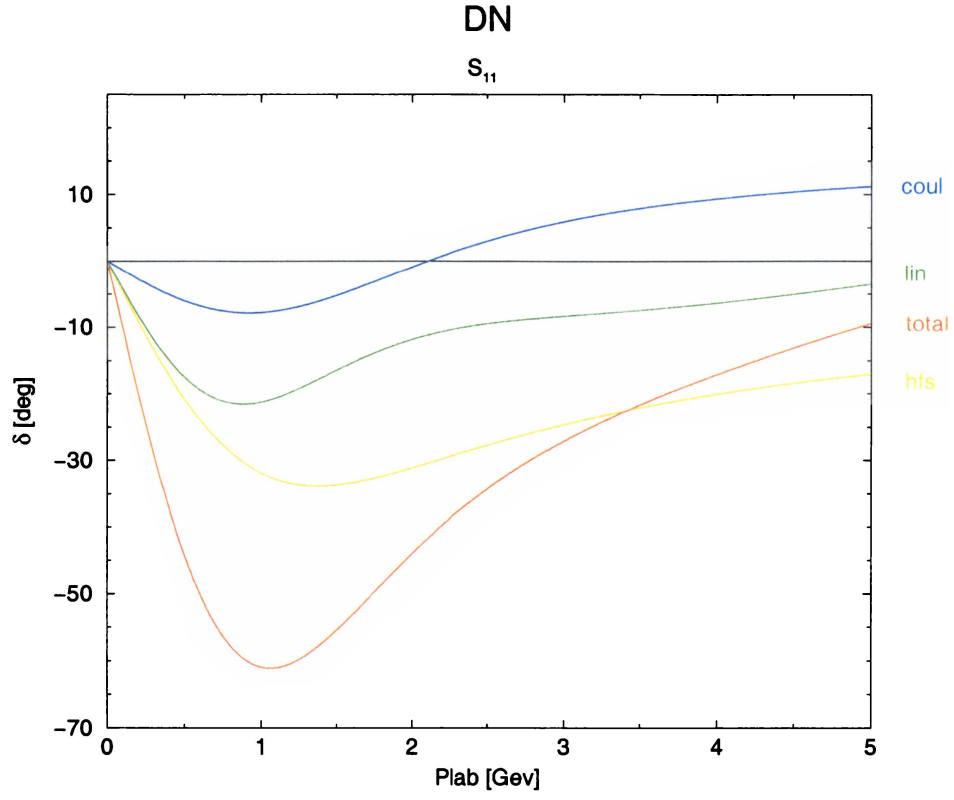


Figure 19: Theoretical S_{11} DN phase shift.

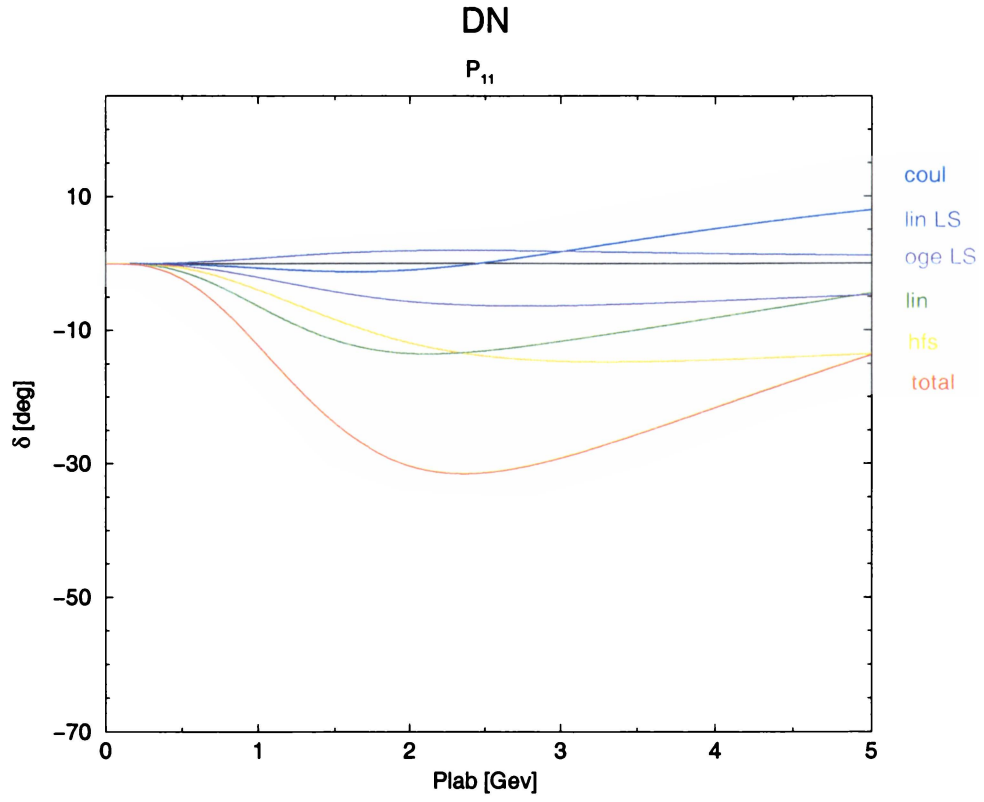


Figure 20: Theoretical P_{11} DN phase shift.

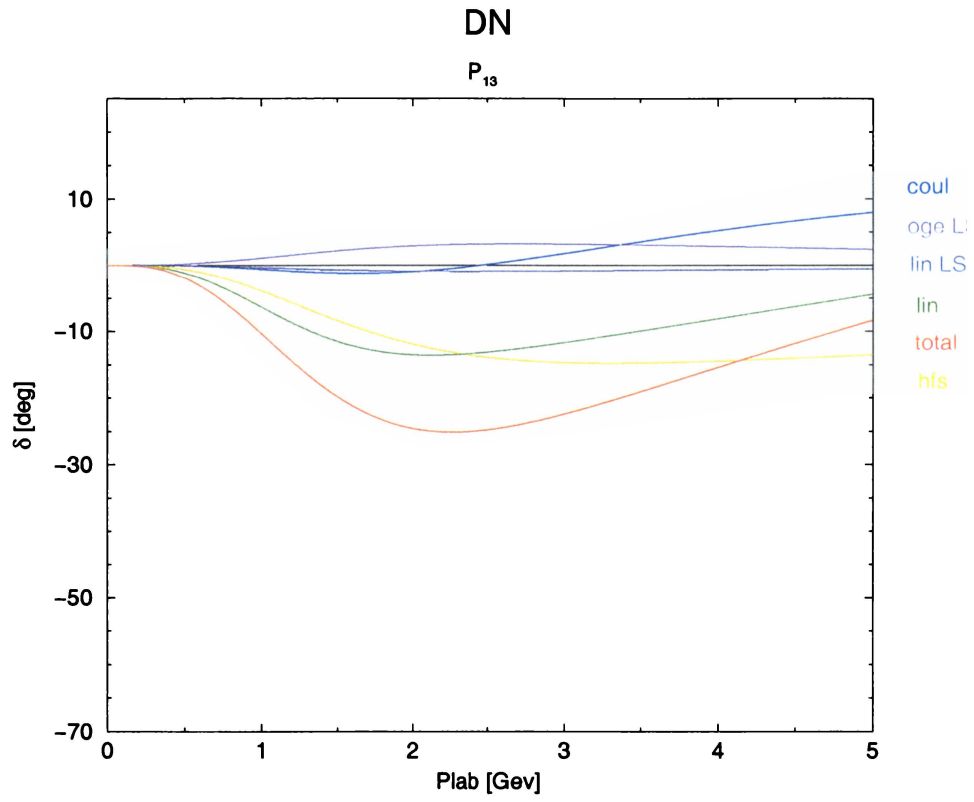


Figure 21: Theoretical P_{13} DN phase shift.

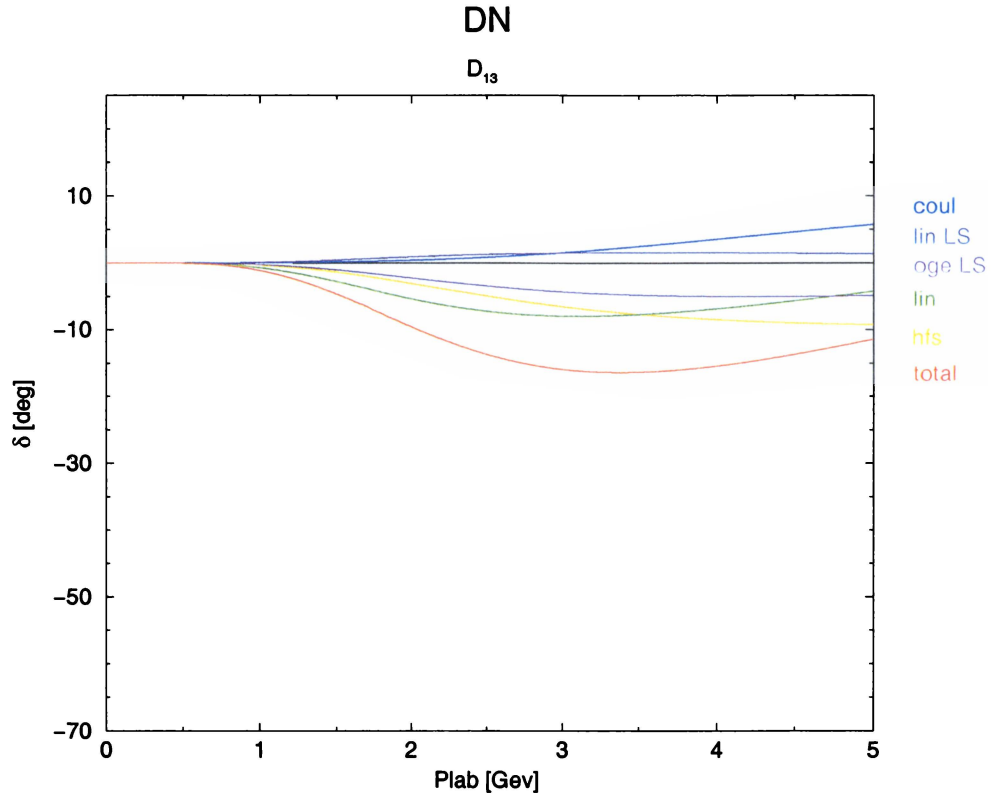


Figure 22: Theoretical D_{13} DN phase shift.

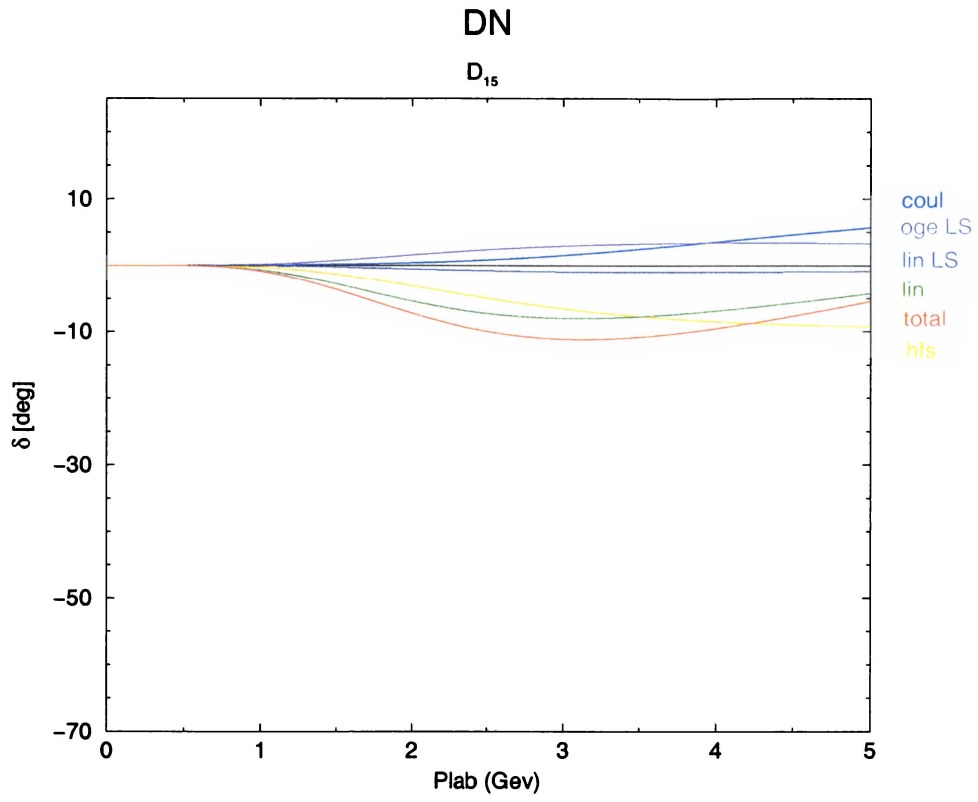


Figure 23: Theoretical D_{15} DN phase shift.

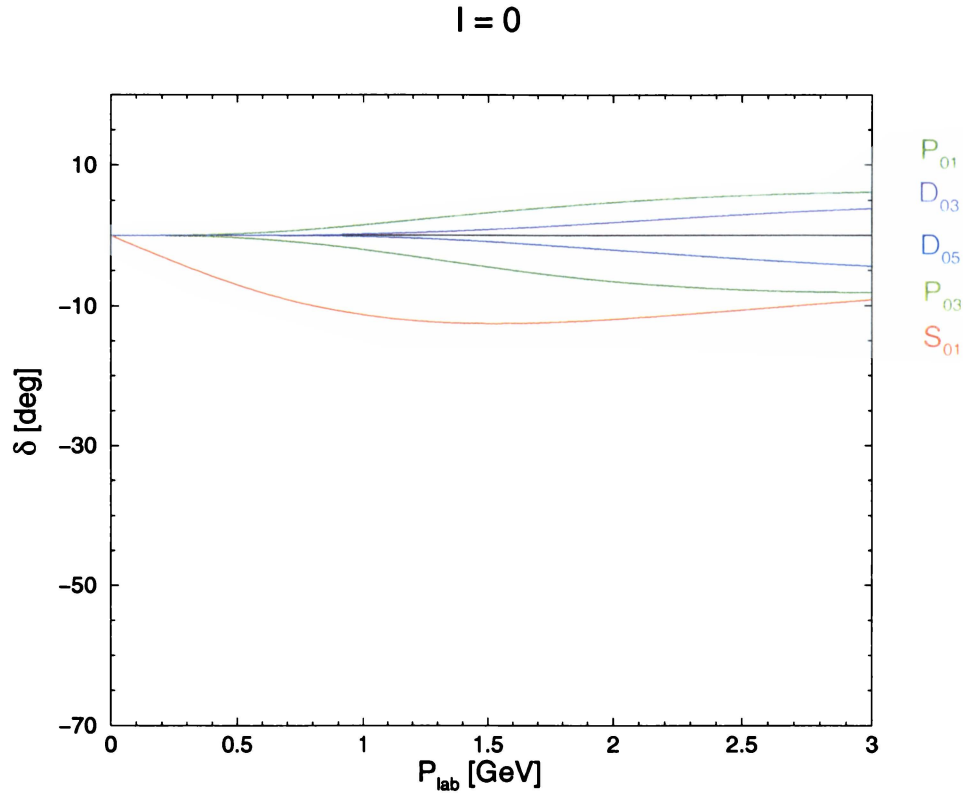


Figure 24: Theoretical $I=0$ DN phase shifts.

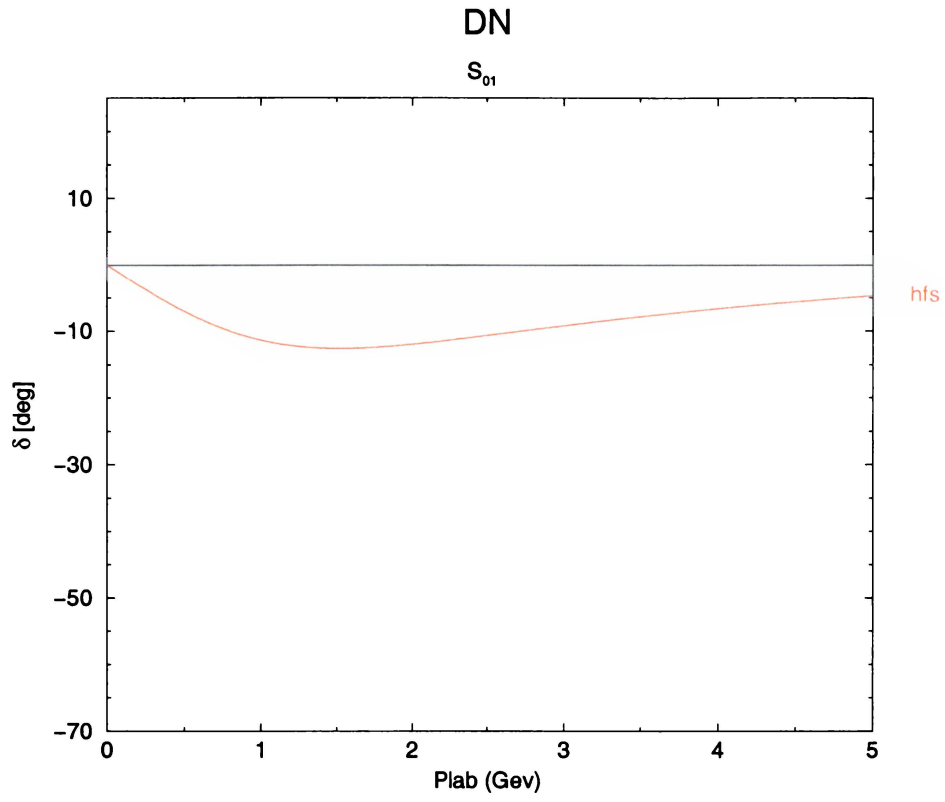


Figure 25: Theoretical S_{01} DN phase shift.

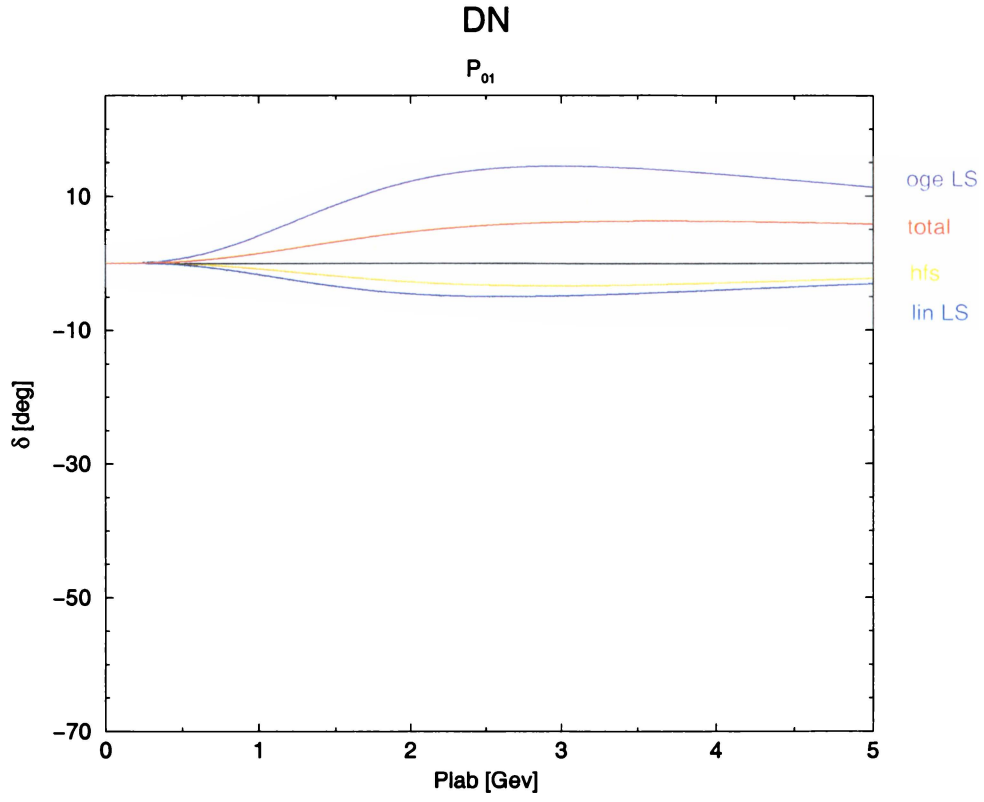


Figure 26: Theoretical P_{01} DN phase shift.

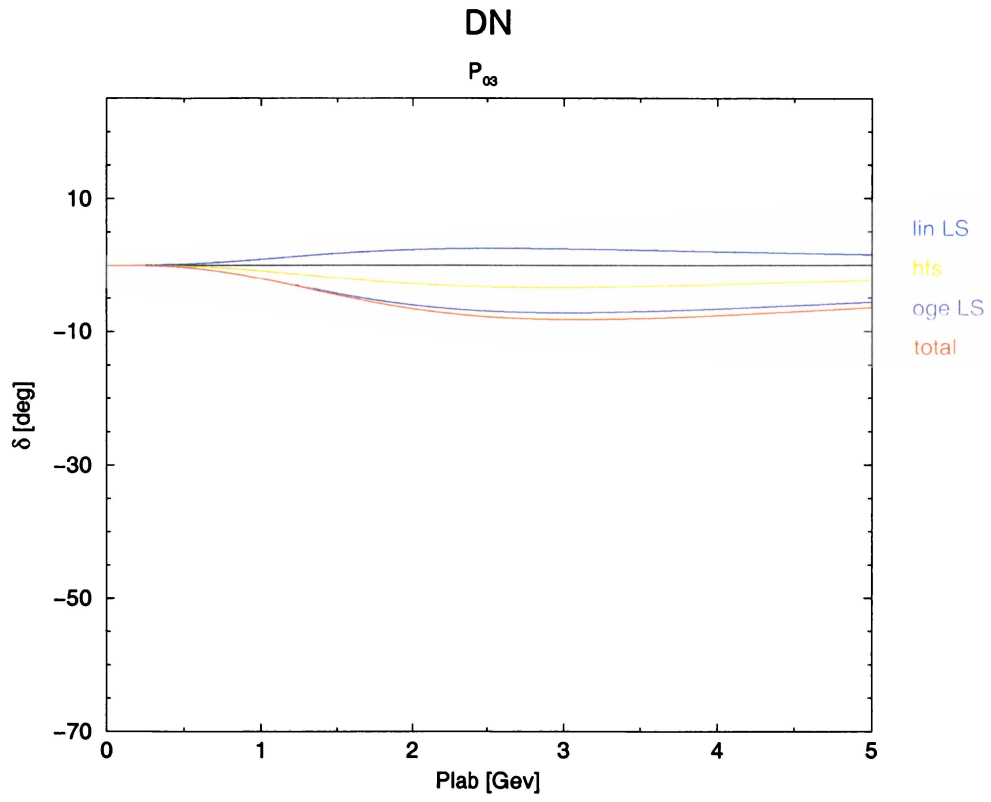


Figure 27: Theoretical P_{03} DN phase shift.

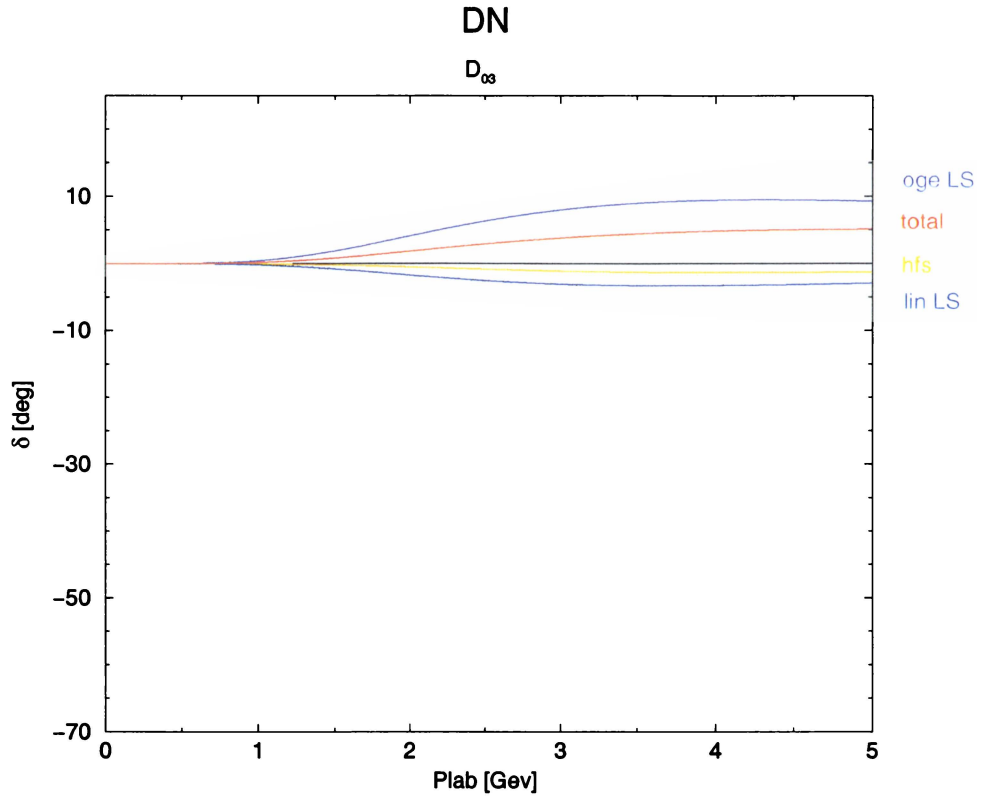


Figure 28: Theoretical D_{03} DN phase shift.

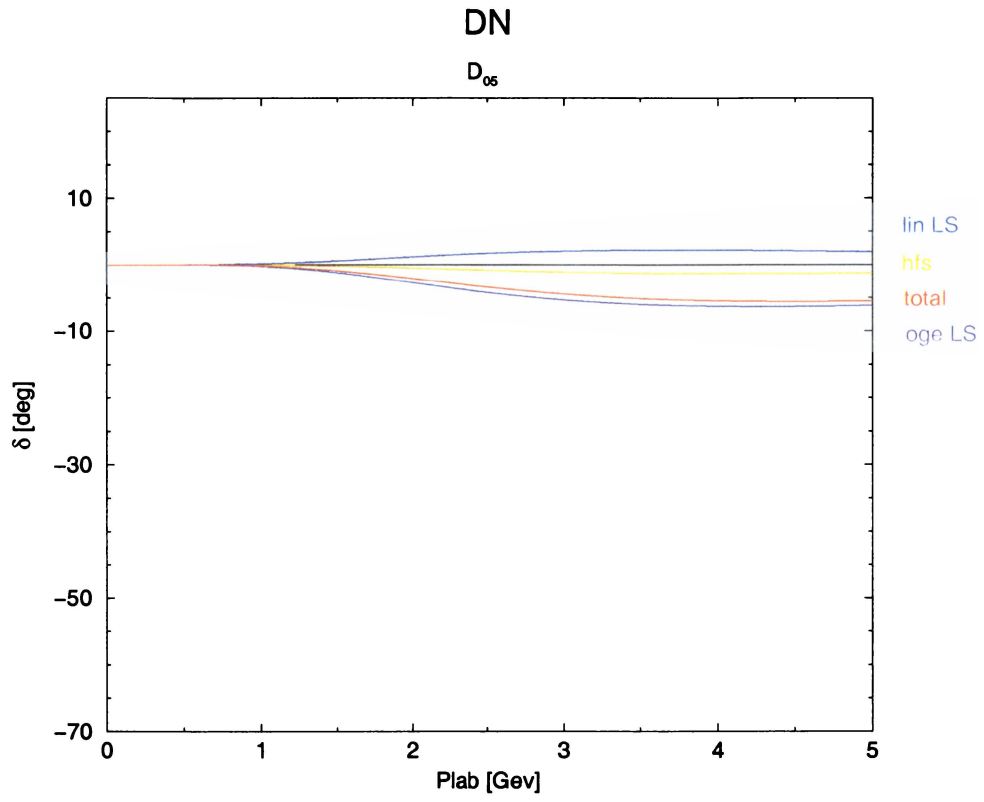


Figure 29: Theoretical D_{05} DN phase shift.

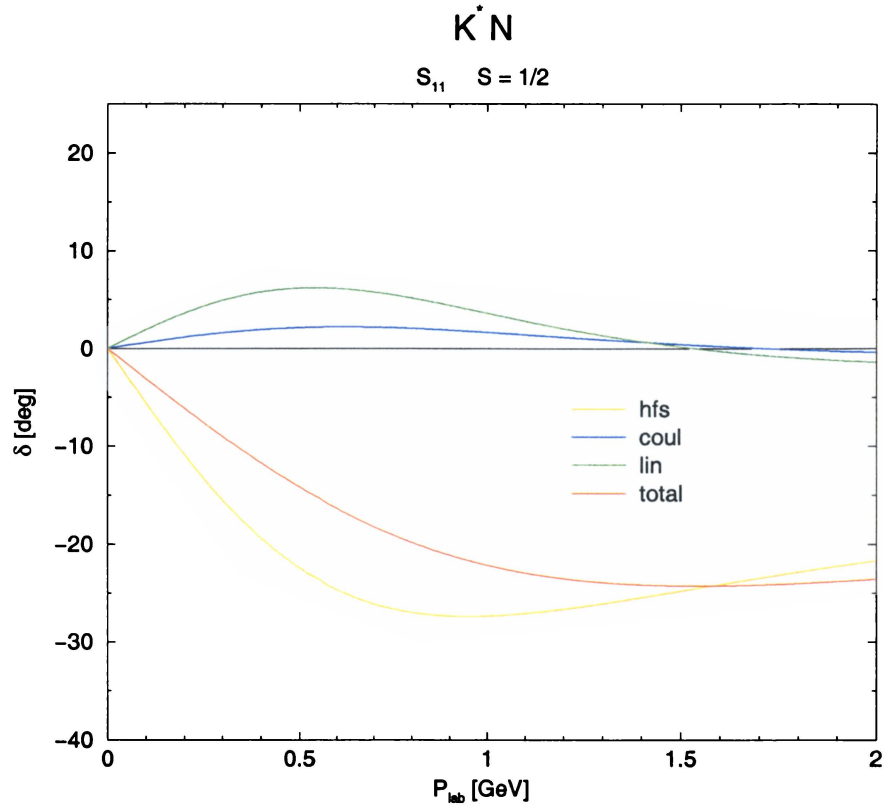


Figure 30: Theoretical $S=1/2 \ S_{11} \ K^* N$ phase shift.

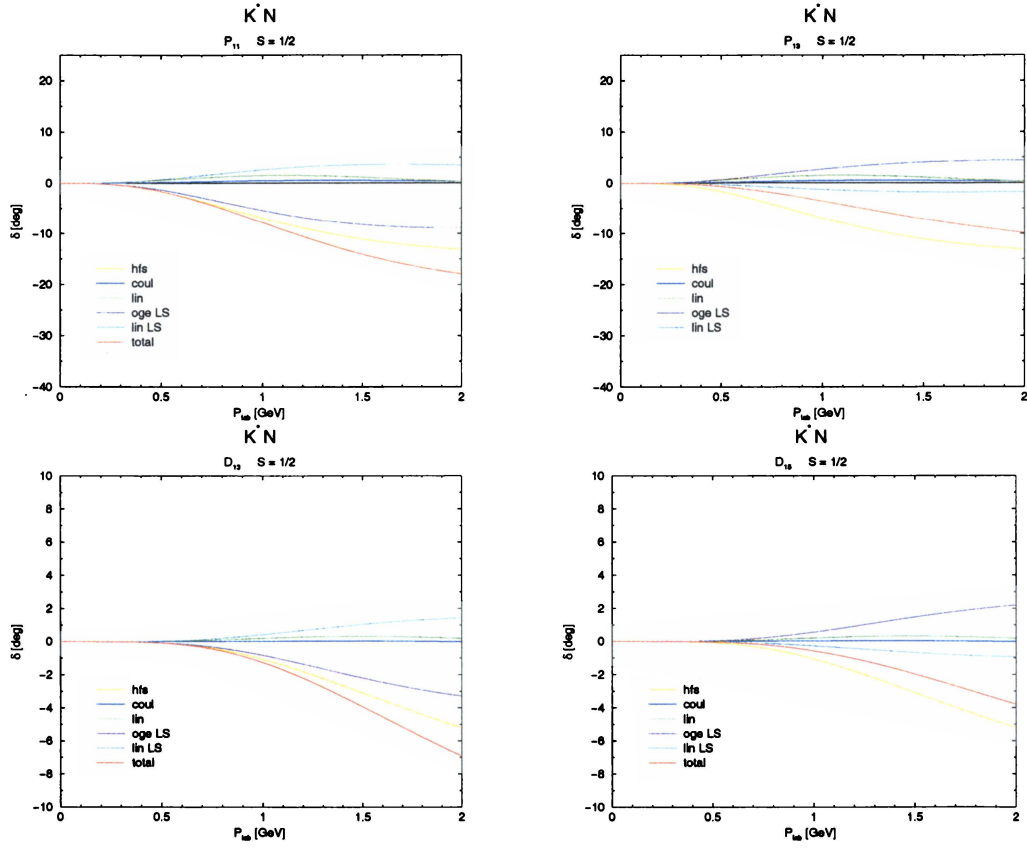


Figure 31: Theoretical $I=1$ $S=1/2$ P- and D-wave K^*N phase shifts.

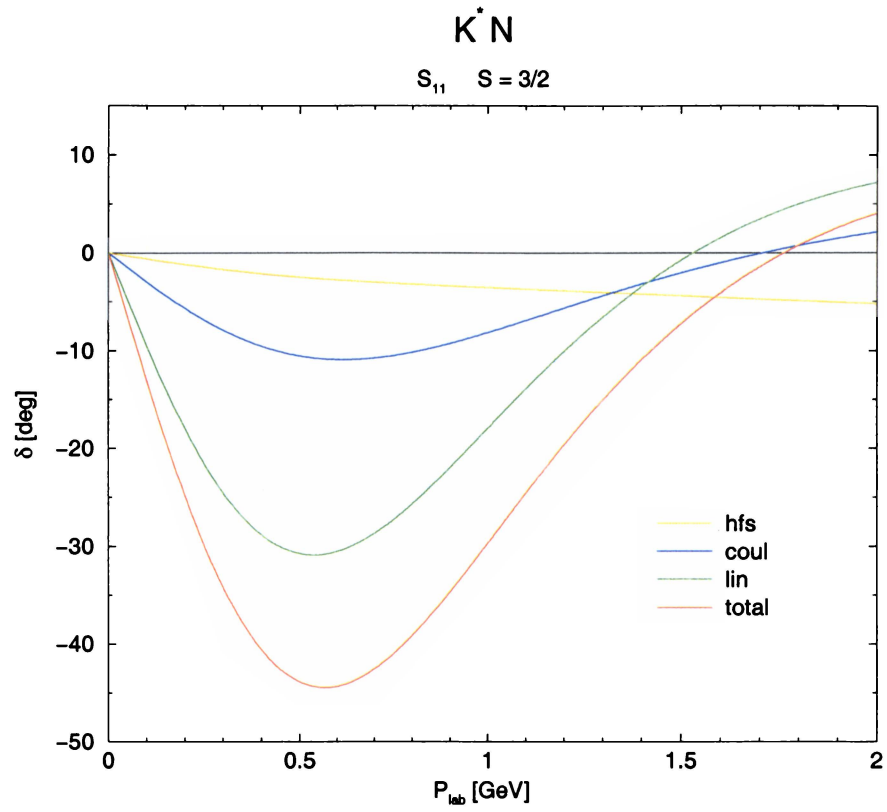


Figure 32: Theoretical $S=3/2 \ S_{11} \ K^* N$ phase shift.

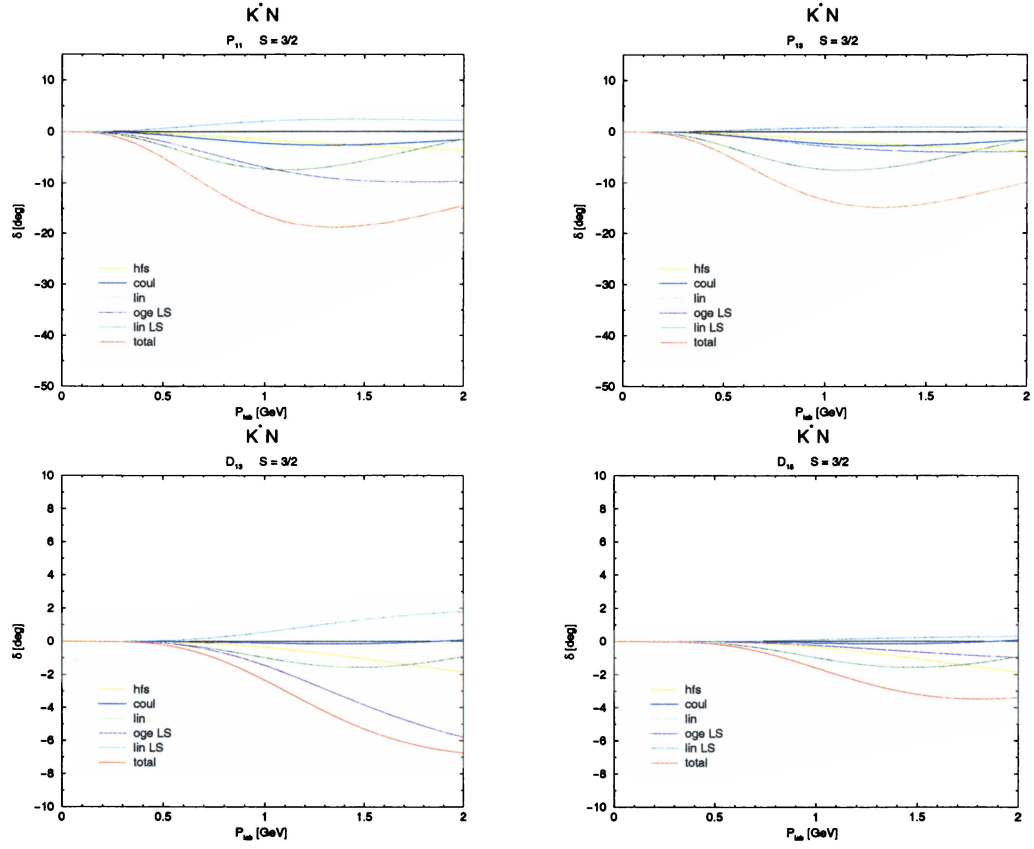


Figure 33: Theoretical $I=1$ $S=3/2$ P- and D-wave K^*N phase shifts.

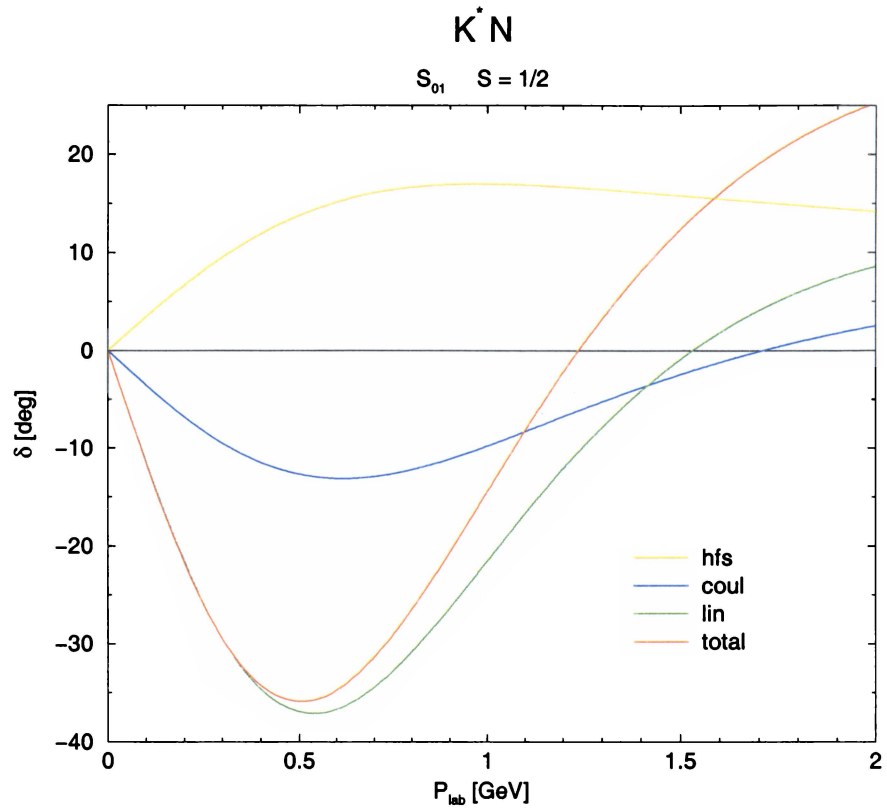


Figure 34: Theoretical $S=1/2$ S_{01} K^*N phase shift.

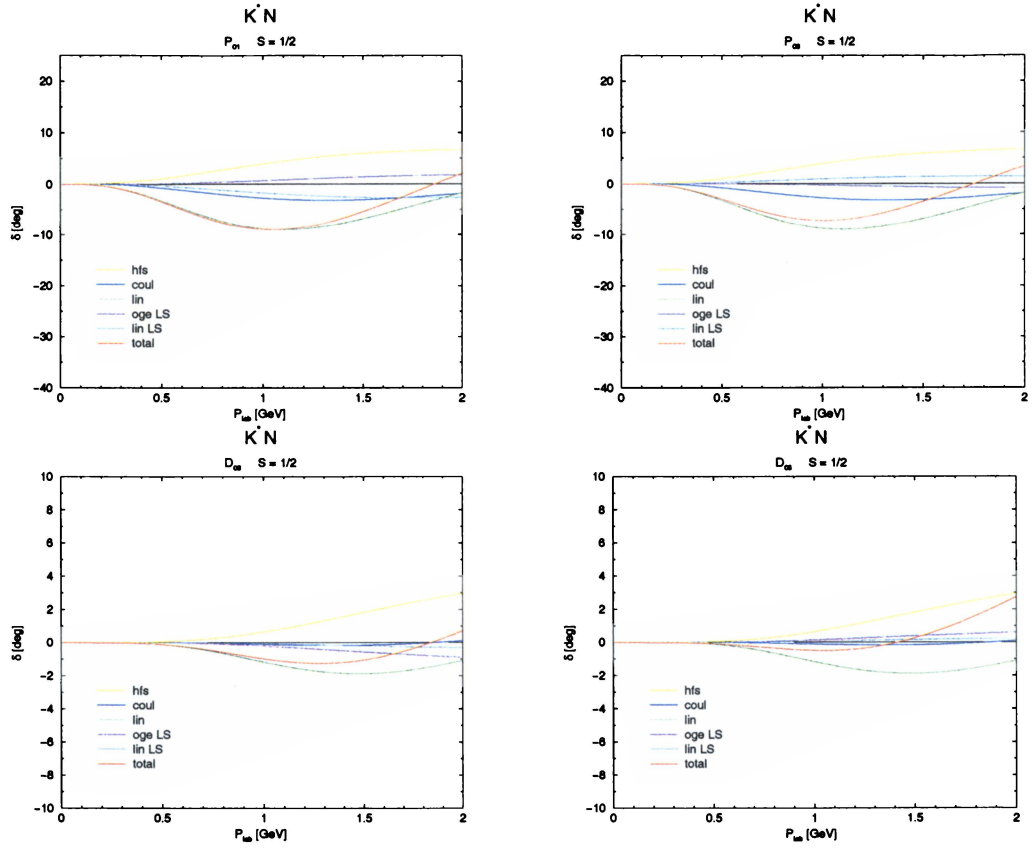


Figure 35: Theoretical $I=0$ $S=1/2$ P- and D-wave K^*N phase shifts.

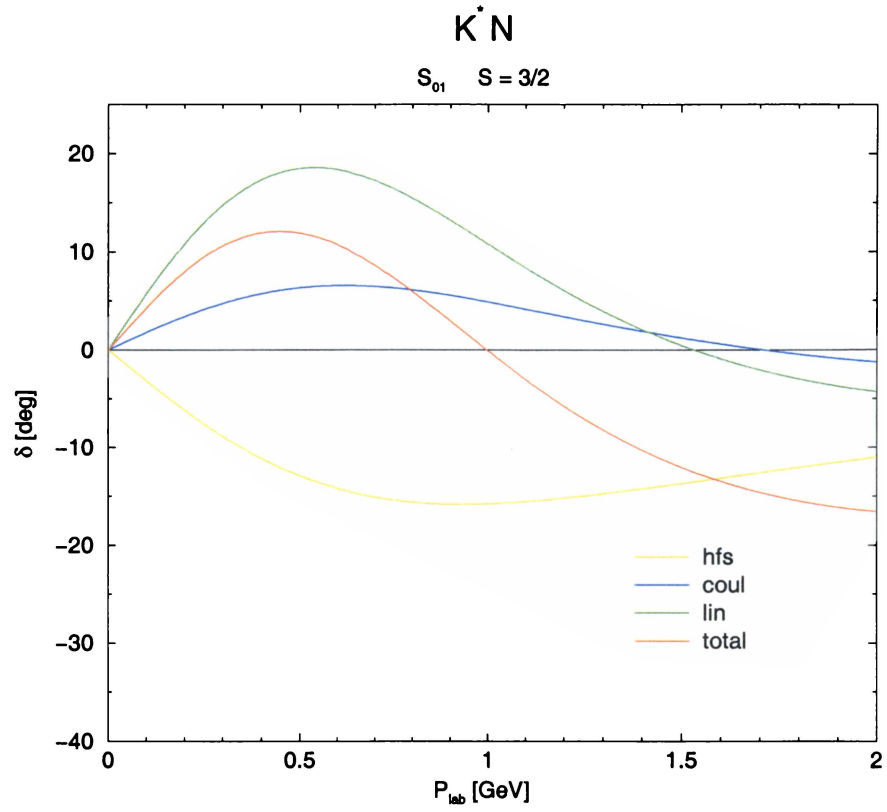


Figure 36: Theoretical $S=3/2$ S_{01} $K^* N$ phase shift.

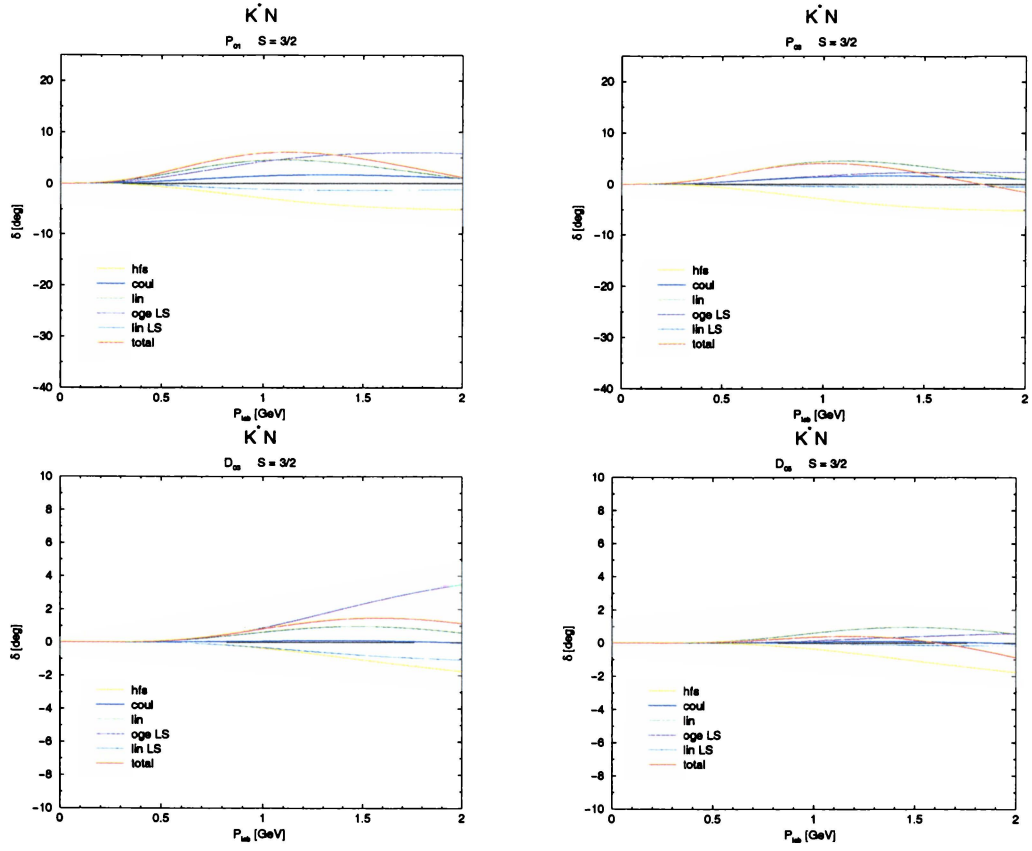


Figure 37: Theoretical $I=0$ $S=3/2$ P- and D-wave K^*N phase shifts.

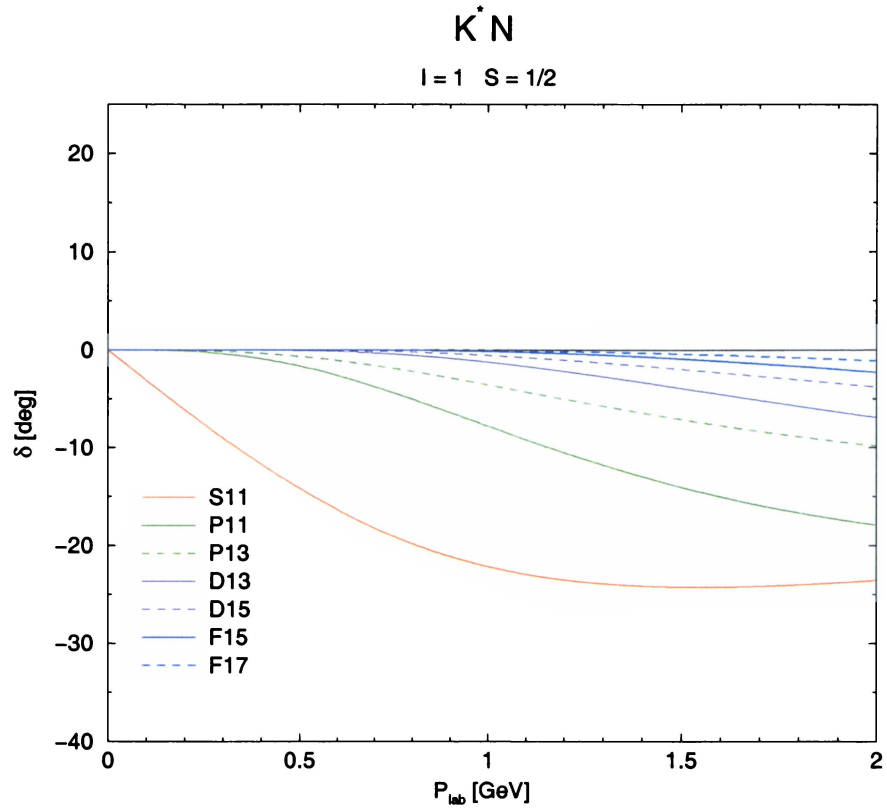


Figure 38: Theoretical $I=1$ $S=1/2$ K^*N total phase shifts.

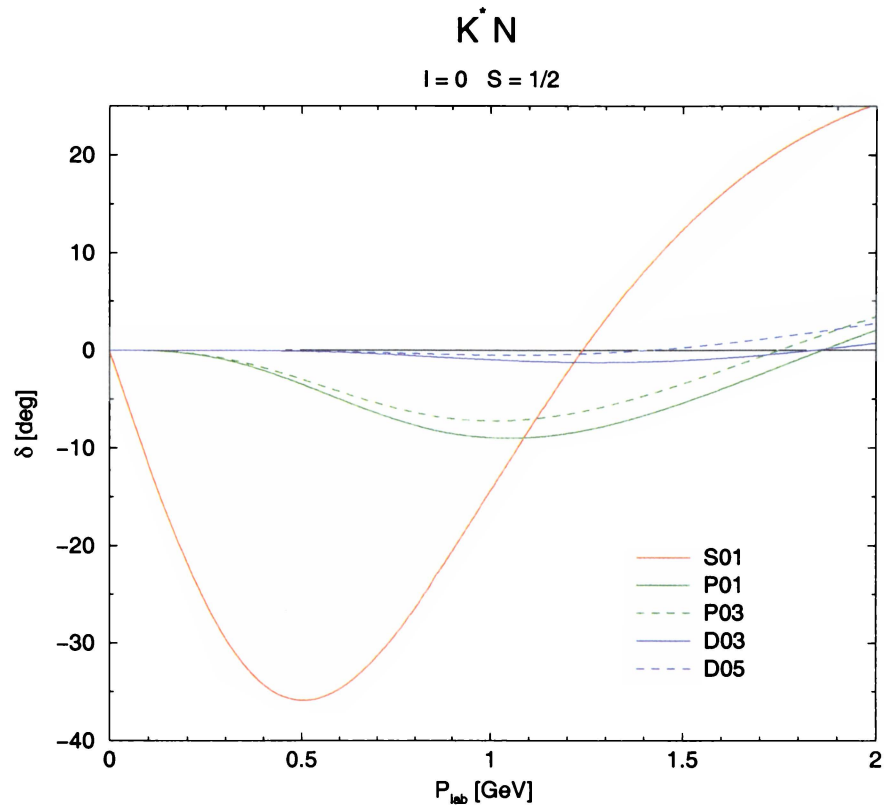


Figure 39: Theoretical $I=0$ $S=1/2$ K^*N total phase shifts.

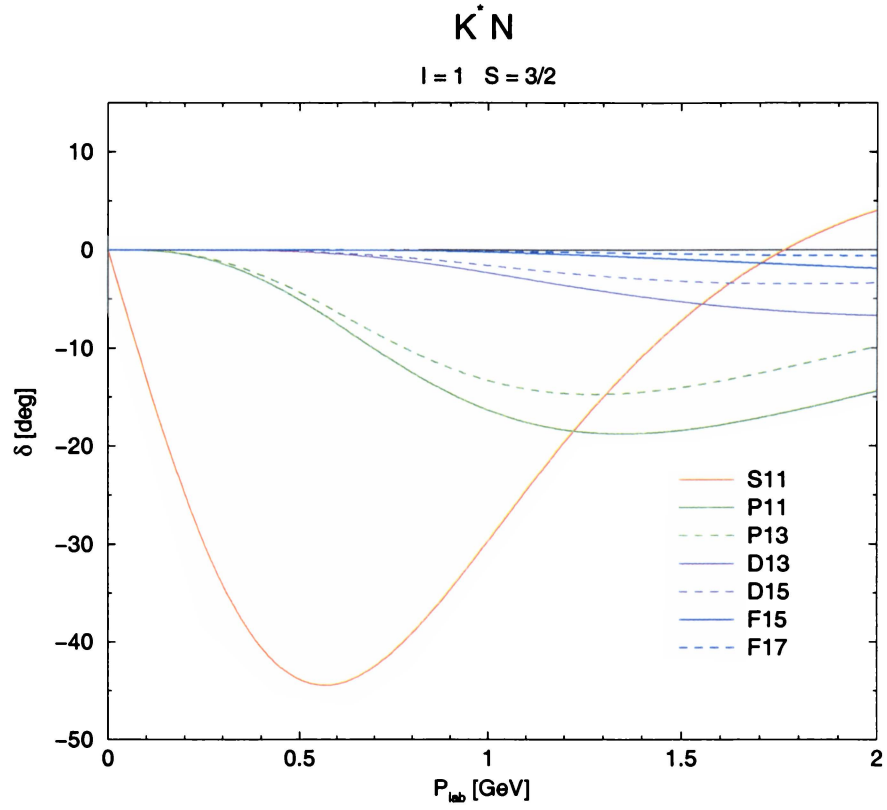


Figure 40: Theoretical $I=1$ $S=3/2$ K^*N total phase shifts.

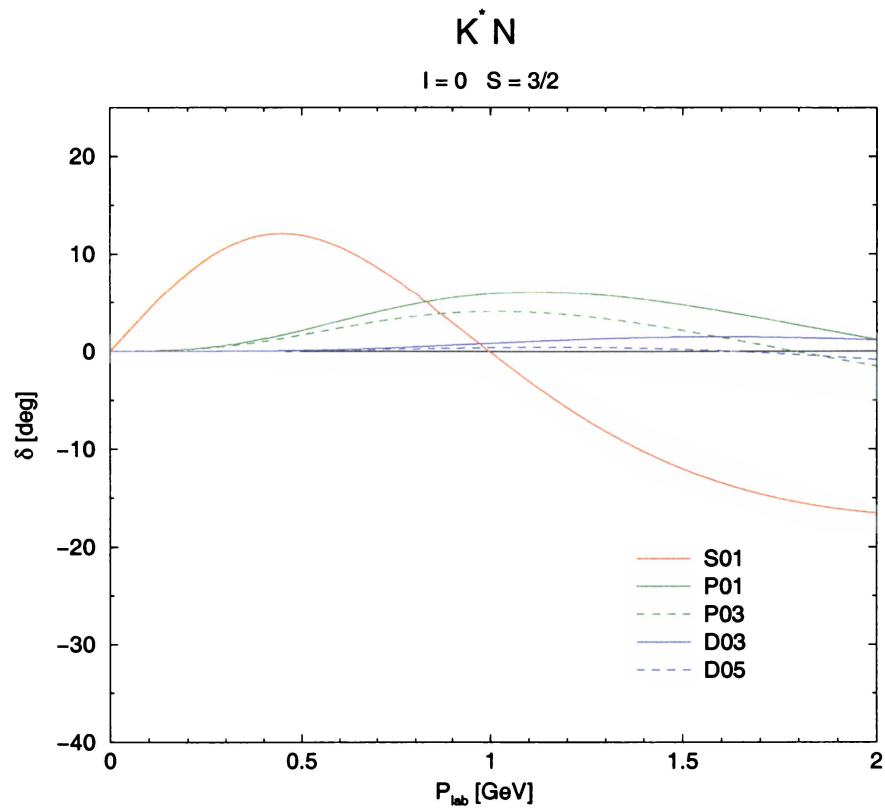


Figure 41: Theoretical $I=0$ $S=3/2$ K^*N total phase shifts.

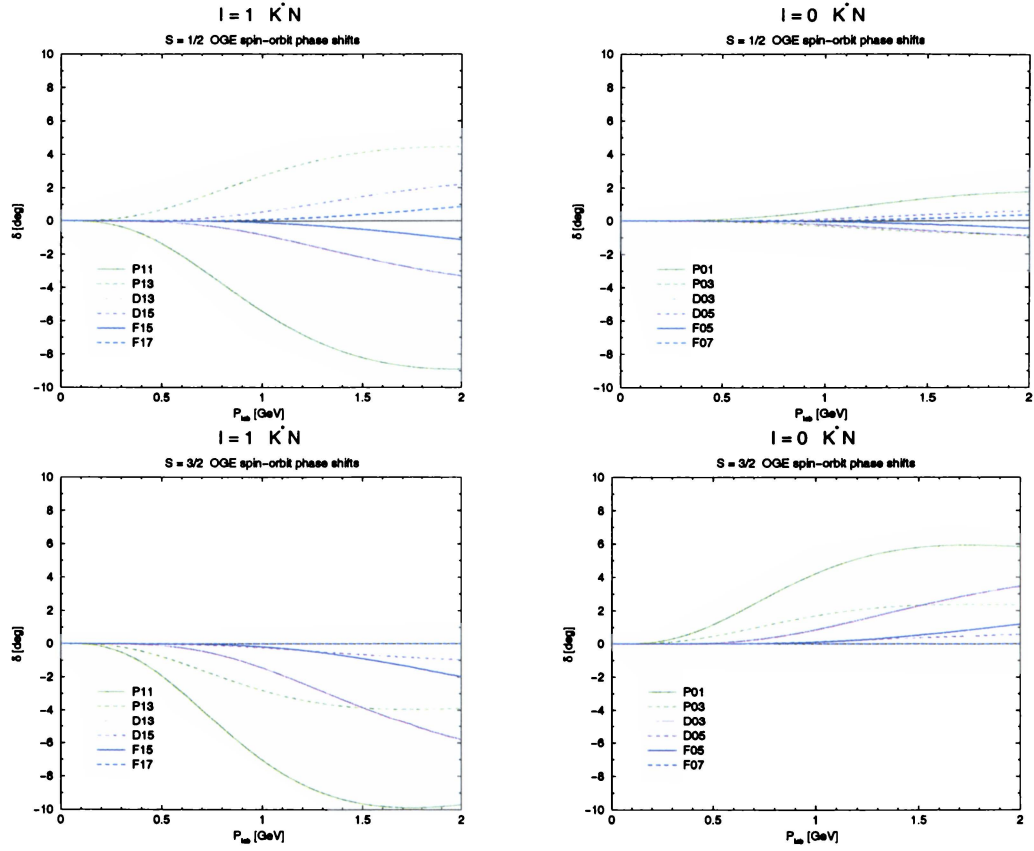


Figure 42: Theoretical $I=1,0$ $S=1/2,3/2$ K^*N OGE spin-orbit phase shifts.

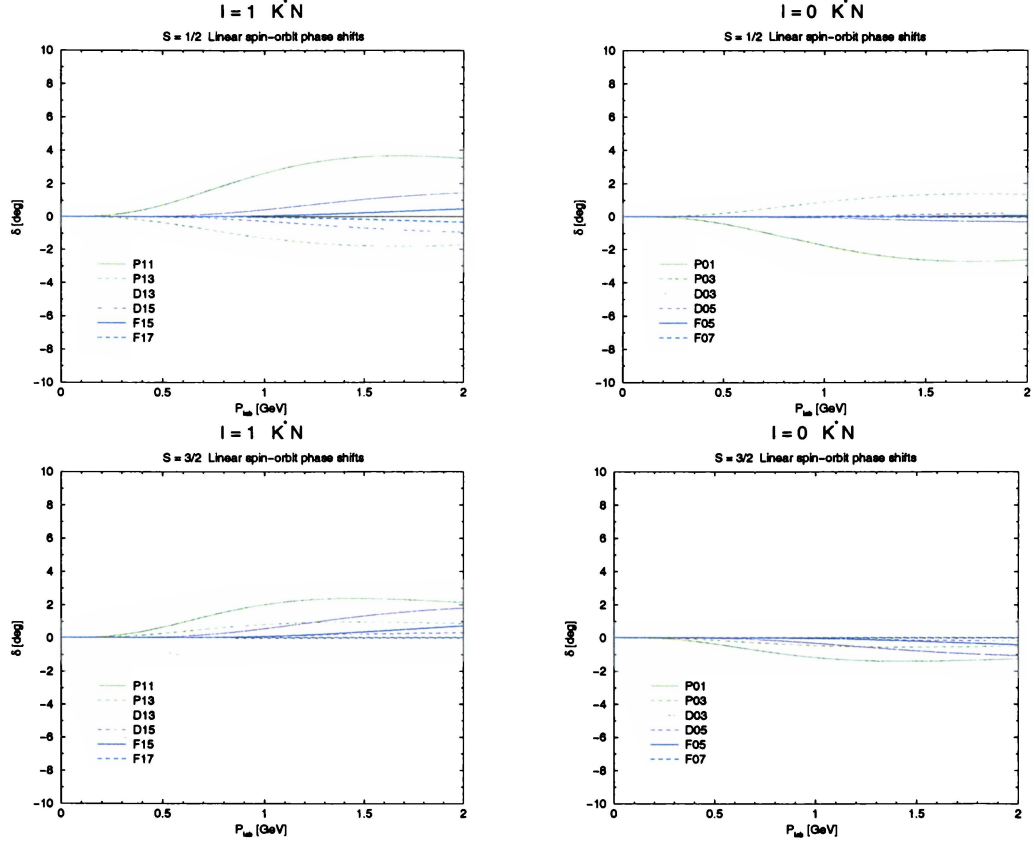


Figure 43: Theoretical $I=1,0$ $S=1/2,3/2$ K^*N confinement spin-orbit phase shifts.

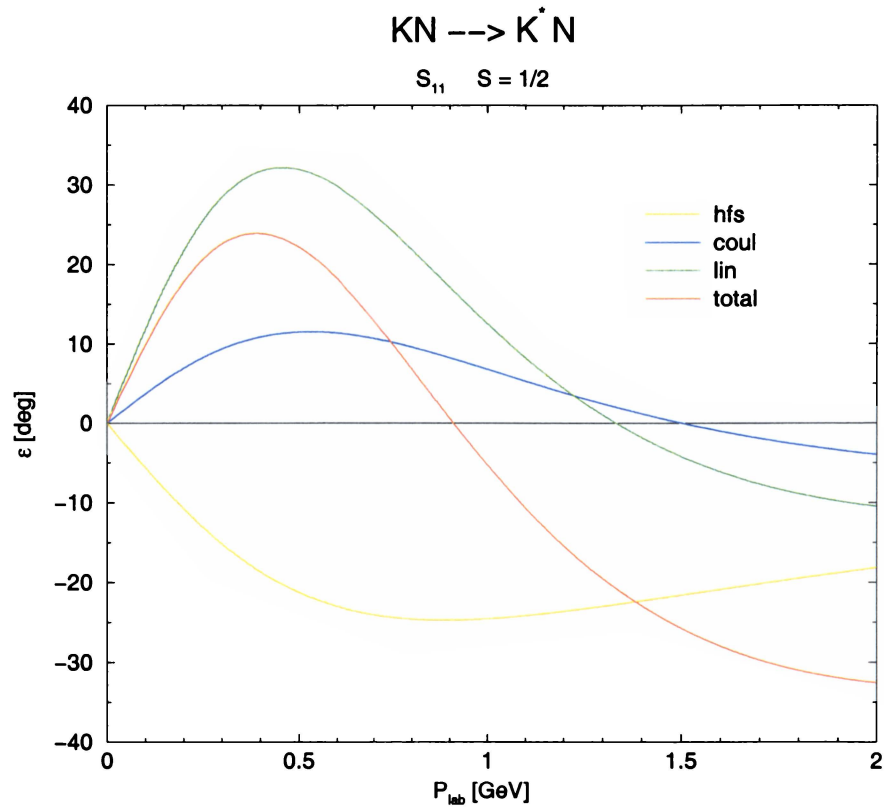


Figure 44: Theoretical S_{11} $KN \rightarrow K^*N$ inelasticity.

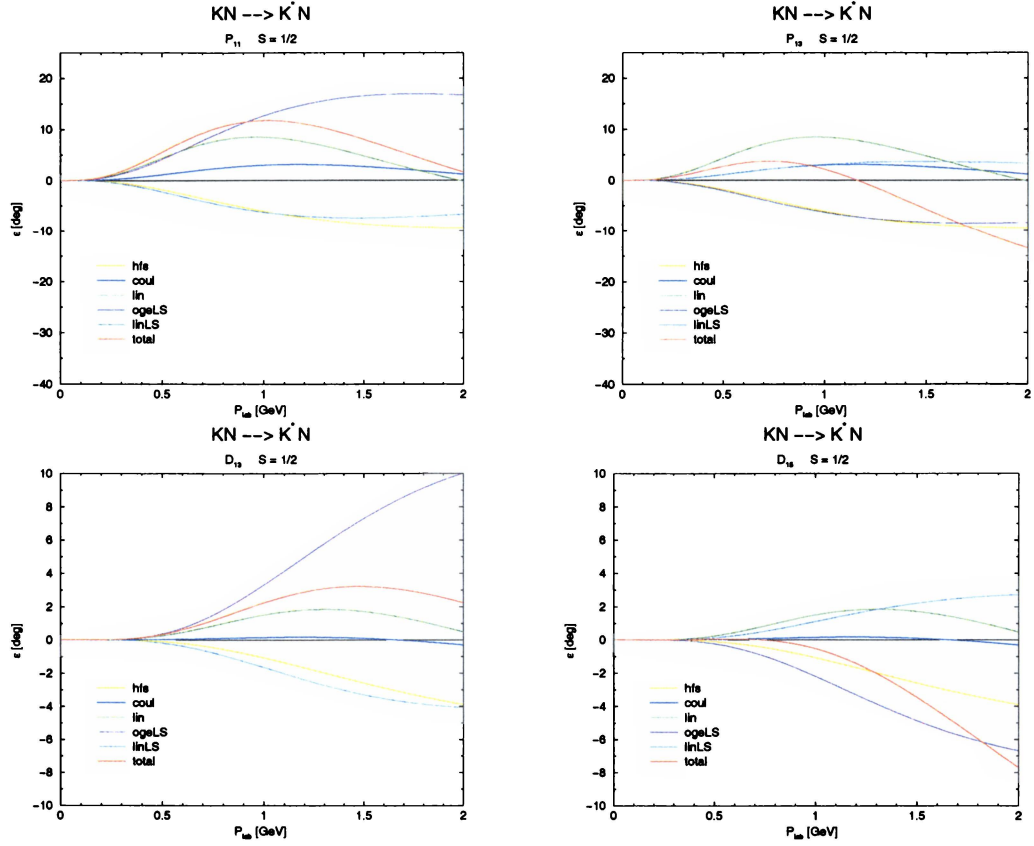


Figure 45: Theoretical $I=1$ P- and D-wave $KN \rightarrow K^*N$ inelasticities.

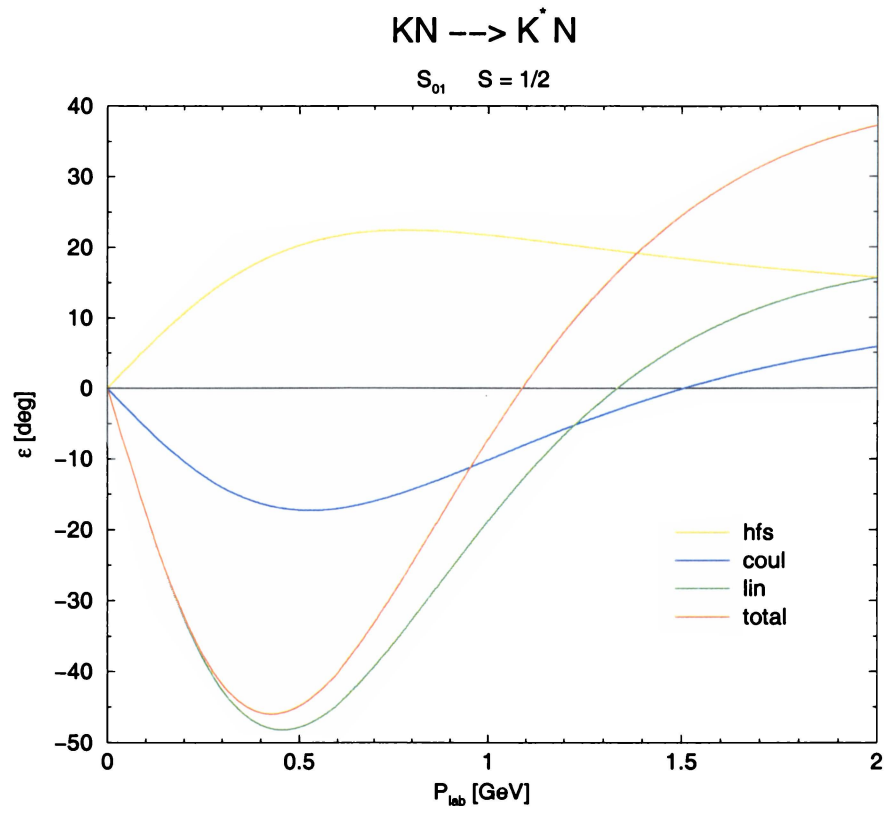


Figure 46: Theoretical S_{01} $KN \rightarrow K^* N$ inelasticity.

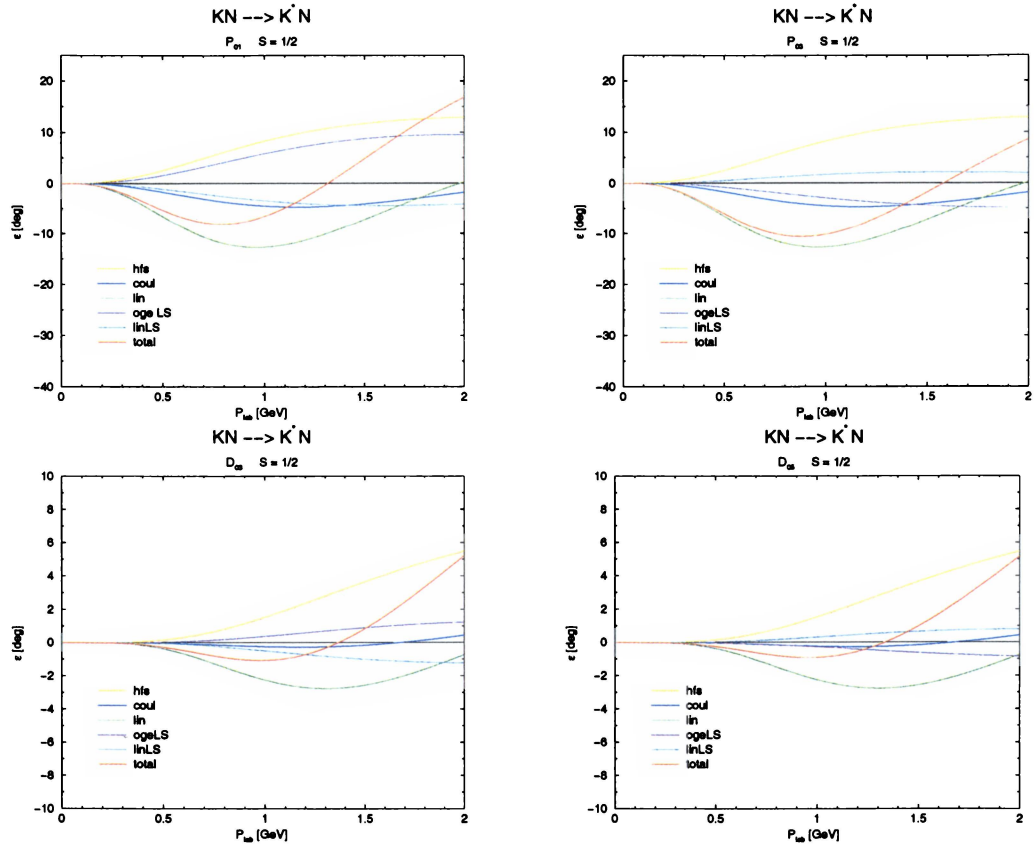


Figure 47: Theoretical $I=0$ P- and D-wave $KN \rightarrow K^*N$ inelasticities.

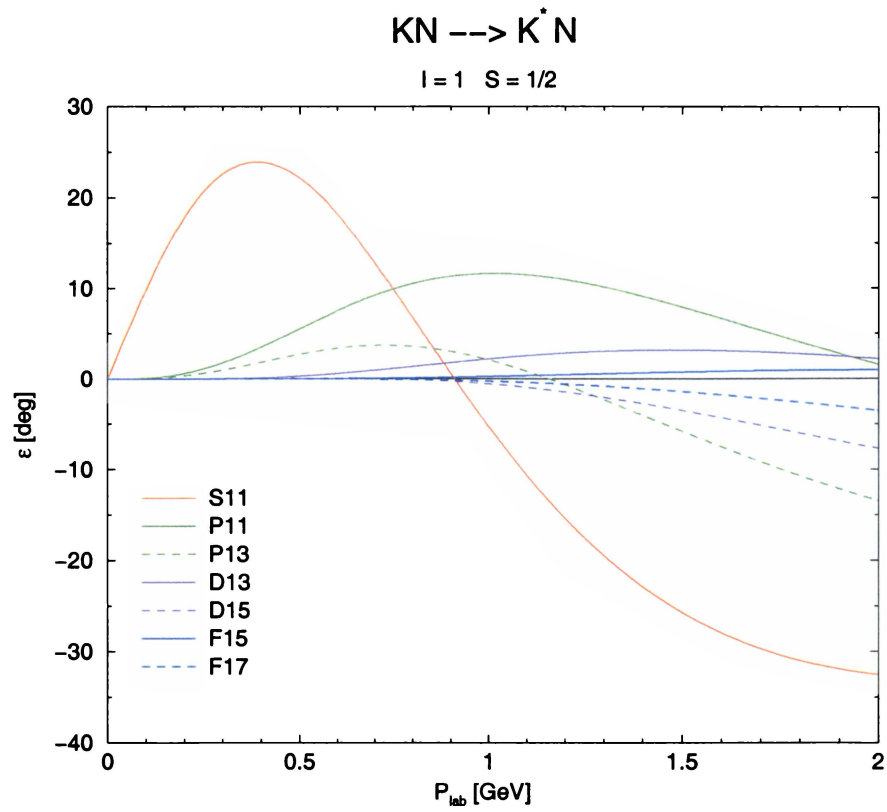


Figure 48: Theoretical $I=1$ $KN \rightarrow K^*N$ total inelasticities.

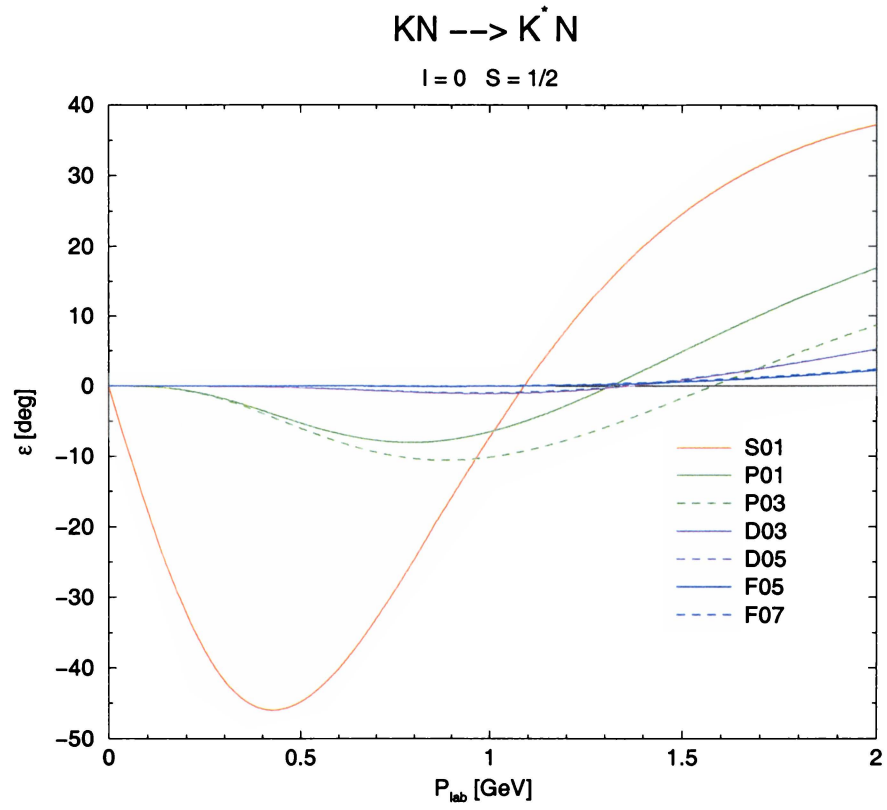


Figure 49: Theoretical $I=0$ $KN \rightarrow K^*N$ total inelasticities.

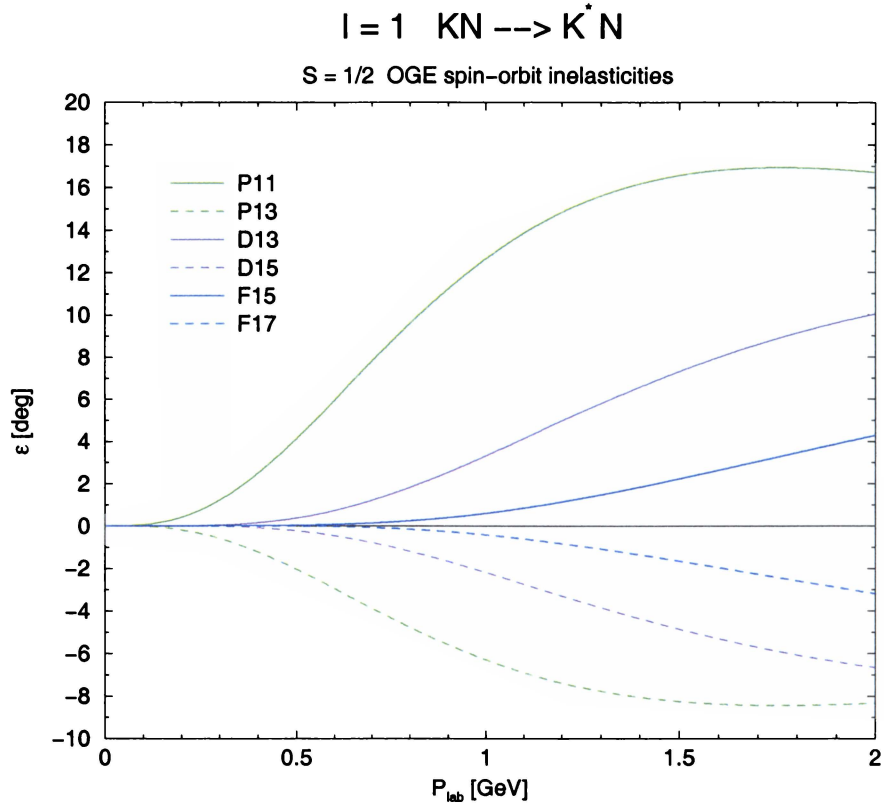


Figure 50: Theoretical $I=1 \quad KN \rightarrow K^* N$ OGE spin-orbit inelasticities.

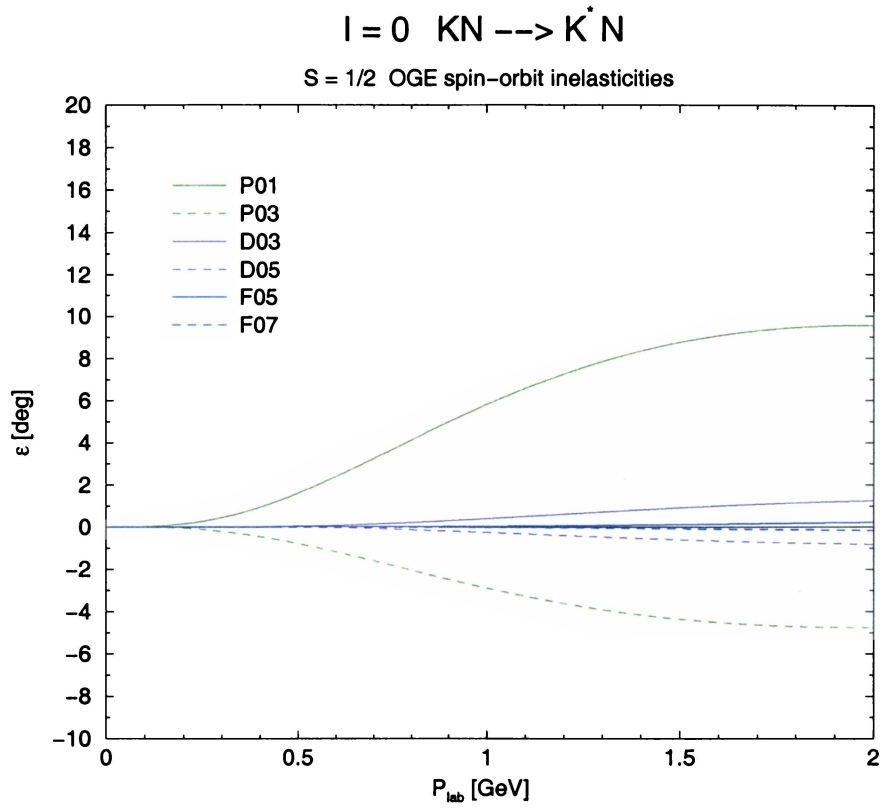


Figure 51: Theoretical $I=0 \quad KN \rightarrow K^* N$ OGE spin-orbit inelasticities.

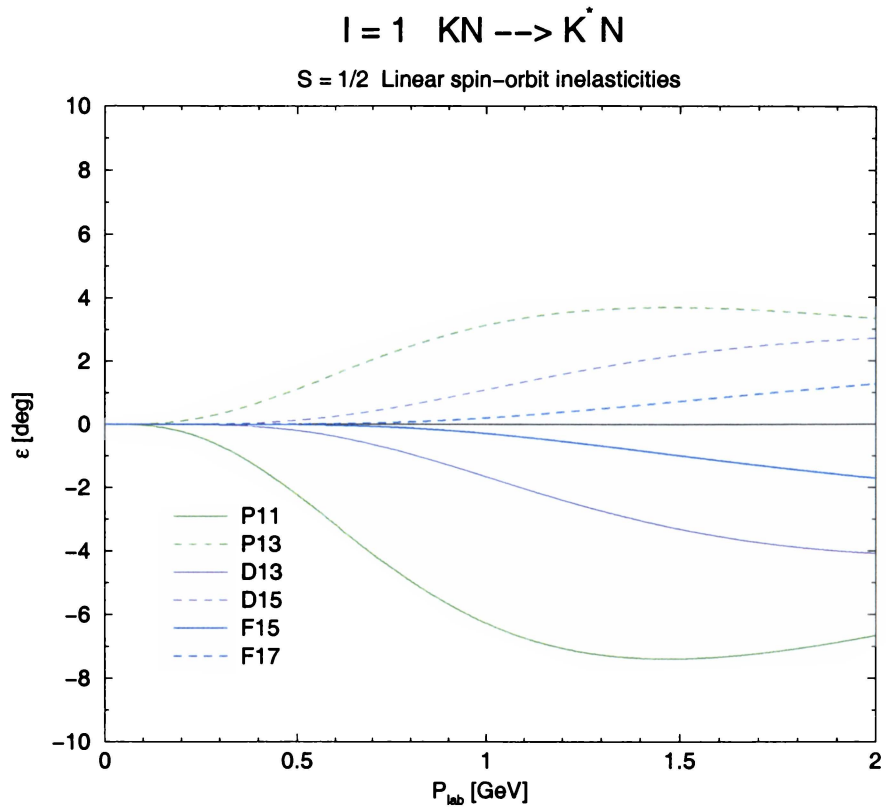


Figure 52: Theoretical $I=1 \quad KN \rightarrow K^* N$ confinement spin-orbit inelasticities.

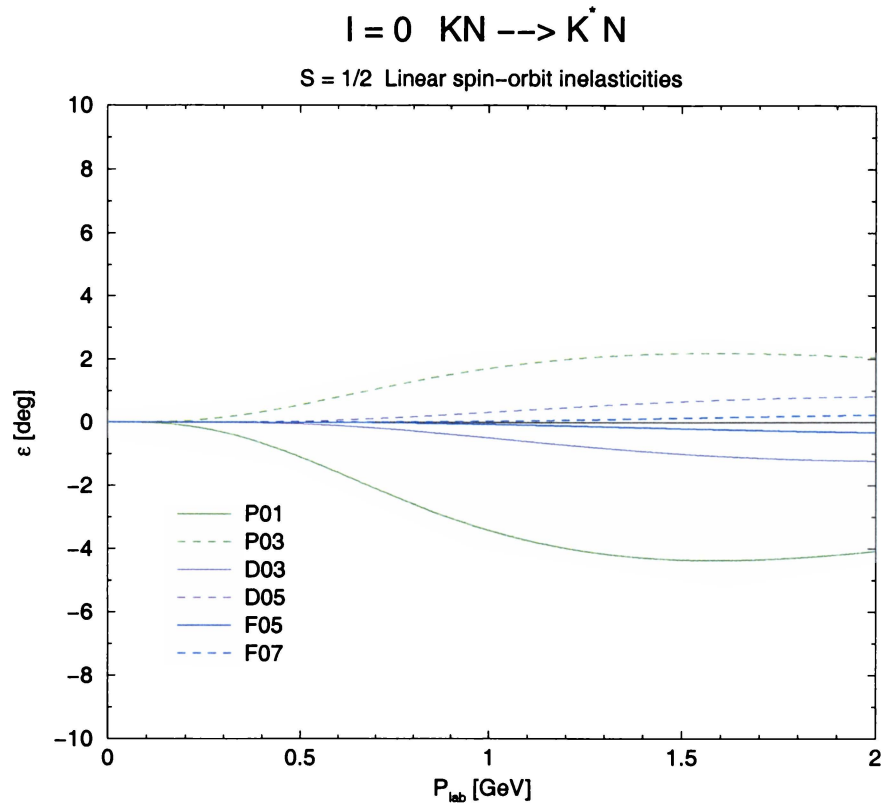


Figure 53: Theoretical $I=0 \quad KN \rightarrow K^* N$ confinement spin-orbit inelasticities.

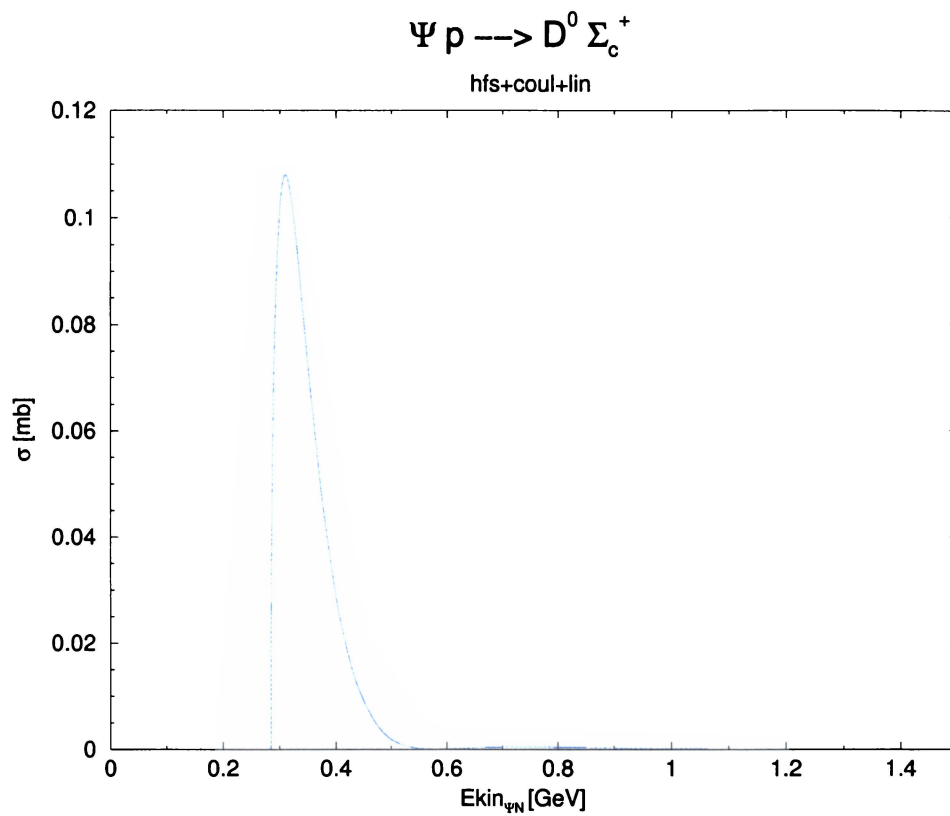


Figure 54: Theoretical $J/\psi p \rightarrow \bar{D}^0 \Sigma_c^+$ cross section.

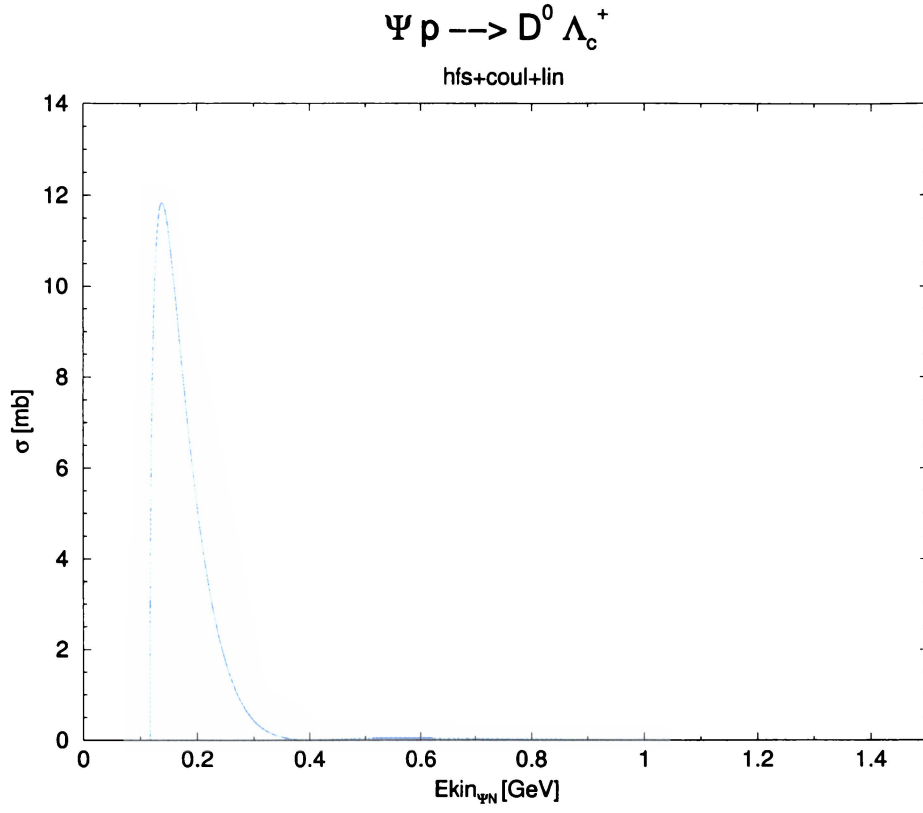


Figure 55: Theoretical $J/\psi p \rightarrow \bar{D}^0 \Lambda_c^+$ cross section.

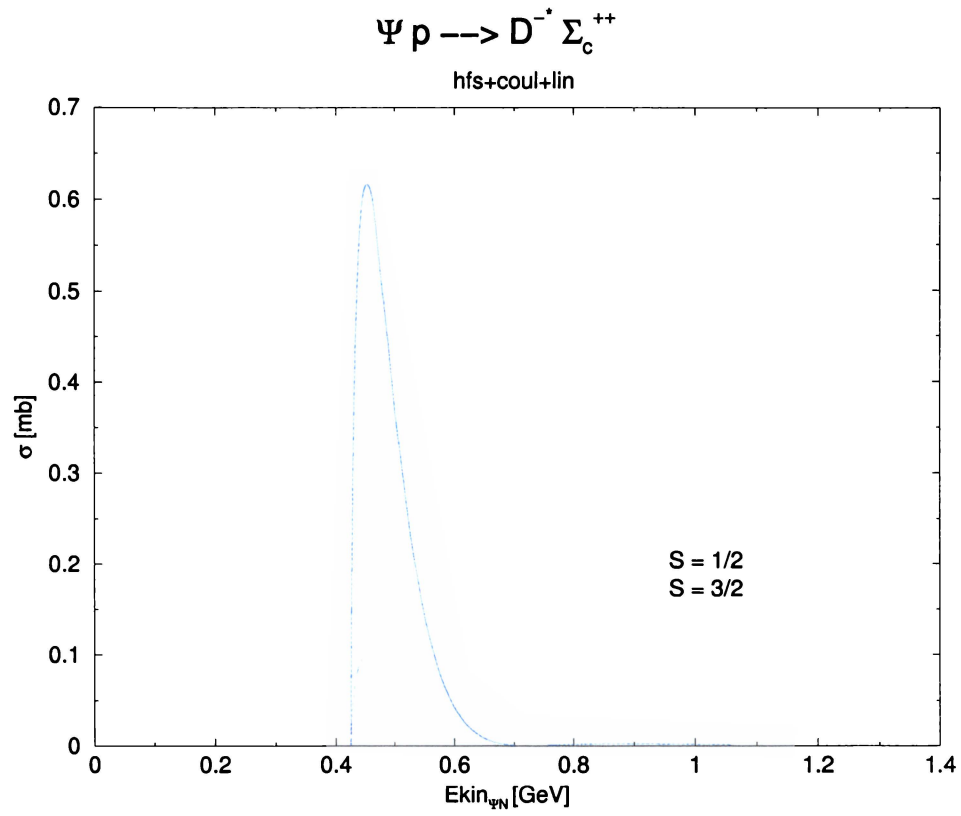


Figure 56: Theoretical $J/\psi p \rightarrow \bar{D}^{*-} \Sigma_c^{++}$ cross section.

Vita

Noel Franklin Black was born March 6, 1968, in Houston, Texas. He graduated from Lamar High School in Houston, Texas, 1986. He was awarded a B.A. in physics from Rice University in 1992, specializing in theoretical condensed matter physics. He has been a graduate student at The University of Tennessee since 1994, specializing in theoretical particle physics. He has published two refereed papers and one conference report, and has maintained a GPA of 4.0.

